ELSEVIER

Regionalization of a national integrated energy system model: A case study of the northern Netherlands

Somadutta Sahoo [a,b,*], Joost N.P. van Stralen [b], Christian Zuidema [a], Jos Sijm [b], Claudia Yamu [a], André Faaij [b,c]

[a] *The Department of Planning, Faculty of Spatial Sciences, University of Groningen, the Netherlands*
[b] *Netherlands Organization for Scientific Research Energy Transition, Amsterdam, the Netherlands*
[c] *The Energy Research and Sustainability Institute Groningen, Faculty of Science and Engineering, University of Groningen, the Netherlands*

HIGHLIGHTS

- Primary and secondary energy mixes at regional and national scales vary greatly.
- Some regional building types and industrial activities potentially save energy.
- Interregional secondary energy flows, notably hydrogen, are massive.
- System costs and energy infrastructure investments differ vastly across regions.

ARTICLE INFO

ABSTRACT

Integrated energy system modeling tools predominantly focus on the (inter)national or local scales. The intermediate level is important from the perspective of regional policy making, particularly for identifying the potentials and constraints of various renewable resources. Additionally, distribution variations of economic and social sectors, such as housing, agriculture, industries, and energy infrastructure, foster regional energy demand differences. We used an existing optimization-based national integrated energy system model, Options Portfolio for Emission Reduction Assessment or OPERA, for our analysis. The modeling framework was subdivided into four major blocks: the economic structure, the built environment and industries, renewable energy potentials, and energy infrastructure, including district heating. Our scenario emphasized extensive use of intermittent renewables to achieve low greenhouse gas emissions. Our multi-node, regionalized model revealed the significant impacts of spatial parameters on the outputs of different technology options. Our case study was the northern region of the Netherlands. The region generated a significant amount of hydrogen (H_2) from offshore wind, i.e. 620 Peta Joule (PJ), and transmitted a substantial volume of H_2 (390 PJ) to the rest of the Netherlands. Additionally, the total renewable share in the primary energy mix of almost every northern region is ~90% or more compared to ~70% for the rest of the Netherlands. The results confirm the added value of regionalized modeling from the perspective of regional policy making as opposed to relying solely on national energy system models. Furthermore, we suggest that the regionalization of national models is an appropriate method to analyze regional energy systems.

1. Introduction

Developing a low-carbon energy system necessitates attention to various spatial dimensions [1]. The establishment of extensive infrastructures for low-carbon sources, such as wind, solar, and biomass energy, requires large amounts of space [2] because their low power densities. In addition, there are substantial regional differences between the potentials of existing renewable energy supply options and available energy infrastructures [1]. Area-based and bottom-up strategies are crucial for improving regional environments and stakeholders' interaction in the pursuit of a low-carbon energy system [3]. Such strategies are especially critical in densely populated areas where high energy demands and a lack of spaces can lead to serious competition over land use and instigate societal resistance. This situation also applies to the Netherlands [4], which is the location of our study.

The Netherlands aims to rapidly reduce greenhouse gas (GHG) emissions [5] and significantly increase in the share of renewables [6] in line with European Union targets [7]. However, the country is currently among the lowest performing European countries in terms of the share of renewables in its energy production [8]. This deficit can be attributed to high energy demands and limited renewable energy generation, which is partly caused by serious societal conflicts centering on the development of wind and solar projects. Furthermore, the Netherlands only recently began to implement region-based policy development. In this context, "region" refers to the provincial or supra-provincial level, covering areas up to 10,000 km^2, with population ranging from approximately 500,000 to a few million inhabitants. This geographical scale facilitates regional support and implementation of future energy policies through the development of effective coordination between different levels of government within a country [9]. Additionally, the balancing of energy demands and supply potentials can be better understood at this geographical scale, necessitating an analysis of regional energy systems [10]. Performing a region-based analysis enables an investigation of different spatially sensitive parameters that are too detailed to be analyzed at the national scale. Regions can differ in terms of their economic structures, particularly those relating to the built environment (BE) and industries. In addition, there are atypical regional differences in the energy supply and demand that contribute to profound mismatches of primary as well as secondary energy mixes, requiring extensive inter-regional flows in energy infrastructures to maintain regional balances. Energy system modeling tools can be used to conduct critical analyses of such issues and inform policy makers about areas requiring strategic planning.

Energy system modeling tools operate at different geographical scales. Models such as TIMES-DENMARK [11] and TIMES-UK [12] are usually applied in analyses at the national scale, while TIAM-ECN [13] and POLES-JRC [14] operate at even larger scales. These models do not represent the energy supply and demand spatially and generally assume copper plates for regions. In this context, the term copper plates refers to energy infrastructures, for example, related to electricity, that are not considered for inter-regional energy flows when the modeling is done on a higher geographical scope, such as the national level, i.e. energy demand and supply are assumed to be met within a region. These models consider neither distance and capacity-related constraints nor investment and transmission costs of interregional connections. Sometimes these models might apply lump sum prices for interregional energy transmission linked to average national energy demand. Additionally, these models do not account for regional infrastructure, land use patterns, or economic structures and activities. Therefore, they are not suitable for conducting regional analyses.

Few models conduct sub-national analyses of energy systems. Among these models are RIEP [15] and Neplan [16], which specifically target the provincial level, while NetSim [17] and SynCity [18] focus on the municipality or city level. However, these models are not integrated energy system models and do not adequately represent different sectors and the interactions between energy carriers. Other models that focus on the regional scale, include some of the geographical information system (GIS)-based models, such as ENERGIS [19] and GISA SOL [20]. However, the detailed granularity of these models influences data requirements and processing times, making them less appealing, and they do not adequately represent the interactions among regions. Moreover, none of these regional models focus on optimization or long-term futures which were the key considerations in this study.

Attempts to incorporate multiple regions into the modeling frameworks of existing energy system models with a higher level of spatial detail are even rarer. Few examples of such models are OSeMOSYS [21], ReEDS [22], NEMS [23], ESME [24], oemof [25]), and PRIMES [26]. For example, OSeMOSYS has been used for long-term rural energy system planning [27]. ReEDS model focuses on energy demand and supply attributes of specific regions within the United States (US). Similarly, NEMS considers various regional classifications for different energy-related activities on the supply and demand side in the US. ESME subdivides the United Kingdom to twelve onshore and twelve offshore regions. PRIMES applies stylized regional categories, such as rural, semi-urban, and urban. Furthermore, the Temoa energy system optimization model, which can analyze different geographical scales ranging from local to global, has been used for state level energy planning in North Carolina region [28] and Puerto Rico island [29] in the US. Nevertheless, because they operate at multiple levels, these models provide clues for integrating spatial parameters into a national energy system model.

We chose an integrated modeling-based approach for our regional analysis, which included crucial energy-related sectors and the interactions between them. Such an integrated approach has been applied within a few Dutch models, such as MARKAL-NL-UU [30,31], OPERA [32], and IESA-Opt [33,34] which are optimization-based models, and ENSYSI [35,36], which is a simulation-based model. However, none of these models include spatial parameters that are appropriate for performing regional analyses. Additionally, their structures do not sufficiently facilitate the integration of different regionally-relevant spatial parameters into a national energy system modeling tool. Our originality lies in integrating these parameters for different sectors and energy supply sources. Nevertheless, these models can serve as starting points for performing a regional analysis using similar technology databases, algorithms, sectoral coupling, and energy carrier interactions that have previously been used at the national scale. Hence, rather than developing an all new regional energy system model, we aimed to regionalize one of these models by modifying its structure.

Regional analysis is important to highlight regional differences in energy supply and potentials, particularly related to renewables. High spatial resolution used in regional analysis is important for investigating heat demand and supply dynamics. Outcomes of regional analysis are important to underpin formulation of regional policies and planning. Specifically, policies can be linked to identifying future regional renewable and emission targets; identifying and understanding changes in energy demand of building stocks and industries; and estimating increases in investment in energy infrastructures, building stocks, or industrial processes. Furthermore, detailed analysis of industrial activities is another key category because industrial activity can be (and is) very regionally specific.

This paper presents the first step for conducting a detailed regional energy system analysis. Specifically, we aimed to regionalize an existing national model by including regional differences in the energy demand and supply, the BE and industrial sectors, potentials of renewable energy sources (RES), and energy infrastructures. Moreover, we aimed to determine whether important spatial parameters could be integrated into a national model and whether a regionalized national model would produce significantly different outcomes compared with the average results of the national model. Thus, we formulate the following research question:

How can important spatially sensitive parameters at the provincial level be incorporated into an integrated energy system model in the context of the
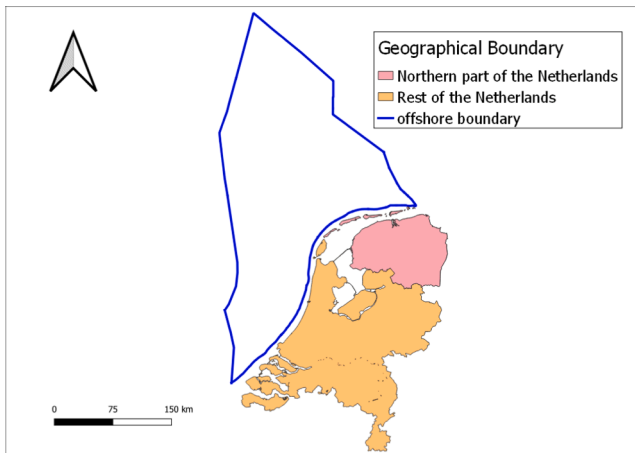
Fig. 1. The geographical scope for the analysis.

Netherlands?

To answer the above question, we formulated three sub-questions:

- *What are the relevant spatially sensitive parameters for different sectors at the provincial level in the Netherlands?*
- *How can a modeling framework be developed that incorporates relevant spatial parameters within an existing integrated energy system model at the national scale?*
- *What are the differences between the constructed regionalized energy system model and the national-average energy system model?*

We decided to use the Options Portfolio for Emission Reduction Assessment (OPERA) model for the following reasons. First, it offers a large selection of technology options for every sector along with energy carriers. Second, it has been intensively applied in recent years. Third, it is accessible through the Netherlands Organization for Applied Scientific Research (TNO in Dutch) Energy Transition, our partner institution. OPERA currently models all of the Netherlands as a single region (node) in which infrastructure costs are included via lump-sum transmission prices. Consequently, sectoral demands are met without considering the actual spatial distribution of sources of energy production and consumption. Existing mismatches between regional production and consumption necessitates a thorough analysis of regional energy landscapes and related infrastructure. Energy landscapes in our context encompass the physical landscape (e.g., the BE), agriculture, transport, industries, and energy infrastructures along with the allocation and availability of RES. We aimed to increase the geographical granularity of the model by creating explicit regions and enabling these regions to interact via energy infrastructures within the OPERA modeling framework. Anticipating a greater role for renewables in the future energy system mix of the Netherlands, we chose a scenario that strongly endorsed high renewable potentials. Defining and using proper indices is important to measure inputs and formulate outcomes in any regional energy system analysis. For example, demand of final main product is a better unit of measuring industrial activities rather than energy demand as energy demand may change over time due to efficiency improvements or process changes. Similarly, the number of projected dwellings is a better index for measuring household activity compared to energy demand. Proper cost indices are also highly relevant in any optimization modelling. For example, investment cost in an energy infrastructure is defined as a unit of distance. Similarly, investment and production costs in industries are a function of unit final main product.
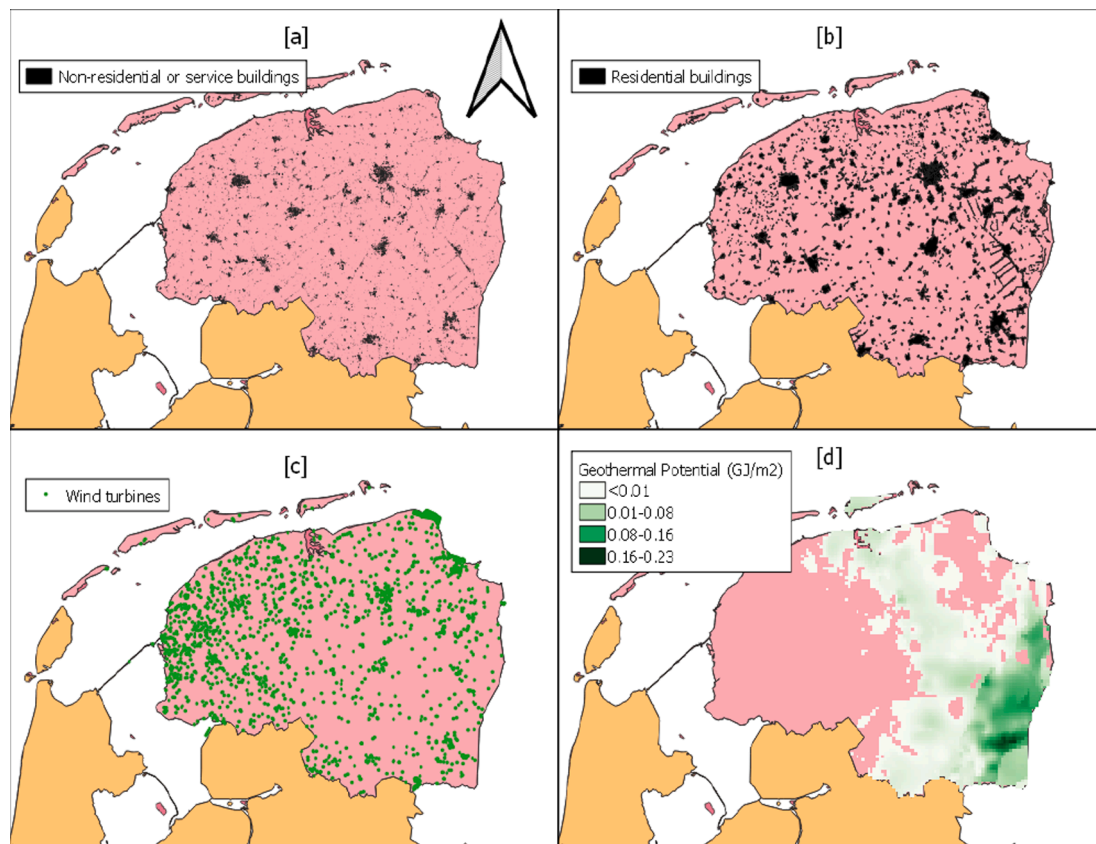
Fig. 2. Energy landscape of the NNL region for illustrative purposes. [a], [b], [c], and [d] show non-residential or service buildings, such as offices and educational buildings; residential buildings; onshore wind farms; and geothermal potential, in GJ/m^2; respectively. Geodienst [44] processed data on residential buildings and non-residential buildings. Data source: ArcGIS online [45,46] and ThermoGIS [41] for wind turbines and geothermal potential maps, respectively.
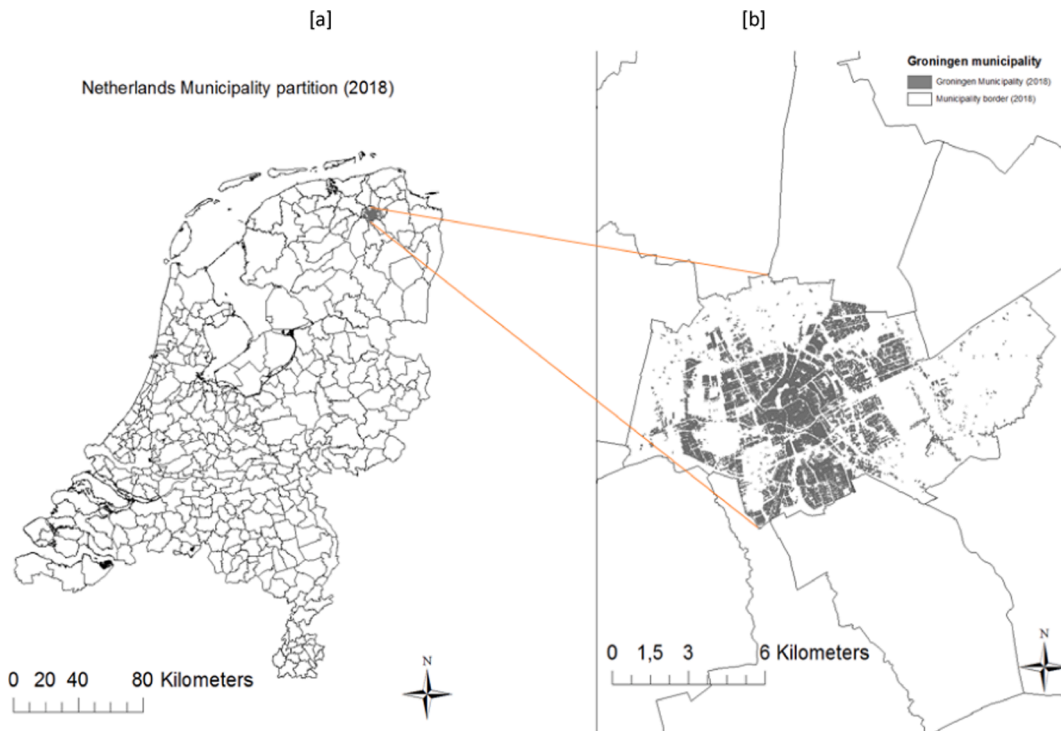
Fig. 3. [a] shows the municipality partition of the Netherlands in 2018, and [b] shows a zoomed-in image of the municipality of Groningen and its built-up area, such as households and services or non-residential buildings, including industries and power plants.
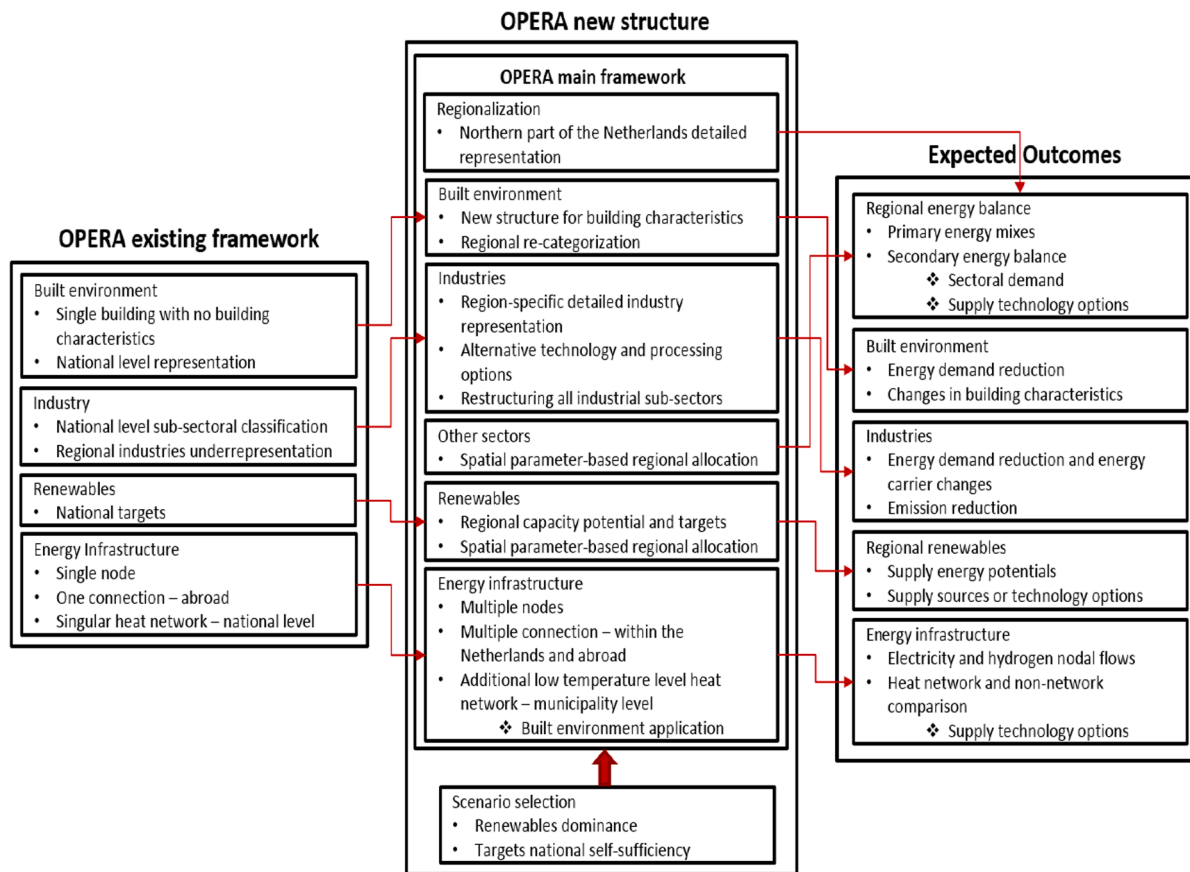
Fig. 4. Block diagram indicating the OPERA model use and expected outcomes in this study.
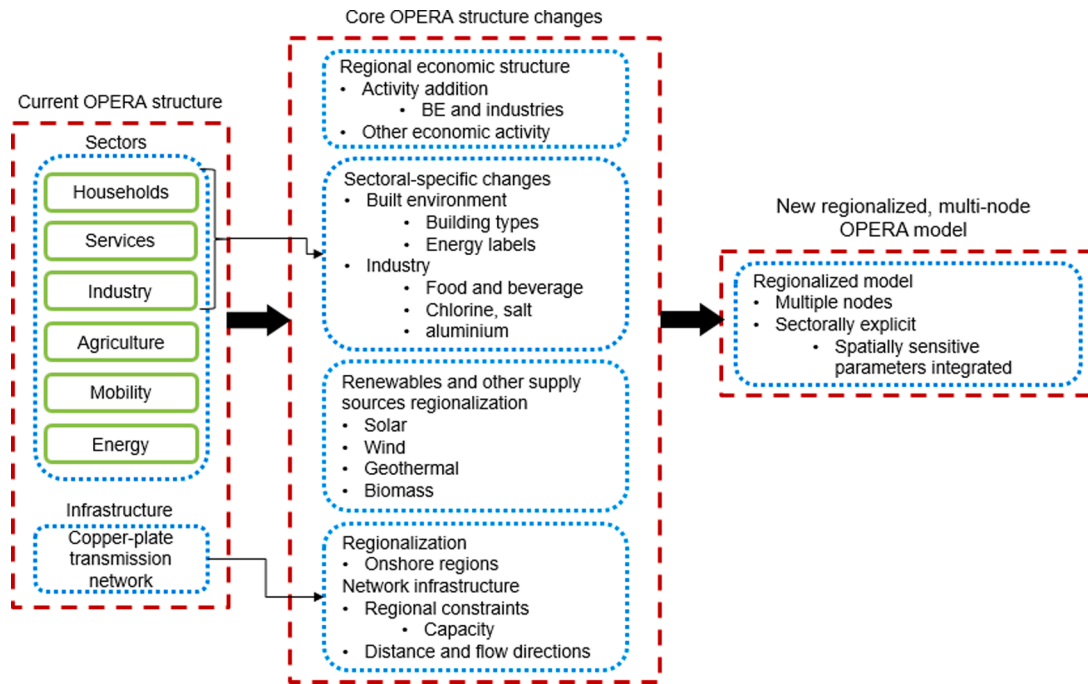
Fig. 5. Schematics of the modeling framework integrated in the OPERA structure.
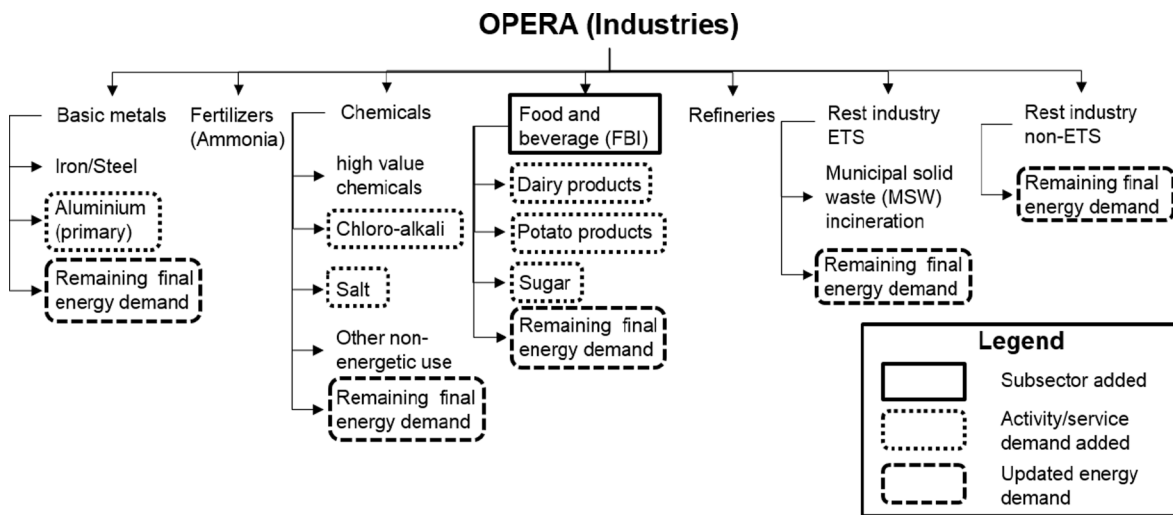
Fig. 6. Schematics of the industrial sector for regional analysis in OPERA.

We began by reviewing the literature to identify important spatially sensitive parameters for all energy-related sectors. We subsequently analyzed other (inter)national integrated energy system models to develop an understanding of how the parameters we had identified as relevant were integrated in these models. Next, we integrated spatial parameters using sector-specific methods to create a new regionalized OPERA model. Finally, we analyzed the impacts of different spatial parameters on the modeling outcomes at the regional scale by comparing the national-average and new regionalized models.

Section 2 includes the methodology of this paper which describes the geographical scope and major modeling framework changes of the integrated national energy system model, incorporating spatially sensitive parameters. Sections 3 and 4 respectively present the scenario applied in the study and the modeling results and analyses. In Section 5, we discuss the implications of the methodology and the results of the study. Our conclusions and future work are presented in Section 6.

2. Methodology

This section describes the geographical scope of our analysis (Section 2.1), followed by the methodological framework creation in OPERA (2.2). The geographical scope incorporates atypical characteristics of the northern part of the Netherlands (NNL) in Section 2.1.1 and explicit regions for our analysis in Section 2.1.2. The integration of our modeling framework in OPERA entailed the following key steps. (1*) We created a regional economic structure by allocating activities and production and demand volumes to regions (Section 2.2.1). (2*) We modified the modeling structures for the BE and industries sectors (2.2.2). (3*) We analyzed regional renewable potentials and related sensitivities (2.2.3). (4*) We connected regions via energy infrastructures (2.2.4).

2.1. Geographical scope

The geographical scope of the modeling encompassed both onshore

5

Table 1

Approach applied to determine region specific potential per type of renewable. Appendix D presents a detailed discussion on the approach used for renewables allocation.

Renewable energy source		Approach [Source/Reference]
Solar PV	Households	Land-use dedicated to BE as equivalent to rooftop space. From this the regional share is determined and multiplied to the national total [78].
	Services	Identical approach as households
	Agriculture	Based on the land dedicated to horticulture [78].
	Industry	Based on the land dedicated to industries [78].
	Roadside	Based on the regional share of provincial roads [78].
	Ground based	Available from the ENSPRESO project [43]. This project considers 17% of agricultural area and 100% of non-agricultural area for GB-PV.
	On (inland) water	Provincial data on inland water areas [78].
Wind	Onshore	Distribution is based on the provincial targets for 2020 [79].
	Offshore	Based on distance to existing/potential connection points and offshore space potential from [80].
Geothermal		We used the GIS-based 'overview technical potential' raster map of TNO [41,81].
Biomass	Wet manure	Regional livestock population [75] multiplied with its manure production [82].
	Co-substrate for manure digestion	Identical approach as wet manure
	Biogenic municipal solid waste (MSW)	Based on annual MSW burnt in existing incinerators [83].
	Vegetable, fruit, and garden (VFG) waste	Population-based distribution
	Sewage sludge	Population-based distribution
	Sugar and starch	Available from Elbersen *et al.* [84], which estimate future biomass potentials by considering existing land-use policy measures, i.e. business-as-usual, for different provinces in the Netherlands.
	Woody	Identical approach as sugar and starch

Table 2

Different sensitivity cases considering RES changes compared to the reference scenario along with application regions. Table D.1 describes cases in more details along with regional allocation.

Sensitivity case name	RES changes compared to reference scenario	Application regions
High onshore wind (*C1*)	Potential wind onshore is doubled	All regions
Low onshore wind (*C2*)	Potential kept at the 2020 target	All regions
Low GB-PV (*C3*)	Utilization of GB-PV as compared to reference is halved	All regions
Low geothermal (*C4*)	Utilization of geothermal as compared to reference is halved	All regions
High woody biomass (*C5*)	Potential of woody biomass is almost doubled (to round values)	All regions
Low woody biomass (*C6*)	Potential of woody biomass is more than halved (to round values)	All regions
High RES potential NNL (C7)	Combination of C1 and C5	Only NNL regions
Low RES potential NNL (C8)	Combination of C2, C3, C4, and C6	Only NNL regions

and offshore sections of the Netherlands (Fig. 1). Although our focus was on the NNL, we considered the entire country because energy infrastructures are strongly interconnected at the national level, and other infrastructures, such as carbon, capture, and storage (CCS) are also defined at this level. Moreover, future emission targets are set nationally. Modeling the NNL in isolation would have required making several
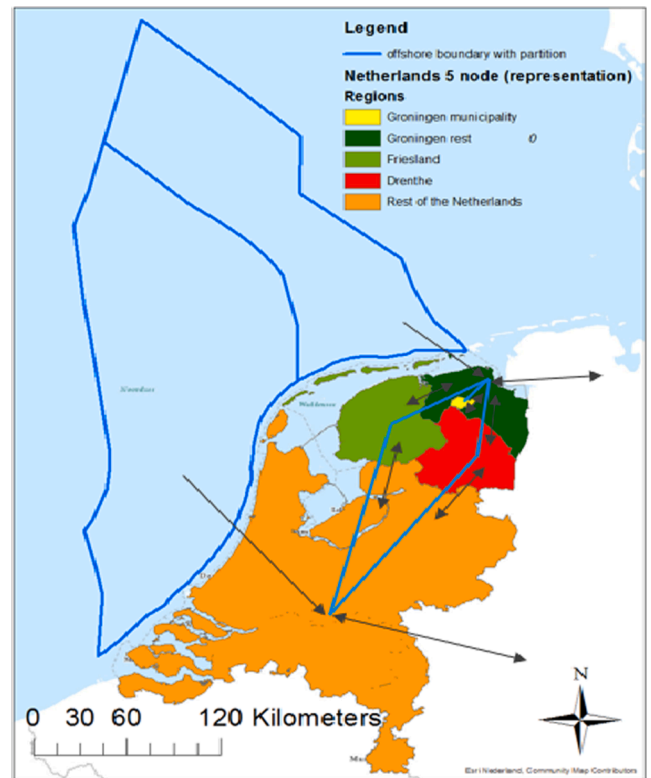
Fig. 7. Explicit regions or nodes and the network infrastructures along with flow directions in OPERA.

Table 3

Definitions of variables, parameters, and indices used in the equations (1)–(6).

Variables		Parameters		Indices	
TC	Total system cost in million Euro (M€)	P	tax on emissions	te	emission type
ET	Activity per emission type	VC	variable cost	n	region/node
G	Activity/ generation per option	CC	Annualized capital investment	to	technology option
CAP	Capacity of option	CO	Fixed O&M cost	t	time slice
EC	Activity per energy carrier	E	Energy cost/price of energy carrier	c	energy carrier
I	Import	TT	Transmission tariff	l	lower bound
E	Export	IC	Investment cost of transmission network	u	upper bound
CAPA	Transmission network capacity	D	Demand	N	national level
		A2C	factor linking activity to energy carrier		
		C	Network capacity limit		

allocation assumptions related to the share of the national emission reduction target to be achieved by the NNL, the share of the CCS potential that can be utilized by the NNL, and electricity and hydrogen prices. By embedding the NNL within a national model, we avoided making such prior assumptions. Therefore, we suggest modelers analyzing regions to consider national scope to avoid making similar assumptions. Appendix B provides detailed information on the analyzed region.

2.1.1. Atypical characteristics of the northern part of the Netherlands

The NNL region comprises of three provinces: Groningen, Friesland,

Table 4
Summary of major modeling framework modification in OPERA.

Core OPERA structure changes	Methodology summary

Regional economic structure	- Generating a regional economic structure through statistical data. New regional activity allocation is based on:
	   - the number of dwellings for households sector
	   - gross floor area for non-residential buildings
	   - unit of final main product for industries

Improvements of the BE and industries sectors in the model	- The BE sector detailed modeling with consideration of building types and energy labels of buildings at a regional level. Comparison of the reference case with optimized results to analyze energy savings. Inclusion of normalized heat demand and shell improvement cost for every building type in the model database - Detailed modeling of industries important for the NNL with a few activities addition. For these activities, considering a set of alternative technology options for meeting final main product demand. Comparison of optimized results with reference case to analyze energy savings and emissions reductions considering investment in new processes for each activity - Added a new subsector called FBI within the industries sector with explicit heat connection options and a new sub-sectoral energy carrier stream called biogas (FBI)
Regional allocation of supply-related sources	- Allocation of supply-related sources, namely solar, wind, biomass, and geothermal, to different nodes based on different spatially sensitive parameters - Sensitivity analyses on supply-side resources considering uncertainties faced regarding both technology and policy developments
OPERA regionalization and infrastructure creation	- Creating five nodes both in the database and model to adequately represent the NNL - Creating network infrastructures for movement of major energy carriers: electricity, H_2, NG, and heat - Network capacity constraints at a regional level along with investment cost consideration - change from lump-sum capacity to a function of distance with capacity constraints

and Drenthe. Important atypical features of the region include (see also Fig. 2):

- Industry: Region-specific industries are the food and beverage industries, including dairy products, potato products, and sugar; chemicals, including chloro-alkali and salt; and primary aluminum [37]. The NNL region also has significant potential for large-scale hydrogen (H_2) production [38].
- Energy: The region favors wind farms installation [39,40] (Fig. 2 [c]). In addition, the region has significant potential for geothermal energy production [41,42] (Fig. 2 [d]) and large-scale solar PV systems [43].

2.1.2. Selection of explicit region

We selected Groningen municipality (GM) at a city or municipality level as an explicit region for our analysis of the NNL. GM clearly illustrates the impacts of a heat network at the city level. Similar to other contemporary integrated energy system models, such as ENERGYPLAN [47] and BALMOREL [48], a consideration of energy infrastructures, for example, district heating (DH) networks, was central to our analysis. DH feasibility is confined to regions with high heat demand densities at low temperatures due to high network losses [49,50]. Within the NNL, GM population (230,000 inhabitants) is considerably larger than that of other municipalities in the NNL, resulting in high heat demand densities

within the BE [51]. Additionally, DH has low penetration in GM [52], leading to its high potential [53]. Fig. 3 presents a graphical zoomed-in representation of GM and its built-up area.

The appropriate geographical resolution for a detailed analysis of the rest of the NNL is NUTS2 [54] or the provincial level. Therefore, the explicit regions or nodes in our model are Groningen rest (GR), i.e. Groningen Province excluding GM; GM; Friesland Province; Drenthe Province; and the rest of the Netherlands (RNL). For our analysis, we identified important spatially sensitive parameters based on a literature review. To allocate these parameters regionally, we extracted and compiled data from the Dutch Central Bureau of Statistics (CBS) databases; TNO, the Netherlands Environmental Assessment Agency (PBL in Dutch), and other Dutch-specific reports; and other European reports. Data from these sources for the Netherlands are mostly available at a provincial level resolution. Additionally, existing provincial policies can be quantitatively implemented within an energy system model.

We enhanced the geographical granularity of the NNL without detailing the remaining region of the RNL because we are interested in understanding how major spatially sensitive parameters affect regional energy supply, particularly renewables, and demand; how regional energy supply can affect regional policy choices and planning; and how industries and energy infrastructures (including investment related to renewables infrastructure) are major part of regional economic structure. This analysis will assist provinces in becoming proactive towards setting future renewable targets and identifying the economic impacts of their choices. Similar to our study, Hers *et al.* [55] increased the spatial resolution of only the Netherlands for analyzing congestion management at a national level within a pan-European electricity network context. Our method can be replicated to other regions within the Netherlands and abroad. Results clearly showed the impact detailed spatial analysis has on understanding the differences in regional energy balances and interregional energy flows. We acknowledge that enhancing the resolution of the whole analyzed region would have resulted in more realistic results related to aspects such as inter-regional energy flows and energy infrastructure prices. However, since we considered regional allocations of a large number of energy-related activities in OPERA (see Table 5, for example), it was not possible to consider every province with the same detail as the NNL. Fig. 4 presents a block diagram of the OPERA model use and expected outcomes in this study.

2.2. Methodological modeling framework

We integrated our modeling framework within OPERA, an existing national energy system model. OPERA is a long-term, optimization-based model covering all of the Netherlands. Sectoral energy demands in OPERA is linked to the National Energy Outlook Modeling System (NEOMS) [56], which is used to produce future-oriented sectoral projections for governmental agencies in the Netherlands. OPERA has been applied in analyzing demand and supply flexibility [57] and exploring the possibilities of power-to-gas conversion [58] in the context of the Netherlands. Appendix A provides a detailed description of OPERA's current structure. Appendix B details sectoral modeling changes and added equations specific to OPERA. Fig. 5 schematically depicts the modeling framework.

2.2.1. Regional economic structure

Regional energy demands differ from the national average due to differences in the regional economic structure. In this section, we describe the economic activities that were allocated on a region-specific basis and explain how we made this allocation. We first identified important spatially sensitive parameters for the relevant sectors and integrated those parameters into the OPERA modeling framework. We subsequently allocated those parameters regionally. Regional allocations of energy demands are described for the BE (Section 2.2.1.1), industries (2.2.1.2) and for the activities in other sectors (2.2.1.3).

Table 5
Demand-side activities and their standardized unit representation for activities or subsectors added to the OPERA model in this paper. Supply-side options present national potentials based on the existing NM2050 scenario. The table additionally includes regional allocation for both demand- and supply-side activities or options.

Category	Standardized unit	2050					
		Drenthe	Friesland	GM	GR	RNL	NL
Demand							
Households-Apartments	Mh	0.04	0.05	0.05	0.03	2.40	2.56
Households-Terraced houses	Mh	0.04	0.06	0.03	0.03	2.02	2.17
Households-other	Mh	0.16	0.21	0.01	0.13	2.80	3.31
Services-offices	km^2	0.99	1.73	0.38	1.29	56.44	60.83
Services-education	km^2	0.71	1.33	0.21	1.40	30.24	33.89
Services-Industrial halls	km^2	5.30	0.67	0.80	3.39	123.18	133.33
Services-hospitals	km^2	0.62	0.77	0.14	0.90	17.75	20.17
Services-other	km^2	4.58	6.72	1.83	3.88	150.99	168.00
Primary aluminium	Mt_liquid_aluminium	0.00	0.00	0.00	0.138	0.00	0.138
Dairy product	Mt_dairy_product	0.19	0.44	0.00	0.10	0.48	1.20
Potato product	Mt_potato_product	0.00	0.10	0.00	0.02	1.54	1.66
Sugar	Mt_sugar	0.00	0.00	0.60	0.00	0.60	1.20
Chloro Alkali	Mt_Chlorine	0.00	0.00	0.00	0.13	0.83	0.96
Salt	Mt_salt	0.00	0.94	0.00	2.95	3.19	7.08
Industry rest ETS-electricity demand	PJ	0.08	0.08	0.00	2.93	23.07	26.16
Industry rest ETS-heat demand	PJ	0.11	0.11	0.00	4.03	31.69	35.93
Industry rest non-ETS-electricity demand	PJ	0.60	0.70	0.00	4.65	35.95	41.89
Industry rest non ETS-heat demand	PJ	0.81	0.95	0.00	6.33	48.89	35.95
Supply							
Solar PV potential-households	GW	1.65	1.65	0.66	0.66	28.38	33.00
Solar PV potential-services	GW	0.24	0.48	0.36	0.12	10.80	12.00
Solar PV potential-Agriculture	GW	0.98	0.51	0.00	0.41	37.16	39.05
Solar PV potential-Industry	GW	0.72	1.20	0.48	0.72	20.88	24.00
Solar PV potential-Roadside	GW	1.50	2.00	0.50	0.75	20.25	25.00
Solar PV potential-Ground-based	GW	7.40	5.18	0.00	7.40	54.02	74.00
Solar PV (Onland) water	GW	0.02	0.28	0.01	0.02	1.22	1.55
Wind onshore potential	GW	0.80	1.44	0.00	2.24	11.52	16.00
Wind offshore potential	GW	0.00	0.00	0.00	33.84	38.16	72.00
Geothermal	PJ	10.00	46.00	2.00	18.00	124.00	200.00
Biomass-Sugar and Starch	PJ	2.00	0.50	0.00	2.18	9.31	14.00
Woody biomass	PJ	0.91	0.86	0.00	0.73	24.21	26.70
Biogenic MSW	PJ	1.32	0.52	0.00	0.69	12.83	15.37
Sewage Sludge	PJ	0.21	0.28	0.08	0.16	6.66	7.4
Co-product Manure Digestion	PJ	0.58	1.26	0.00	0.49	9.01	11.33
Wet Manure	PJ	1.56	3.39	0.00	1.31	24.25	30.5
VFG waste from households	PJ	0.29	0.38	0.11	0.22	9.00	10

2.2.1.1. Built environment. A consideration of building characteristics in the regional allocation of energy demand in the BE is preferable to basing this allocation on the proportion of the population, which is a comparatively crude method. In light of our review of the literature, we selected dwelling types [59,60] and energy labels [61] as important spatial parameters for households and building type as an important spatial parameter for service buildings, including offices [62], and hospitals and educational buildings [63].

Single dwellings and single service buildings were respectively used to represent all Dutch households and services sectors within OPERA. We introduced three dwelling types: apartments, terraced houses, and other dwelling types because of considerable differences in their average energy consumption and regional distribution [52]. Similarly, we categorized service buildings as offices, educational buildings, industrial halls, hospitals, and others. For this categorization, we followed other contemporary integrated energy system models, such as ENSYSI [36], NEMS for households [64] and services [65], and IKARUS [66]. We gathered region-specific data on the numbers of dwellings of different types and their average annual energy consumption from CBS databases [52,67]. We referred to existing studies to extract region-specific data on gross floor area of service buildings [62,68,69]. Table C.6 and Table C.8 present the current regional distribution of households and service buildings, respectively, which we added to the OPERA database. Given a lack of data, we did not consider distinct demand profiles for different building types. Section 2.2.2.1 presents detailed analysis of energy demands and savings for the BE buildings in OPERA.

2.2.1.2. Industries. Industrial economic activities differ significantly among regions within the NNL and between the NNL and the RNL. We performed an explicit analysis of key industrial activities in the NNL. Fig. 6 presents the overall structure of industries covered in OPERA along with an added subsector and integrated activities or service demands, including newly added activities (see Section 2.1.1). Table G.7 shows the current nodal distribution of activities that are added in OPERA. This distribution is derived from the MIDDEN reports [37], which analyzes decarbonization options for different industrial subsectors in the Netherlands. Existing OPERA activities, namely iron/steel, ammonia, refinery, and high value chemicals (HVC), are all allocated to the RNL node as these activities are only present there. Following other contemporary integrated energy system models, such as NEMS [70], PRIMES [71], SimREN [72], and ESME [24], we created food and beverage industry (FBI) as a new subsector.

Apart from creating the FBI subsector, we also created new activities/service demands (Fig. 6). Referring to the MIDDEN reports [37], we identified the energy demand for one unit of activity (related to final main product production) for the existing technology option, termed as reference/standard option for these processes. We then introduced a set of alternative technology options with lower energy demands, emissions, or both, and we analyzed their investment and variable costs, including possible additional non-GHG emissions (see Tables G.1–G.6). We did not consider explicit demand profiles for the added activities. We subsequently projected future demands for the main products for 2050 based primarily on the projections used in the latest Dutch Climate Agreement and Energy Outlook (KEV in Dutch) [73]. As a final step, we allocated future final product demands to regions based on the current shares of these products.
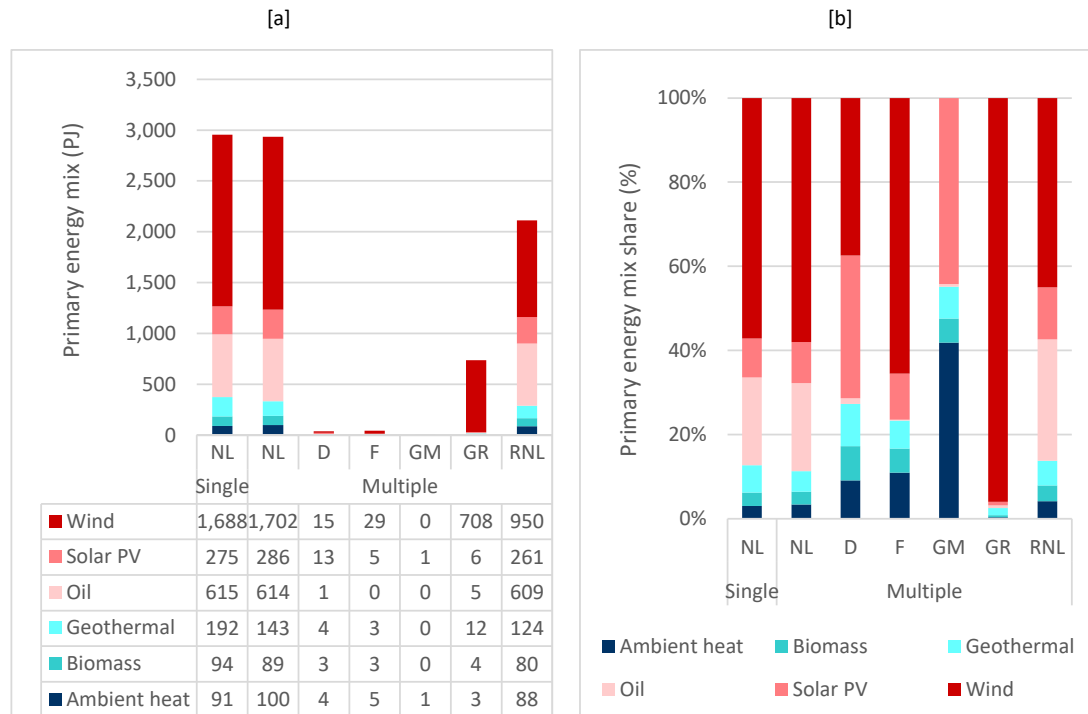
Fig. 8. Primary energy mix for the single- and multi-node models. [a] shows absolute values in PJ and [b] depicts the relative share of energy carriers for every node in both the models (in %). The data table in [a] is the same as [b]. D, F, GM, GR, and RNL are Drenthe, Friesland, Groningen municipality, Groningen rest, and the rest of the Netherlands, respectively.

2.2.1.3. Other economic activities. We considered agriculture and transport as two additional economic activities for regional allocation. Within the agriculture sector, horticulture is a highly energy-intensive activity in the Netherlands [74]. Because this activity is unevenly distributed across the country [75], we included horticultural area as a spatial parameter. Therefore, the regional allocation of sectoral energy demands and related mobile machinery was based on land use for horticulture. For the transport sector, our allocation of regional energy demands was based on 'klimaatmonitor.nl' [76]. This source provides the regional allocation of energy demands for transport-related activities based on CO_2 emissions. We used these data to calculate the regional share of activities for passenger cars, light duty vehicles, and heavy duty vehicles. Existing international shipping and aviation activities were all allocated to RNL, where they are prevalent.

2.2.2. Improvements for the BE and industries

In this section, we describe improvements relating to the BE and industries in the OPERA model and database.

2.2.2.1. Built environment. Energy label categorization, similar to building types, is another important spatial parameter from the perspective of energy savings potential. Therefore, we introduced an energy label categories for every building type similar to those in ENSYSI [36]: GFE, DC, B, A, and A+. We only considered improvements in heat demands resulting from changes in energy labels, as there has been hardly any reduction in electricity demands associated with improvements in energy labels [36,62]. Data on the normalized heat demands of different building types for different energy labels and shell improvement costs compared to the GFE label were obtained from ENSYSI [36] (see Tables C.1–C.5). Additionally, for office buildings, we considered the current distribution of regional energy labels, as reported in the literature [62,77] (see Table C.7). For other buildings, we assumed that this distribution is the same as the current national distribution given the lack of available data.

The model determined whether it is cost effective to improve energy labels for different building types considering overall GHG targets, reductions in heat demands, and shell improvement costs. Overall, the changes in the energy labels were responsible for reducing sectoral energy demands. We compared energy savings potentials of residential and service buildings with respect to the reference case, i.e. a case where no additional energy savings are achieved compared to the model input, to identify the energy savings potentials achieved by introducing building characteristics in OPERA. Appendix C details on the reference case and its inputs for the BE.

2.2.2.2. Industries. We compared the optimized model run with the reference case for the newly added industrial activities. In the reference case, every added activity corresponded to a situation in which all of the projected final product demand was met by an existing/standard production process. The model determined whether it is cost effective to change processes and energy carriers to meet final product demand considering energy savings, emission reductions, and investment costs in the new processes for each activity.

For the newly added sub-sector FBI (Fig. 6), we created and regionally balanced a new energy carrier, biogas (FBI), to account for the production and utilization of biogas associated with different activities, such as potato products, within the FBI subsector and within a region. We introduced heat supply options along with an external heat network connection for each activity within the FBI subsector. This network enables heat interaction between an activity and the overall FBI subsector to occur via some general heat supply options, such as combined heat and power (CHP) plants, biomass boilers, and heat pumps (HP), assigned to the overall subsector.

2.2.3. Regional allocation of renewables

We considered four renewables: solar PV, wind, geothermal, and biomass. Table 1 shows the approaches used to determine region-specific renewable energy potentials. Appendix D provides a detailed description of the approach used for performing the regional allocation of different renewables. Table 5 in Section 3 provides the regional
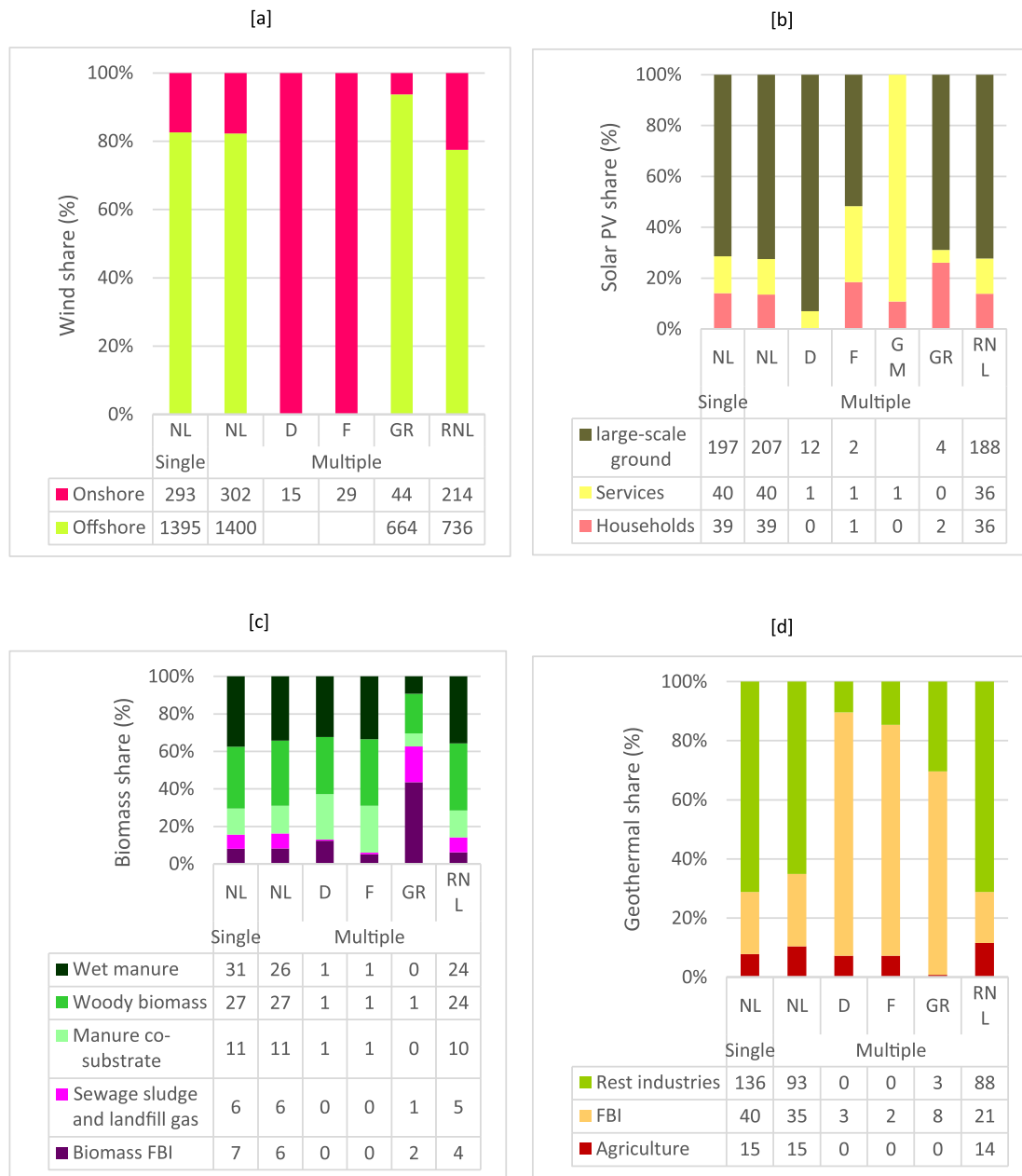
[a]

	NL	NL	D	F	GR	RNL
	Single		Multiple			
■ Onshore	293	302	15	29	44	214
■ Offshore	1395	1400			664	736

[b]

	NL	NL	D	F	G M	GR	RN L
	Single		Multiple				
■ large-scale ground	197	207	12	2		4	188
■ Services	40	40	1	1	1	0	36
■ Households	39	39	0	1	0	2	36

[c]

	NL	NL	D	F	GR	RN L
	Single		Multiple			
■ Wet manure	31	26	1	1	0	24
■ Woody biomass	27	27	1	1	1	24
■ Manure co-substrate	11	11	1	1	0	10
■ Sewage sludge and landfill gas	6	6	0	0	1	5
■ Biomass FBI	7	6	0	0	2	4

[d]

	NL	NL	D	F	GR	RN L
	Single		Multiple			
■ Rest industries	136	93	0	0	3	88
■ FBI	40	35	3	2	8	21
■ Agriculture	15	15	0	0	0	14

Fig. 9. Technology options and sectoral demand of different primary energy carriers. [a], [b], [c], and [d] present technology options utilizing wind energy, technology options utilizing solar energy, biomass-related supply sources, and sectors utilizing geothermal energy, respectively. The tables below diagrams present absolute values in PJ.

renewables allocation based on the approach described here.

The future potentials of renewables are highly variable and therefore uncertain. These potentials are also strongly dependent upon future policy choices at both the national and regional levels. We chose an aggressive reference scenario in which renewables were strongly emphasized, as the presence of more renewables results in greater spatial differences in their potentials. Given the uncertainties encountered in the areas of technology as well as policy making, we performed sensitivity analyses to assess different situations in the future pertaining to renewables. Table 2 presents sensitivity cases and changes made relative to the reference scenario and the regions to which these changes were applied. Most cases were paired as a high case and a low case. High cases entailed doubling the potential supply of a specific resource relative to the values shown in Table 5, whereas in low cases, the potentials were halved. For cases in which full potentials were not utilized, we only analyzed potentials corresponding to half the level of utilization

compared to the reference scenario (cases C3 and C4). Table D.1 in Appendix D provides a more detailed description of the cases.

2.2.4. Regionalization of the OPERA model and the creation of network infrastructures

In this section, we describe the energy infrastructures for electricity, natural gas (NG), and H_2 at the national level and the DH network at the municipality level.

2.2.4.1. Electricity, natural gas, and hydrogen network analysis. As a national model, OPERA represented all network infrastructures as copper plates, using lump-sum prices to account for network capacity changes. With regionalization, we introduced transmission networks as functions of distances and network capacities.

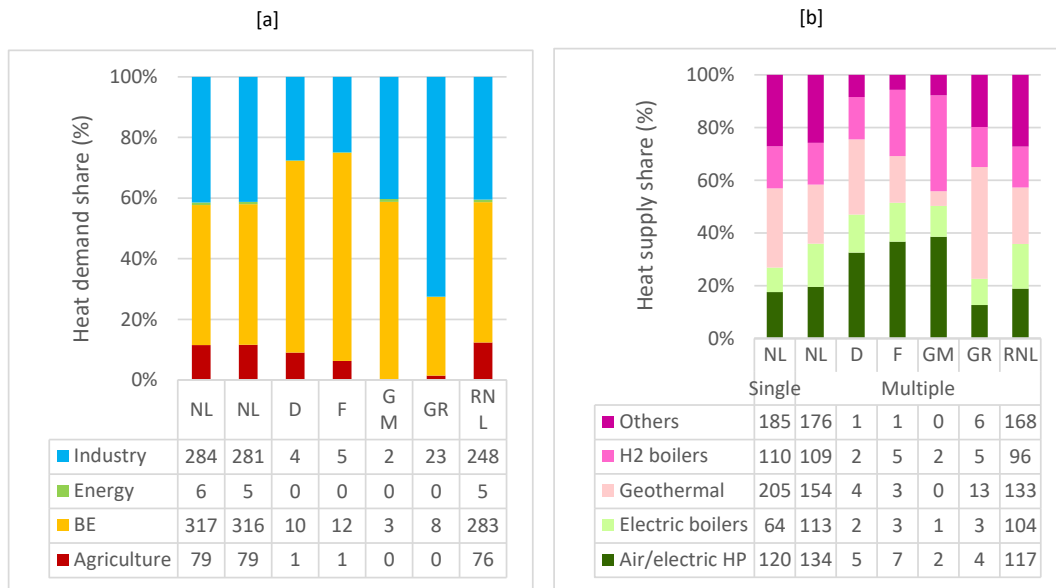We constructed a multi-node network infrastructure in which each

	NL	NL	D	F	GM	GR	RNL
Industry	284	281	4	5	2	23	248
Energy	6	5	0	0	0	0	5
BE	317	316	10	12	3	8	283
Agriculture	79	79	1	1	0	0	76

	Single	Multiple					
	NL	NL	D	F	GM	GR	RNL
Others	185	176	1	1	0	6	168
H2 boilers	110	109	2	5	2	5	96
Geothermal	205	154	4	3	0	13	133
Electric boilers	64	113	2	3	1	3	104
Air/electric HP	120	134	5	7	2	4	117

Fig. 10. [a] and [b] show heat demand-related sectors and heat supply-related technology options, respectively. The tables below the diagrams present absolute values in PJ.
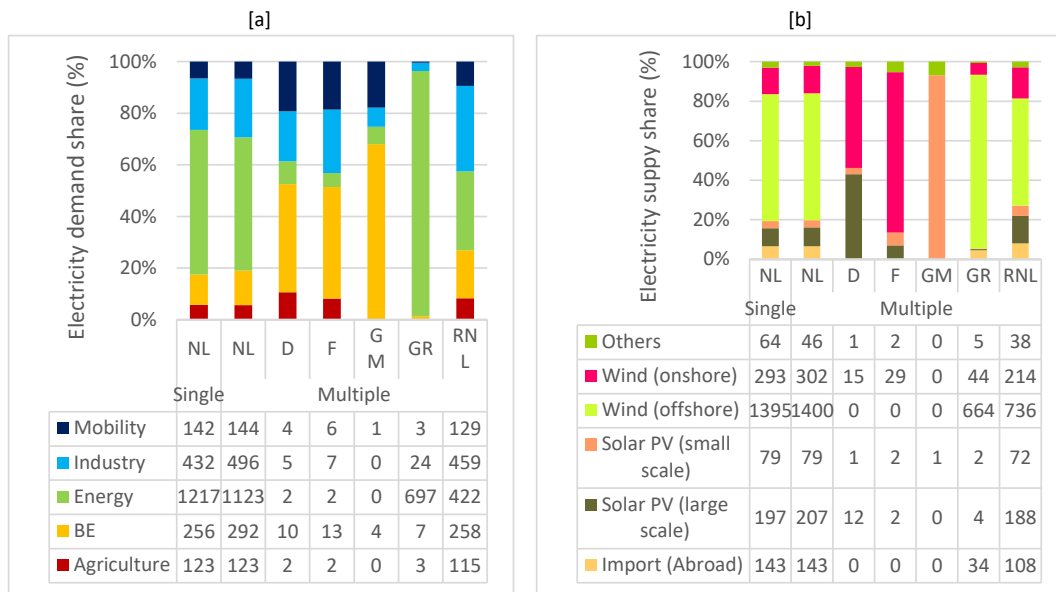

	Single	Multiple					
	NL	NL	D	F	GM	GR	RNL
Mobility	142	144	4	6	1	3	129
Industry	432	496	5	7	0	24	459
Energy	1217	1123	2	2	0	697	422
BE	256	292	10	13	4	7	258
Agriculture	123	123	2	2	0	3	115

	Single	Multiple					
	NL	NL	D	F	GM	GR	RNL
Others	64	46	1	2	0	5	38
Wind (onshore)	293	302	15	29	0	44	214
Wind (offshore)	1395	1400	0	0	0	664	736
Solar PV (small scale)	79	79	1	2	1	2	72
Solar PV (large scale)	197	207	12	2	0	4	188
Import (Abroad)	143	143	0	0	0	34	108

Fig. 11. [a] and [b] show electricity demand-related sectors and electricity supply-related technology options, respectively. The tables below the diagrams present absolute values in PJ.

node represented an explicit region. This approach is also used in other models, such as COMPETES, the pan-European electricity market model [55,85], and ESME [24]. The data requirements for our method were relatively low compared with the data requirements of GIS-based methods because of the modest geographical resolution. In the current version of OPERA, it is not feasible to consider more than one node per region. Therefore, each region represented an explicit node in our analysis. Each node is positioned at the centroid of each region.

We provided straight connections between nodes to establish a new transmission network between regions/nodes in OPERA (Fig. 7). This connection pattern was inspired by the high voltage (HV) electricity transmission network connections of TenneT, which is the national electricity transmission system operator in the country [86]. The actual network connections are more complex (Fig. H.1).

To reduce computational complexity, we used the same transmission network structure for electricity, NG, and H$_2$. We established a bidirectional flow between onshore regions for all energy carriers. Two nodes, GR and RNL, were used to depict electricity interactions with other countries. Considering existing electricity capacity connections between the Netherlands and other countries, we allocated 24% and 76% capacities to GR and the RNL, respectively. As in the BALMOREL model [87], we excluded inter-nodal heat transmission as heat movement over long distances is uneconomical. The added equations are shown below, and the symbols applied in the equations are defined in Table 3.

a) The new objective function is minimization of total system cost considering transmission-related variables and parameters:
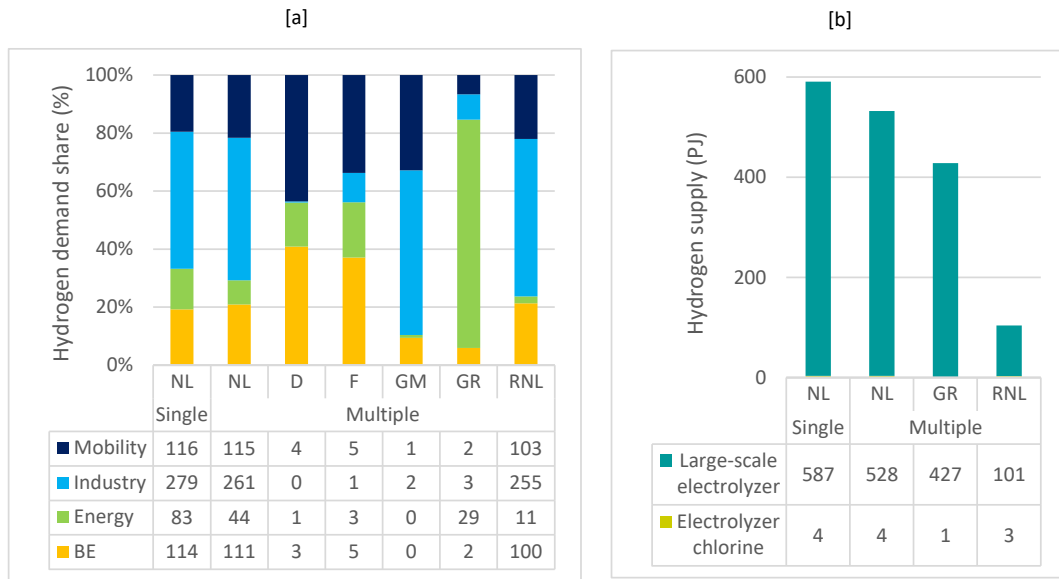
Fig. 12. [a] and [b] show H$_2$ demand-related sectors and H$_2$ supply-related technology options, respectively. The tables below the diagrams present absolute values in PJ.
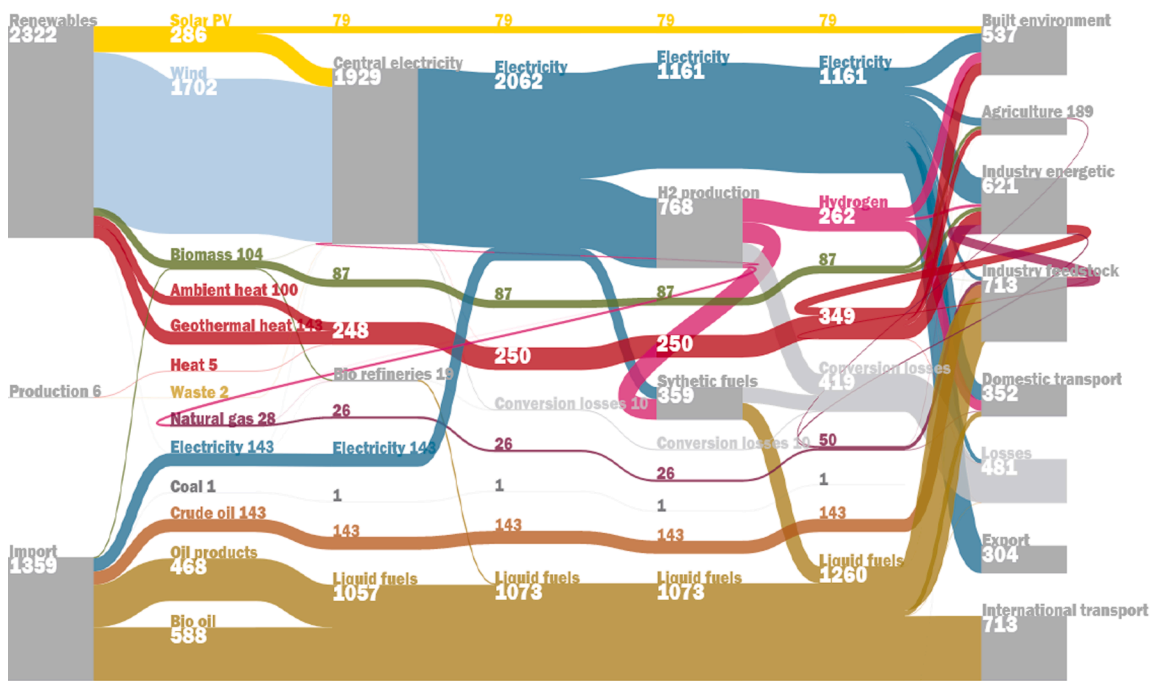

Fig. 13. Sankey diagram of the multi-node model at the national level (all data in PJ).

$$TC = \sum_{te,n,to,t} ET_{te,n,to,t}*\mathbf{P}_{te} + \sum_{n,to}\sum_{t}(G_{n,to,t}*\mathbf{VC}_{n,to,t}) + CAP_{n,to}*(\mathbf{CC}_{n,to}+\mathbf{CO}_{n,to})$$

$$+ \sum_{n,to,c} EC_{n,to,c}*\mathbf{E}_{n,to,c} + \sum_{t,n_1\to n_2,c}\left((I_{t,n_1,n_2,c}-E_{t,n_1,n_2,c})*\mathbf{TT}_{t,n_1,n_2,c}\right)$$

$$+ \sum_{n_1\to n_2,c} CAPA_{n_1,n_2,c}*\mathbf{IC}_{n_1,n_2,c} + \sum_{t,c}\left((I_{t,N,c}-E_{t,N,c})*\mathbf{TT}_{t,N,c}\right)$$

$$+ \sum_{c} CAPA_{N,c}*\mathbf{IC}_{N,c},$$

(1)

b) New energy balances at regional and national levels:

$$\mathbf{D}_{t,n,c} = \sum_{to} G_{n,to,t}*\mathbf{A2C}_{to,c} + \sum_{n\to n_1}\left(I_{t,n,n_1,c}-E_{t,n,n_1,c}+L_{t,n,n_1,c}\right) \quad \forall t,\ n,\ and\ c,$$

(2)

and

$$\mathbf{D}_{t,N,c} = \sum_{n,to} G_{n,to,t}*\mathbf{A2C}_{to,c} + \sum_{n\to n_1} l_{t,n,n_1,c} + I_{t,N,c}-E_{t,N,c} \quad \forall t\ and\ c,$$

(3)

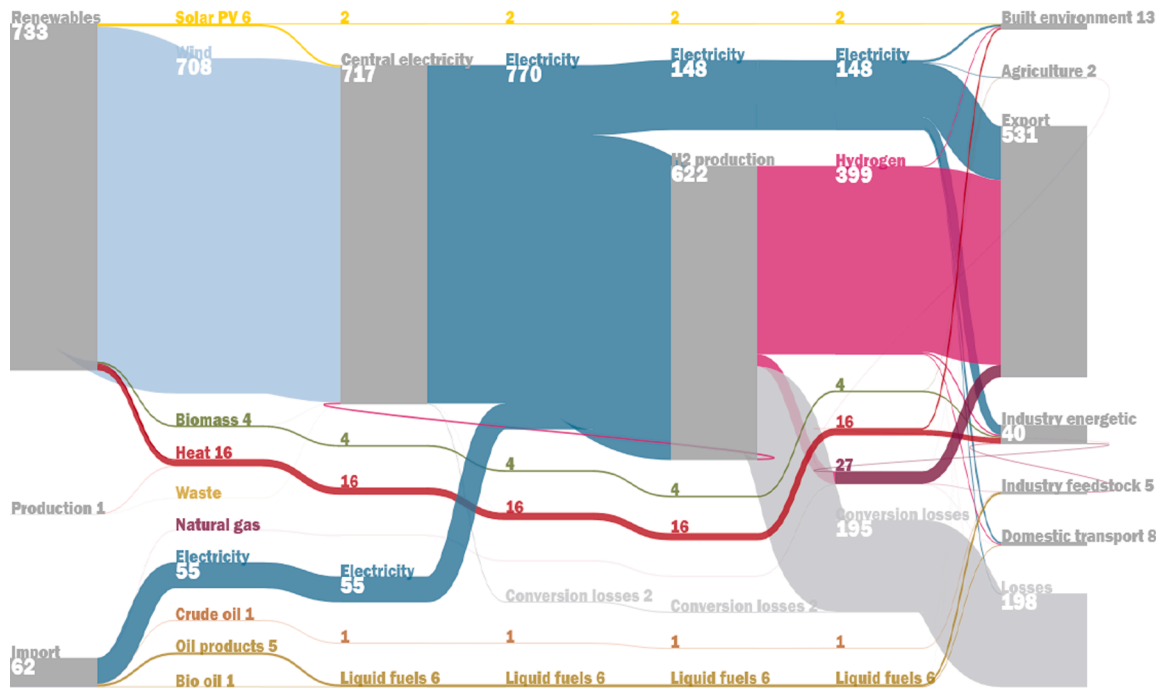These energy balances are subject to the following constraints:

Fig. 14. Sankey diagram of the multi-node model at the regional level for GR (all data in PJ).
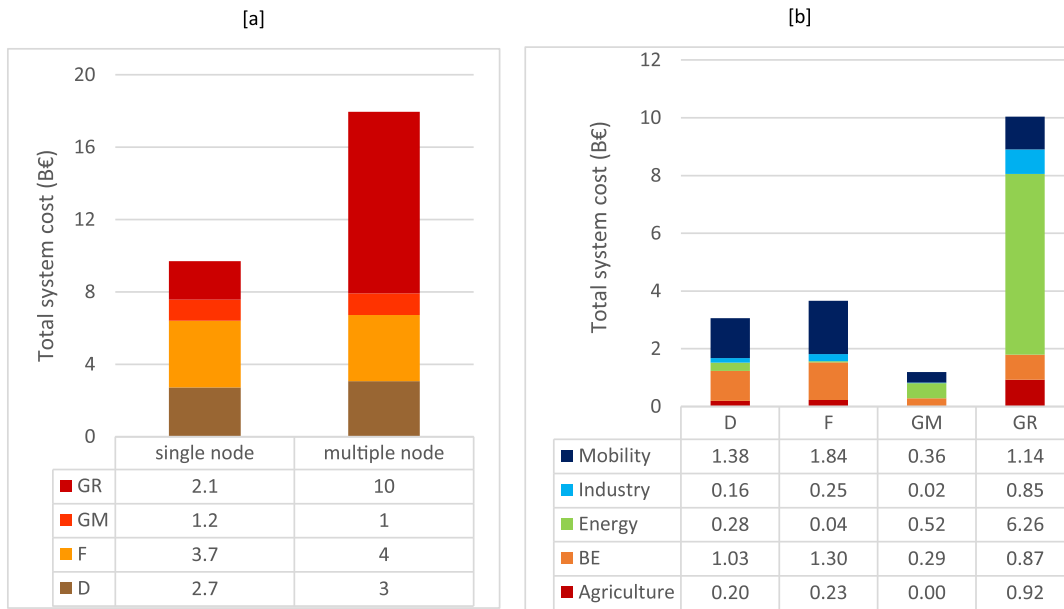

Fig. 15. Total system costs for all of the northern part of the Netherlands (NNL) nodes (in B€). [a] presents a comparison between the single- and multi-node models. For the single-node, we used the population share for nodal segregation. [b] presents sector-wise disaggregation of total system costs.

$$0 \leq g_{n,to,t} \leq CAP_{n,to}, \tag{4}$$

$$\mathbf{C}_{l,n_1,n_2,c} < I_{t,n_1,n_2,c}, E_{t,n_1,n_2,c} < CAPA_{n_1,n_2,c} \leq \mathbf{C}_{u,n_1,n_2,c}, \text{ and} \tag{5}$$

$$\mathbf{C}_{l,N,c} < I_{t,N,c}, E_{t,N,c} < CAPA_{N,c} \leq \mathbf{C}_{u,N,c} \tag{6}$$

In this study, we implemented capacity constraints only for electricity, as we assumed that existing other network capacities, NG and H_2, will use the NG network in the future via retrofitting. NG networks in the Netherlands are considered over-dimensioned. Appendix H presents database information on energy infrastructures and related constraints.

2.2.4.2. District heating network analysis. OPERA did not include an

adequate representation of a DH network. Moreover, similar to electricity, lump-sum values were applied for all network cost components. We established a DH network only for GM. For this purpose, we calculated the heat distribution cost taking account of aspects such as the heat demand density, population density, linear heat density, and the average pipe diameter. Appendix E presents the equations and method used to calculate the heat distribution cost. This cost is represented as the variable operation and maintenance (O&M) for the heat network in OPERA. Other network cost components, such as fixed O&M and capital expenditure (CAPEX), remained the same as the existing lump-sum cost in the OPERA database. We allocated explicit heat supply options or sources, such as geothermal electric pumps, woody biomass boilers, and
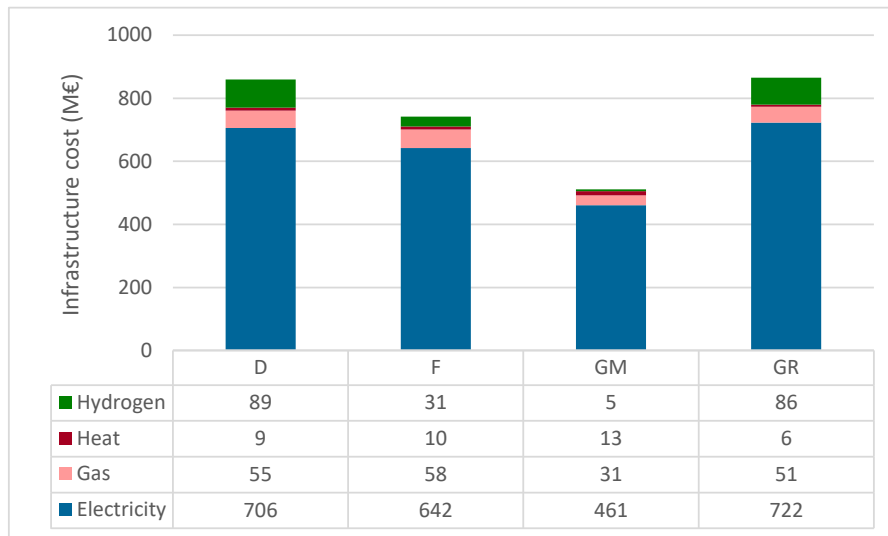
Fig. 16. Electricity, gas, heat, and hydrogen infrastructure costs in the multi-node model (in M€).

	D	F	GM	GR
■ Hydrogen	89	31	5	86
■ Heat	9	10	13	6
■ Gas	55	58	31	51
■ Electricity	706	642	461	722

[a]

	D		F		GM		GR	
	R	O	R	O	R	O	R	O
■ A+	0.03	0.23	0.04	0.31	0.01	0.09	0.02	0.19
■ A	0.13	0.00	0.17	0.00	0.04	0.00	0.11	0.00
■ B	0.05	0.00	0.06	0.00	0.03	0.00	0.04	0.00
■ DC	0.03	0.00	0.04	0.00	0.01	0.00	0.02	0.00

[b]

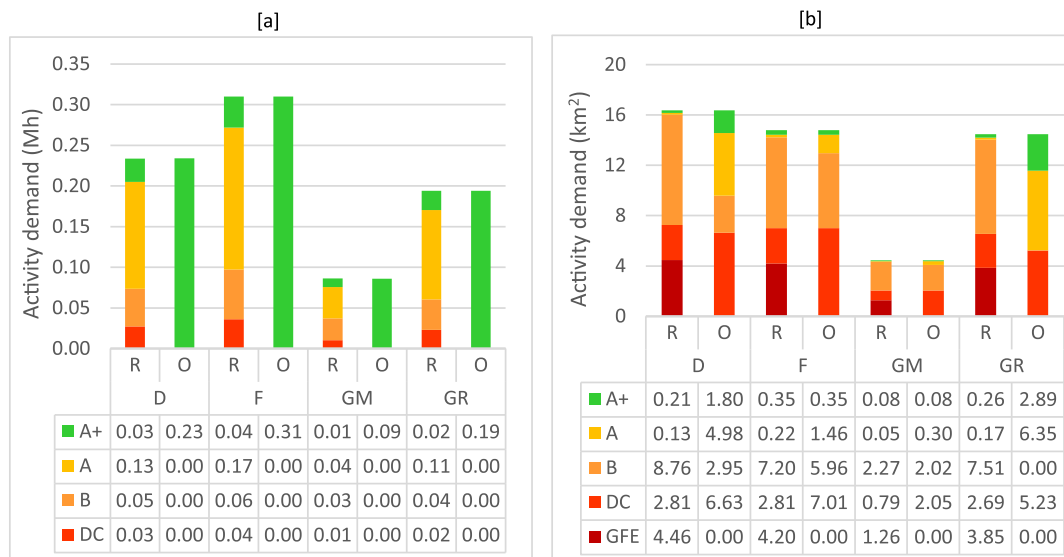|	D		F		GM		GR	
	R	O	R	O	R	O	R	O
■ A+	0.21	1.80	0.35	0.35	0.08	0.08	0.26	2.89
■ A	0.13	4.98	0.22	1.46	0.05	0.30	0.17	6.35
■ B	8.76	2.95	7.20	5.96	2.27	2.02	7.51	0.00
■ DC	2.81	6.63	2.81	7.01	0.79	2.05	2.69	5.23
■ GFE	4.46	0.00	4.20	0.00	1.26	0.00	3.85	0.00

Fig. 17. Comparison of activity demands between the reference case and optimized case model run regarding energy labels at different nodes in the NNL for the multi-node model. [a] shows the households activity demand in 'Mh' and [b] shows the services sector activity demand in 'km^2'. R and O represent the reference and optimized cases, respectively.

compression HPs, for this network, referring to the DH-related technology databases of the Danish Energy Agency [88,89]. Following the introduction of this network, we analyzed the proportion of the heat demand of GM that will be met by a DH network (i.e., DH penetration) in an optimized energy system in the future. The DH network analysis application is relevant in cases where low temperature (60–100°C) heat demand density is high. In such a case, a centralized DH network can show significant increase in heat supply contribution compared to individual heat sources.

Even though our modeling has been applied to the NNL, the method is universal. For example, if the regional data on the distribution of various buildings types for the BE are available, with or without energy label classifications, the regional BE-related energy demand differences can be modeled and the possibilities of energy saving potentials can be investigated. An important methodological addition is the creation of energy infrastructures for the movement of energy carriers between regions. The equations applied in this regard are generic and can be introduced in any regional analysis provided information on future

capacity limitations, and investment and transmission costs, are available. Table 4 presents a summary of major changes made to the OPERA modeling framework.

3. Description of reference scenario and regional allocation

Our reference scenario for 2050 was based on the national management scenario (NM2050) developed by Berenschot and Kalavasta [90] to facilitate network operators in the Netherlands. The NM2050 scenario is one of four scenarios explored by Berenschot and Kalavasta in their study. All four scenarios take the national climate agreement for the Netherlands as the starting point for the energy system development up to 2030 and subsequently present four alternative routes for establishing a climate-neutral energy system in the Netherlands by 2050. The selection of this scenario was notably influenced by regional factors, such as the possibility of utilizing large-scale offshore wind for H$_2$ production. Additionally, the low population density in the region is conducive to extensive deployment of intermittent renewables.

[a]

[b]

	R	O	R	O	R	O	R	O
	D		F		GM		GR	
Rest services	2	1	3	2	1	1	2	1
Hospitals	0	0	1	0	0	0	1	0
Industrial halls	1	1	0	0	0	0	1	1
Education	0	0	0	0	0	0	0	0
Offices	0	0	1	1	0	0	1	0

	R	O	R	O	R	O	R	O
	D		F		GM		GR	
Terraced houses	1	1	2	1	1	1	1	1
Other dwellings	7	5	9	7	1	0	6	4
Apartments	1	1	1	1	1	1	1	0

[c]

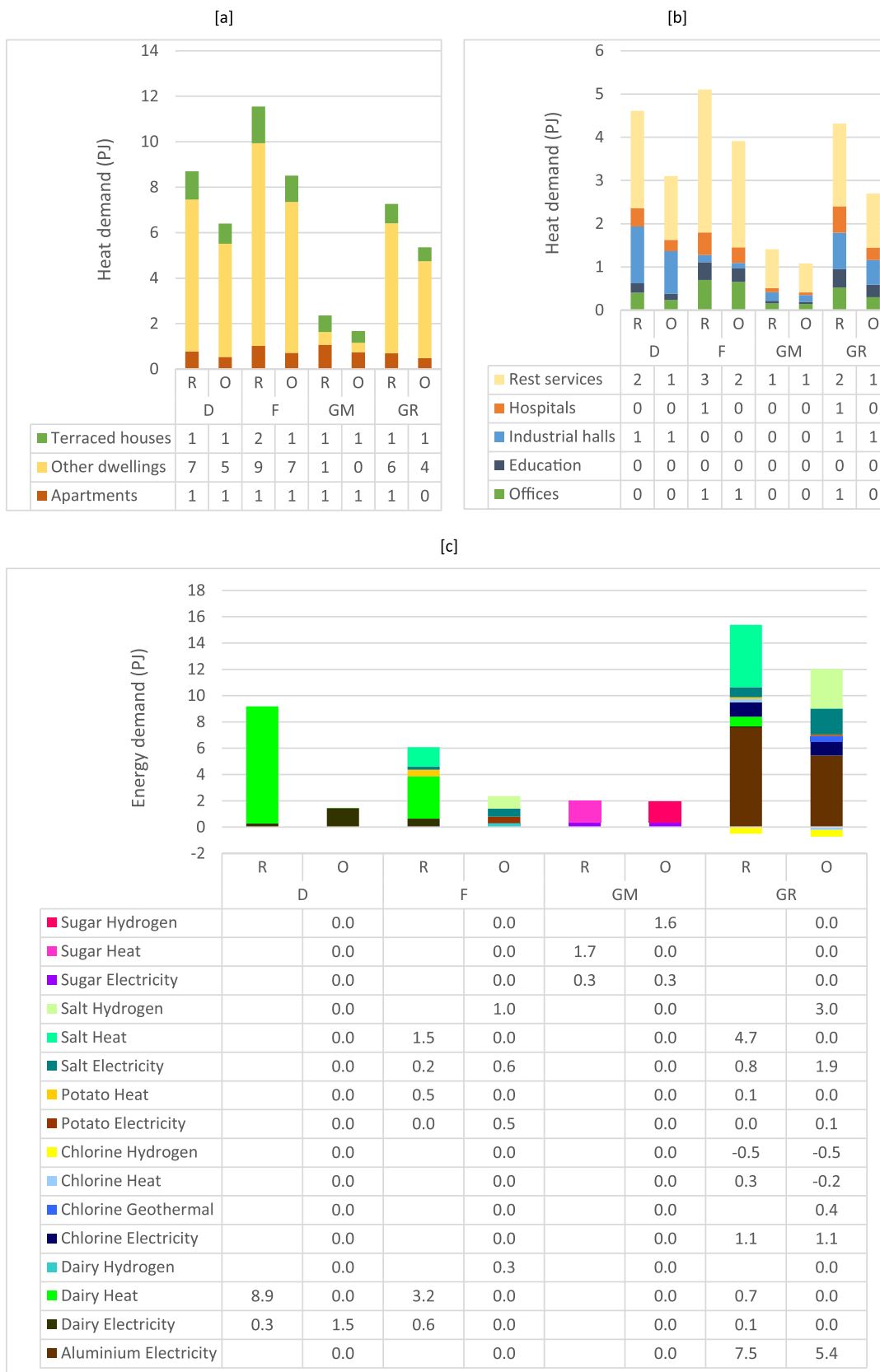|	R	O	R	O	R	O	R	O
	D		F		GM		GR	
Sugar Hydrogen		0.0		0.0		1.6		0.0
Sugar Heat		0.0		0.0	1.7	0.0		0.0
Sugar Electricity		0.0		0.0	0.3	0.3		0.0
Salt Hydrogen		0.0		1.0		0.0		3.0
Salt Heat		0.0	1.5	0.0		0.0	4.7	0.0
Salt Electricity		0.0	0.2	0.6		0.0	0.8	1.9
Potato Heat		0.0	0.5	0.0		0.0	0.1	0.0
Potato Electricity		0.0	0.0	0.5		0.0	0.0	0.1
Chlorine Hydrogen		0.0		0.0		0.0	-0.5	-0.5
Chlorine Heat		0.0		0.0		0.0	0.3	-0.2
Chlorine Geothermal		0.0		0.0		0.0		0.4
Chlorine Electricity		0.0		0.0		0.0	1.1	1.1
Dairy Hydrogen		0.0		0.3		0.0		0.0
Dairy Heat	8.9	0.0	3.2	0.0		0.0	0.7	0.0
Dairy Electricity	0.3	1.5	0.6	0.0		0.0	0.1	0.0
Aluminium Electricity		0.0		0.0		0.0	7.5	5.4

Fig. 18. Comparison of energy demands between the reference and optimized model run in different nodes in the NNL for the multi-node model (all data in PJ). [a] presents the heat demand comparison for different household building types in the BE. [b] presents the heat demand comparison for different service building types in the BE. [c] presents different energy carriers demand for various industrial activities highly relevant for the NNL. '-' values in [c] presents energy production, rather than demand.
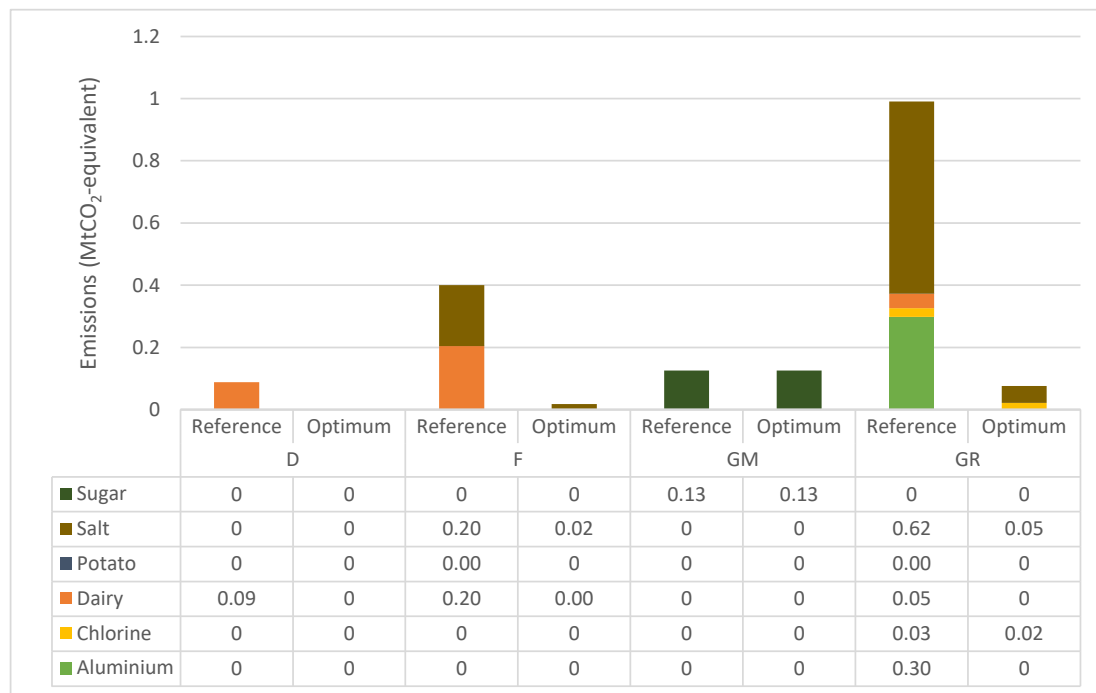
	Reference	Optimum	Reference	Optimum	Reference	Optimum	Reference	Optimum
	D		F		GM		GR	
■ Sugar	0	0	0	0	0.13	0.13	0	0
■ Salt	0	0	0.20	0.02	0	0	0.62	0.05
■ Potato	0	0	0.00	0	0	0	0.00	0
■ Dairy	0.09	0	0.20	0.00	0	0	0.05	0
■ Chlorine	0	0	0	0	0	0	0.03	0.02
■ Aluminium	0	0	0	0	0	0	0.30	0

Fig. 19. Comparison between the reference case and optimized case model run regarding industrial activities-related emissions from the different nodes in the NNL for the multi-node model (all data in $MtCO_2$-equivalent).

NM2050 is characterized by the existence of strong national governance and a high level of self-sufficiency at the national level. This scenario favors electrification through renewable power generation and a relatively high demand and supply of domestically produced green H_2. National-level imports/exports of electricity in our model were based on an import/export profile derived from COMPETES [55,85] using the NM2050 scenario [91]. Table 5 presents the newly added activities under the demand category and the supply potentials/capacities, standardized units, and regional allocation of activities. Table E.1 presents a complete list of economic activities and their national allocation in the reference scenario, while Table E.2 presents a comparison between our reference scenario and the NM2050 scenario.

4. Results

We created a regionalized, multi-node model by integrating changes into the OPERA modeling framework. We compared this model with a single-node model. The latter model integrates core changes in OPERA framework within a single node without creating regions and making regional allocations. This comparison enabled us to quantify differences arising as a consequence of regional variations in energy demands, supply potentials, and economic structures.

This section presents analyses of energy mixes (Section 4.1), regional cost structure (4.2), the overall energy system of the BE and industries (4.3), the impact of supply-side options (4.4), and network infrastructures and inter-nodal flows (4.5).

4.1. Primary, secondary, and total energy mix

Here, we analyze differences in energy shares at the national level between the single- and multi-node models and between the NNL nodes within the multi-node model. Section 4.1.1 focuses on the primary energy mix and related technology options and sectors, Section 4.1.2 discusses the demand and supply of secondary energy carriers, and Section 4.1.3 presents Sankey diagrams depicting the total energy system at the national level and for GR in the multi-node model.

4.1.1. Primary energy mix

Minor differences existed between the single- and multi-node models in terms of absolute values and the relative shares of supplies from primary energy carriers at the national level (Fig. 8), with the exception of geothermal energy. These insignificant differences in the primary energy supply between the single- and multi-node models can be attributed to the use of a restrictive NM2050 scenario. Given the absence of NG and limited biomass availability on the one hand and considerable wind potentials on the other hand, the possibility of changing the primary energy mix was limited. At the national level, the geothermal supply in the single-node model was 34% (49 PJ) higher than that in the multi-node model because of the averaging of the heat demand in the single-node model. Geothermal supply in both the models is a small fraction of total primary energy supply, though. The marked differences in the primary energy mixes of Drenthe and Friesland in the multi-node model were also striking. The shares of wind and solar energy in Drenthe's primary energy mix were 37% (15 PJ) and 34% (13 PJ), respectively, whereas wind and solar energy shares in Friesland were 66% (29 PJ) and 11% (5 PJ), respectively. The total share of the northern offshore wind was allocated to GR leading to a very high share of wind in the primary energy mix of this region (708 PJ or 96% of its total primary energy share). Similarly, there were regional differences in the absolute and relative shares of geothermal energy and biomass in the multi-node model. Drenthe's geothermal energy and biomass supplies were 10% (4 PJ) and 8% (3 PJ) of the total primary energy mix, respectively, whereas both types of energy had equal shares at 6% (3 PJ) of the total primary energy mix in Friesland. GM had a very low primary energy supply as activities there were mainly related to the BE. For example, the solar energy supply in GM was only 1 PJ and was mainly derived from rooftop PV systems. Fig. H.1 shows a comparison of the absolute primary energy mixes for all the NNL nodes in the single- and multi-node models, with the former entailing the use of the population share for nodal segregation. These differences clearly illustrates the value of creating regions for advancing understanding of differences in primary energy supplies between regions and in comparison to the national level, which would not be possible with a standalone national model with average values. Additionally, even though the single-node
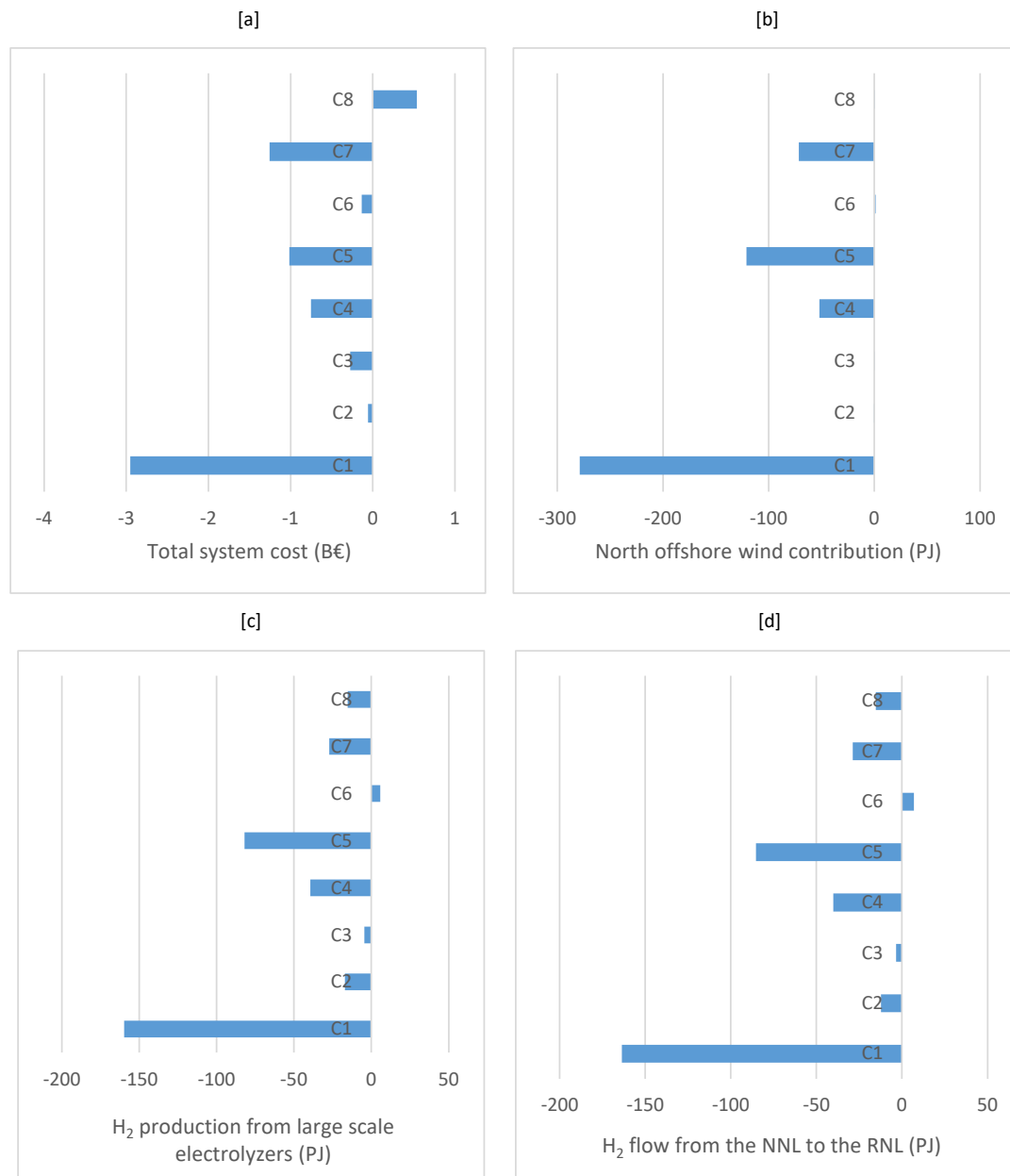
Fig. 20. Sensitivity analyses of all the nodes in the NNL (combining values of all the NNL nodes in all cases) in the multi-node model with respect to the reference scenario. [a] presents total system cost (in B€), [b] presents north offshore wind contribution (in PJ), [c] shows H_2 production from large-scale electrolyzers (in PJ), and [d] depicts H_2 flow from the NNL to the RNL (in PJ).

model predicts the energy mix almost similar to the national energy mix of the multi-node model, the latter is necessary to develop energy-related policies unique to each region as demonstrated by the diverse fuel mix in each province. In addition, identifying such differences in energy mix between regions as well as between regional and national levels is one of the many original findings from our study.

Detailed analysis of primary energy carriers/supply side options

Fig. 9 shows the supply shares of primary energy carriers, namely wind, solar, geothermal, and biomass energy for different nodes and considering various technology options/sectors. In the multi-node model, the offshore wind energy supply of GR and the RNL were 664 and 736 PJ, respectively, (Fig. 9 [a]), and the contribution of the onshore wind supply in the NNL was high (15 PJ, 29 PJ, and 44 PJ for Drenthe, Friesland, and GR, respectively). The high wind capacity potential and wind speeds in the NNL accounted for the high wind energy

supply potentials (in PJ) in this region. The relative shares of offshore and onshore wind in the single- and multi-node models were similar. The onshore wind farm capacity is fully utilized suggesting, application-wise, wind farms installation-related stakeholders should be motivated to install a lot more wind turbines compared to the current capacity for a cost-effective future energy system.

Regional differences relating to solar energy were prominent in the multi-node model (see Fig. 9 [b]) and were partly caused by the degrees of urbanization and available land for ground-based photovoltaics (GB-PV). Moreover, the overall GB-PV capacity was underutilized, with only 60 GW used in the Netherlands compared with the 72 GW potential available in the reference scenario.

Of the different categories of biomass, the supply of woody biomass supply was high in the NNL, followed by manure and FBI-related biomass (see Fig. 9 [c]). Of the nodes in the NNL, GR had the highest biomass demand (4 PJ), of which 2 PJ was from the potato industry in
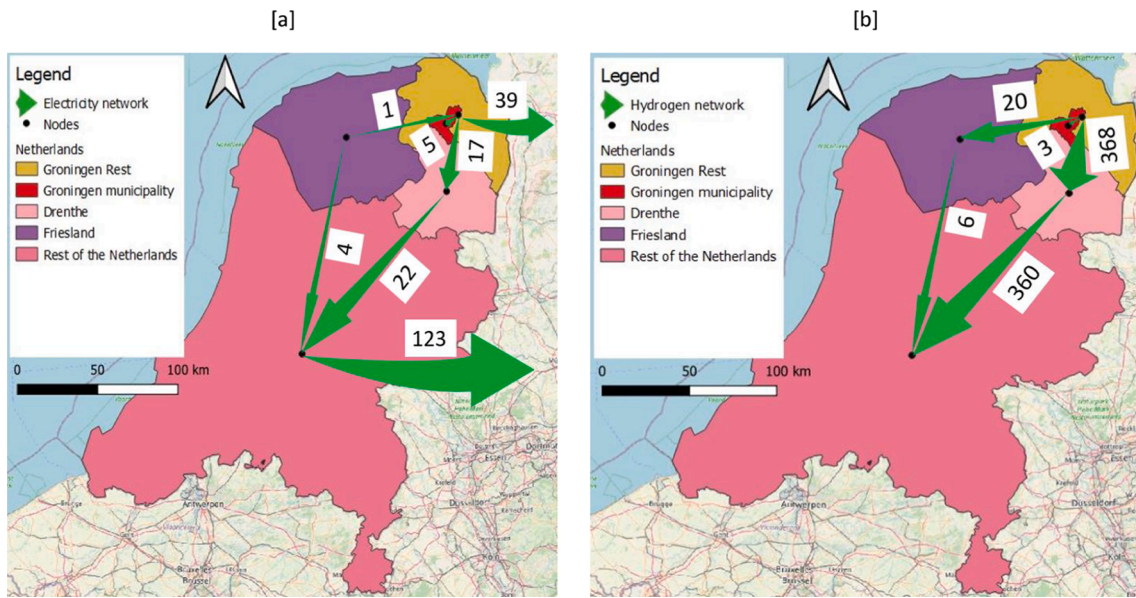
Fig. 21. Inter-nodal flows of electricity and hydrogen (all data in PJ). [a] and [b] present electricity and H_2 network flows, respectively.
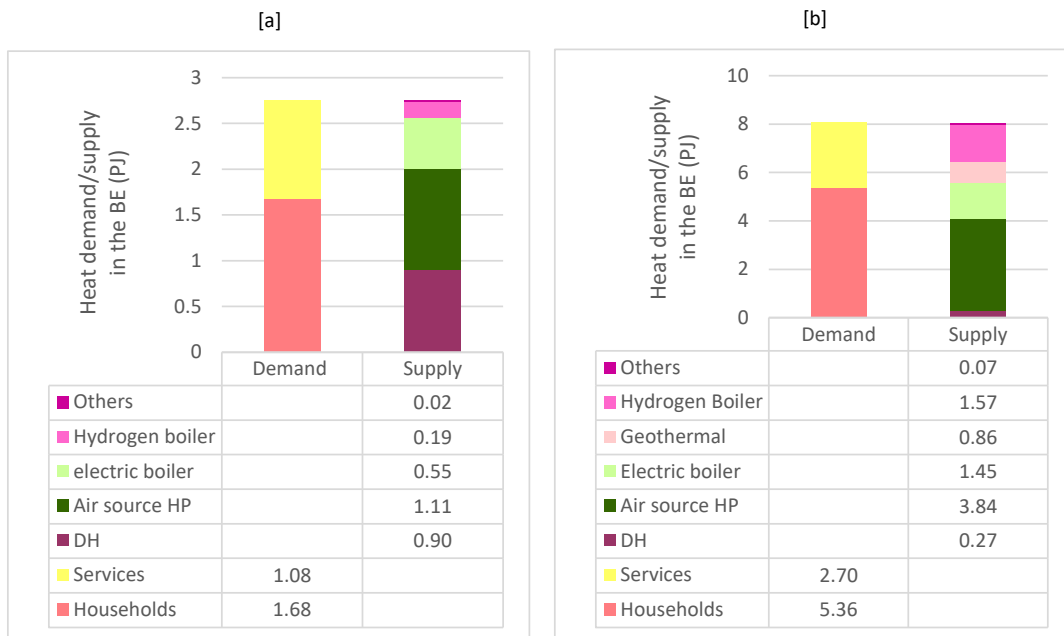

Fig. 22. Heat demand and supply comparison of the BE between GM and GR to understand the impact of modeling a DH network at a city or municipality level in the multi-node model (all data in PJ). [a] shows GM and [b] depicts GR. The left bar in each diagram presents end-use heat demand sectors and right bar presents the heat supply-related options.

the FBI. Drenthe and Friesland were ranked after GR, having equal demands of 3 PJ. The utilization of sewage sludge and biogenic waste was negligible in the NNL compared with the RNL. There was no demand for sugar and starch for bioethanol production. Similarly, there was no demand for vegetable, fruit, and garden (VFG) waste-related biomass for energy production. Similar to wind, allocated biomass potential is fully utilized as biomass can be cost-effectively used in different applications.

As shown in the Fig. 9 [d], the demand for geothermal energy in the FBI industries in the NNL was high and varied. The geothermal energy supplies to just the FBI industries in Drenthe, Friesland, and GR were 3 PJ (82%), 2 PJ (78%), and 8 PJ (69%), respectively. Notably, a lack of demand undermined the potential of geothermal energy, especially in Friesland, despite this province having a relatively high share (23%) of

the entire country's geothermal energy supply. Overall, low utilization of geothermal supply reflect skewed distribution of geothermal supply leading to significant mismatch between demand and supply.

4.1.2. Secondary energy carriers

Of the secondary energy carriers, we explicitly analyzed the demand for and supply of heat, electricity, and H_2.

Heat

Because our model excluded inter-nodal heat transfer, heat was considered to be regionally balanced. Heat demand and supply shares varied among different sectors within the NNL in the multi-node model (Fig. 10). The BE accounted for high shares of the total heat demand in Drenthe (59% or 10 PJ), Friesland (60% or 12 PJ), and GM (60% or 3

PJ), and industry's share of the heat demand was the highest in the GR (72% or 23 PJ). Within the NNL, the supply of the geothermal energy was the highest (20 PJ), followed by air/electric HPs (18 PJ) and H_2 boilers (14 PJ).

Electricity

There were significant sectoral differences in electricity demands among nodes of the NNL in the multi-node model (Fig. 11). The energy sector comprised H_2, electricity, and NG supplies along with large-scale electricity production options. Within the NNL, electricity demands were the highest in the energy sector (701 PJ), followed by the industrial sector (36 PJ) and the BE (34 PJ). Of the NNL nodes in the multi-node model, GR had the highest electricity demand (734 PJ), followed by Friesland (30 PJ) and Drenthe (23 PJ). The demand of electricity within GR's energy sector was 697 PJ or 95% of its total share, and was predominantly associated with large-scale H_2 production. In GM, Friesland, and Drenthe, the maximum electricity demands were associated with the BE, with respective shares of 80% (4 PJ), 42% (13 PJ), and 43% (10 PJ). On the supply side, onshore wind-related technology option played a significant role in Drenthe, Friesland, and GR at 15 PJ, 29 PJ, and 44 PJ electricity supply, respectively. The contribution of offshore wind-related technology option to GR was very high (664 PJ). A comparison of the single- and multi-node models revealed that while the total electricity demands were similar, there were clear variations among sectors and technologies.

Hydrogen

There were significant differences in sectoral demands for H_2 between the national share in both the single- and multi-node models and the regional share in the NNL nodes in the multi-node model (Fig. 12 [a]). At the national level, the H_2 demand was significantly lower in the industrial and energy sectors in the multi-node model. Within the NNL, GR's energy sector had a high demand for H_2 (29 PJ or 79% of its total H_2 demand). This demand for H_2 was linked to H_2 admixing in the NG grid and its use in steam and gas turbines. Only two technology options supplied H_2: large-scale electrolyzers and electrolyzers linked to chlorine production (Fig. 12 [b]). Large-scale electrolyzers in GR produced a significant amount of H_2 (427 PJ out of a total of 528 PJ produced from this option in the Netherlands) in the multi-node model because of the availability of a substantial amount of electricity from offshore wind. Our analysis showing a greater role of H_2 in the NNL energy system conforms with the ongoing experiments to make Groningen the H_2 hub of the Netherlands or even northwest Europe [92].

4.1.3. Total energy system

Fig. 13 depicts Sankey diagram of the total energy system at the national level, and Fig. 14 focuses on GR. These Sankey diagrams clearly show that distinct regions can differ significantly from the national averages. For example, the wind energy supply changed from 46% of the total energy supply at the national level to 89% in GR. H_2 produced via intermediate steps from wind-based electricity played a more significant role in GR relative to the national level. Oil-based carriers had a negligible role in GR given the minor role of feedstock relative to the national total. Export of electricity and H_2 from GR were also higher compared with exports at the national scale.

4.2. Cost analysis

This section presents an overview of the total system cost, a disaggregation of system costs, and analyses of infrastructure costs.

An overview of the total system cost

In the OPERA modeling framework, the total system cost is the sum of total cost of individual options considering every sector. For a region, this cost is the sum of the total cost of all of the options within the region. Fig. 15 [a] depicts a comparison of the total system cost for the different nodes in the NNL using the single- and multi-node models. We calculated total system cost for a region in the single node by using population share, i.e. the number of people living in that region over total

population of the Netherlands. When comparing regions within the models, we found that the total system cost is almost similar for every region, except GR. The total system cost of GR in the multi-node model is €8.4 billion higher compared to the single-node model. The main reason for this difference is investment related to H_2 infrastructure and large-scale H_2 electrolyzers utilizing large amounts of electricity from the northern offshore part of the North Sea. It is important to note that a large portion of the North Sea is linked to GR in the multi-node model. Fig. 15 [b] presents a sector-wise breakdown of the total cost for every node in the NNL in the multi-node model. In GR, investments in renewables and related infrastructure within the energy sector accounted for most of the costs (€6.3 billion or 60% of the total cost in GR). Appendix I details total system cost breakdown into a variety of categories to further illustrate regional differences.

Infrastructure cost analyses

Because infrastructure is an important component of the total system cost at the national and nodal levels, we analyzed options relating to heat, H_2, NG, and electricity infrastructures (Fig. 16). The proportions of electricity network costs were 82% (€0.7 billion), 87% (€0.6 billion), 90% (€0.4 billion), and 83% (€0.7 billion) of the total infrastructure costs in Drenthe, Friesland, GM, and GR, respectively. The heat network cost in GM (€3 million) was related to the variable O&M cost associated with the heat distribution costs of the DH network.

4.3. Analysis of the built environment and industry in the NNL

This section presents detailed analyses of energy labels for the BE, energy savings for the BE and industries, and emission savings for industries. Appendix I presents the energy mixes for the BE and industries.

A comparison of energy levels of the optimized case compared to the reference case in the BE

Fig. 17 shows regional improvements in energy labels in the optimized model run compared to the reference case for the households and services buildings in the multi-node model. In the optimized case, all the household buildings were upgraded to the A + label for all of the nodes in the NNL, irrespective of the energy labels in the reference case (Fig. 17 [a]). The situation was different for services buildings. The buildings in the reference case were mostly GFE, DC, and B buildings for all of the nodes in the NNL, whereas in optimization case, DC, B, A, and A + buildings were predominant (Fig. 17 [b]). Thus, the optimized model run revealed improvements in energy labels for the overall BE throughout the NNL.

Energy savings in the BE and Industrial sectors

Fig. 18 [a] and [b] show that 'other dwellings' were responsible for most of the energy savings in the BE, with reductions in energy demands evident in all regions in the optimized model run compared to those in the reference case. Fig. 18 [c] depicts changes in the energy carriers in the optimized model run along with reductions in the energy demands in all of the nodes in the NNL. To illustrate reduction in the energy demands, the heat and electricity demands for manufacturing dairy products fell from 9 PJ and 0.3 PJ, respectively, to 3.2 PJ and 0.64 PJ, respectively, resulting in a total energy saving of 5.3 PJ. Similarly, the primary aluminum industry in GR evidenced electricity savings of 2 PJ in the optimum model run compared with the reference case. The application of detailed modeling and analysis of the BE and industries results in a better understanding of energy saving potentials of these sectors.

Emission savings in industries

Changes in energy carriers and reductions in energy demands of industries reduced their CO_2 emissions in the optimized model run relative to the reference case (Fig. 19). For example, emissions from both salt and dairy industries in Friesland drop from 0.2 $MtCO_2$-equivalent to 0.01 $MtCO_2$-equivalent for the salt industry and to almost zero for the dairy industry.

The construction of regional nodes enabled us to perform a more fine-tuned analysis of the savings potential of the BE and industries. Our

analyses of the BE and industries revealed significant differences in regional energy demands for these sectors. Additionally, we were able to analyze industries that are not considered high-energy demanding industries from the perspective of a national energy system but are important for the NNL and to identify emission savings associated with the reduced energy demands of industries.

4.4. Understanding the impacts of supply-side options through sensitivity analysis

Table 2 shows the topics selected for sensitivity analyses. Our optimized modeling was aimed at minimizing total system costs, which is generally a priority objective in any modeling exercise. Accordingly, we conducted sensitivity analyses of the total system cost of the NNL (Fig. 20 [a]). Other policy-relevant topics, notably the contribution of the northern offshore wind, H_2 production through large-scale electrolyzers in the NNL, and H_2 flow through the corresponding network from the NNL to the RNL were also included in sensitivity analyses (see Fig. 20 [b], [c], and [d], respectively). We performed all these analyses in the multi-node model.

Of particular note is the finding that the doubling of the onshore wind capacity in all of the regions (case C1) resulted in a decrease in both the contribution of the northern offshore wind (-279 PJ, Fig. 20 [b]) and in the total system cost (€-3 billion, Fig. 20 [a]) compared to the reference scenario. Currently, there is strong opposition to such onshore wind farms, particularly in Groningen Province. The real world application of this result is to make policy makers aware of the future financial benefits of having large onshore wind farms.

Doubling woody biomass (C5) resulted in a decrease in both the northern offshore wind contribution (-121 PJ) and the total system cost (€-1 billion). Case C7 showed a decrease in both the total system cost (€-1.2 billion) and the contribution of the northern offshore wind (-71.4 PJ) resulting from an increase in the contribution of the onshore wind.

Our analysis of H_2, revealed that large-scale H_2 electrolyzers, particularly in GR, created an extensive flow of H_2 from the NNL to the RNL. Our sensitivity analyses showed that H_2 production by large-scale electrolyzers (Fig. 20 [c]) and the H_2 flow to RNL (Fig. 20 [d]) decreased in all of the sensitivity cases, notably in case C1. An exception was the reduction in woody biomass (C6), which resulted in a modest increase in H_2 production.

4.5. Network infrastructure and inter-nodal flows

Flows of major energy carriers, such as electricity and H_2, between regions through their network infrastructures are created through mismatches between regions in the primary and secondary energy mix, differences in sectoral energy demands, and the utilization of renewables. This section presents an analysis of electricity and H_2 network inter-nodal flows in the Netherlands (4.5.1) and the impact of the DH network in GM (4.5.2).

4.5.1. Electricity and hydrogen

We observed a flow of electricity from GR to Drenthe (17 PJ) and GM (5 PJ) (Fig. 21 [a]). Moreover, Drenthe produced more electricity than it consumed. Therefore, the oversupply flowed to the RNL (22 PJ). Net exports of electricity to other countries from the NNL occurred via GR (39 PJ). Net supplies of electricity from Friesland to GR and the RNL were 1 PJ and 4 PJ, respectively. Fig. 21 [b] shows a substantial flow of H_2 from GR to Drenthe (368 PJ) and subsequently to the RNL (360 PJ). This large amount of H_2 was mainly produced by large-scale H_2 electrolyzers in GR. GR also supplied H_2 to Friesland (20 PJ) and ultimately to the RNL (6 PJ) via another route (see Fig. 7). Compared with electricity and H_2 flows, the flow of NG is negligible between regions of the NNL.

4.5.2. The impact of district heating in GM

To acquire a better understanding of the impacts of DH modeling at the city/municipality level within a regionalized model, we compared the heat demand and supply within the BE in GM, where we applied a customized DH network, with the application of the standard existing heat network in GR in the multi-node model (Fig. 22). Fig. 22 [a] shows that DH will provide 33% of the heat demand of the BE in GM in 2050 under optimized conditions. However, Fig. 22 [b] shows that DH only supplies 3% of the BE's heat demand in GR. The DH penetration of GM is remarkable given that a DH network is currently almost non-existent [52]. Thus, creating GM within the regionalized model enabled us to conduct a fine-tuned analysis of the impacts of a DH network at the municipality level. This analysis reflects the originality and usefulness of our study.

The results clearly show the advantages of detailed regional modeling compared to a national average or aggregated representation of a country. Depending upon the atypical attributes of different regions, modelers can highlight differences in primary energy use, energy balance of secondary energy carriers, energy saving potentials of the BE and industries, investments in infrastructure, and inter-regional flows. Results can show whether capacity and energy potential of renewables are underutilized, whether capacity additions are required for energy infrastructures and to what extent, and whether DH networks are cost-effective to implement. Other interesting results are the possibilities to understand the role of the building stock characteristics, i.e. buildings types and energy labels, and its distribution in determining the BE energy saving potentials. Similarly, regional energy savings and emission reductions can depend upon existing processes, alternative processes and their costs, and projected final main products demand. The amount of energy carriers flow in various energy infrastructures can highlight regional mismatches between energy demand and supply, and regional renewable potentials.

5. Discussion

Here, we critically analyze our methodology and findings, focusing on four key topics: the economic structure, the built environment (BE) and industries, renewable potential, and energy infrastructures. Additionally, we compare with previous studies and discuss the possibilities of other regional analysis with our method.

We discuss three considerations regarding the economic structure. First, we assumed that uniform normalized prices applied to energy label upgrades in the BE for all nodes in the multi-node model. However, these costs depend on other regional macroeconomic considerations, such as income levels and economic activities. Second, the NNL's shares of the national total for most economic activities are low, ranging between 8% and 13% of the national total. Third, the default design of the OPERA modeling framework population-based regional allocation for aspects such as technology options, energy carriers, and activities. While we adapted these allocations for most of the key economic activities based on relevant spatial parameters, we did not change default allocations for some of the (less important) aspects. Furthermore, we assumed that the current relative regional shares of demand or supply potentials for activities would remain the same in the future, which may not actually be the case.

When considering the BE, we found that no data were available energy labels for most building types at the regional level. Hence, we assumed that the distribution share was the same for different building types, except for offices, in all regions. In reality, the energy labels of buildings can differ significantly among regions, and our results may not reflect optimized energy labels for buildings in 2050. Furthermore, we applied the same normalized heat demand per building type per region, whereas in reality the heat demand in the NNL may be higher than the heat demand in the southwestern part of the Netherlands given lower outdoor temperatures in the former region. Additionally, we did not consider explicit demand profiles for different building types and

regions because of the lack of relevant data. These profiles can have a major effect on the energy balance and role of technology options in the BE. Among the industries, the dairy industry's energy demand were normalized with respect to a standard type of product, namely milk powder. However, as for potato products, energy demands for different types of dairy products, such as butter and milk powder, vary significantly [37]. For uncategorized activities every industrial subsector, we allocated regional energy demands based on CO_2 emissions, which may not have been completely accurate.

Most literature on regional studies are related to future renewables potentials and comparable to our modeling inputs or results. Van der Niet *et al.* [93] considered onshore wind capacity potential ranges of 0.6–1.7 GW and 0.2–0.9 GW for 2050 in Groningen and Drenthe, respectively, which are similar to our corresponding potential input of 2.2 GW and 0.8 GW, respectively. A Groningen Province report [94] estimates a future potential contribution of 7.2 PJ from solar PV. This value is close to our results which showed a cumulative solar PV contribution of 7 PJ in Groningen Province.

In our analysis of renewables, we considered land dedicated to different sectors to estimate regional shares for small-scale solar PVs. This allocation may have resulted in errors, as not all spaces allocated to different sectors may be equally suitable for PV integration. Moreover, the use or potential use of such spaces may differ significantly among regions depending on regional and national policy choices. Similarly, in the case of onshore wind, we considered the regional distribution shares based on short-term regional targets [79]. However, long-term onshore spatial allocations for wind energy are strongly dependent on policy choices. In the case of geothermal energy, we considered a GIS layer, which denotes the technical potential, i.e. with the present technology how much geothermal energy can be extracted, for allocating shares of geothermal energy among regions. In reality, the actual available geothermal share may be less than this potential. In addition, we did not adequately represent shallow and deep geothermal energy in this study, as we used the same allocation shares for both.

A further limitation of our study was that we did not consider competition over space among different activities when estimating renewable potentials. Multiple activities can coexist within the same space but with important constraints. For example, solar PV can only be partially integrated into agricultural land or the BE, and wind farms may easily coexist with agricultural land but not with the BE. Given that there are spatial constraints, particularly in a densely populated country such as the Netherlands, it is advisable to account for such constraints when modeling a regional energy system.

We applied the same network infrastructure for electricity, H_2, and NG, which does match the reality. In addition, we provided a fixed value of allocation shares for the network capacity for electricity transmission between the Netherlands and other countries, and for electricity transmission within the Netherlands, which may not be applicable in the future. For the demand and supply of heat, wind energy, and geothermal energy that are characterized by considerable spatial variations, a much higher geographical resolution is required to capture spatial variability and potential. In addition, our geographical resolution was too low to conduct an analysis of heat transmission, given that heat networks are associated with high losses and low energy density. We only analyzed the role of DH in GM by calculating heat distribution cost at a municipality level. However, in reality, this cost can differ within different parts of a city [49]. In addition, for other regions we could not impose this cost because of significant differences in heat demand densities within those regions. Our method can be shifted to other regional analyses. For example, equations and methods related to creating and constraining energy infrastructures can be easily adapted based on data availability. Similarly, the BE and industries spatial distribution and energy demand differences can be represented by building types, maybe with energy labels, and industrial activities or processes, respectively. Regional renewable potentials and sectoral allocations can be performed based on our identified spatially sensitive parameters.

6. Conclusions and future research

We conducted an integrated energy system analysis for the northern part of the Netherlands (NNL) using an existing national energy system optimization model Options Portfolio for Emission Reduction Assessment or OPERA. By embedding the NNL within a national model, we avoided the need to make critical assumptions about national targets, resource availability, and secondary energy prices. Our modeling was based on four themes: the regional economic structure, modeling modifications of the built environment and industries, regional potential or capacity allocation of renewables, and the creation of energy infrastructures. We created a multi-node model, entailing regional or nodal allocation and compared it with a national model that did not include regional allocation. Our results showed significant differences in energy balances between models at the national level and between nodes in the multi-node model. Among renewables, we considered wind, solar, geothermal, and biomass options. We performed sensitivity analyses for renewables because the potential of these options vary according to the availability of space and future policy making. Significant modeling results included the generation of a significant amount of hydrogen (H_2) from offshore wind, i.e. 620 Peta Joule (PJ), in Groningen Province and the transmission of substantial volume of H_2 to the rest of the Netherlands (390 PJ). Additionally, the total renewable energy share in the primary energy mix of the northern region is ~90% or more compared to ~70% for the rest of the Netherlands.

Our multi-nodal approach, entailing the use of just five nodes, revealed the significant impacts of spatial parameters on outputs from different technology options. We were able to represent regional differences in available energy sources and their potentials or constraints by integrating important spatial parameters within our modeling framework. Our approach is applicable to other regional energy system analysis contexts for investigating regional energy infrastructure and landscape, as well as for suggesting policy implications regarding regional energy-related planning and decision-making. We will therefore continue to develop and refine our modeling framework to address more complicated spatial issues, such as multiple competing land-use claims, through the inclusion of geographical information system-based analyses. Additionally, by making our framework more interactive, we expect to generate direct inputs for policy makers and other stakeholders regarding the impacts of current choices on the future energy system.

Target Audience: Energy system modelers and analysts

CRediT authorship contribution statement

Somadutta Sahoo: Conceptualization, Methodology, Software, Formal analysis, Data curation, Writing – original draft, Writing – review & editing. **Joost N.P. van Stralen:** Methodology, Software, Writing – review & editing. **Christian Zuidema:** Writing – review & editing, Supervision. **Jos Sijm:** Writing – review & editing, Supervision. **Claudia Yamu:** Writing – review & editing, Supervision. **André Faaij:** Methodology, Writing – review & editing, Supervision, Project administration, Funding acquisition.

Declaration of Competing Interest

The authors declare that they have no known competing financial interests or personal relationships that could have appeared to influence the work reported in this paper.

Acknowledgements

Appendix A. OPERA

OPERA model description

OPERA (Option Portfolio for Emissions Reduction Assessment) was developed by the Energy research Center of the Netherlands (ECN) for analysis of the Dutch energy system. OPERA is a bottom-up, technology rich, optimization based techno-economic model of the entire energy system of the Netherlands. It offers high temporal resolution as compared to other similar national energy system models. It covers the entire range of GHG and particulate emissions, and is thus suitable for assessment of future low carbon energy systems. It specifically considers the impact of energy efficiency improvement, technology diffusions and a broad range of policy interventions. Therefore, the model is already extensively used for climate change mitigation and policy advice on energy decarbonization for the Dutch government [58,95]. This model determines the configuration and operation of the energy system combined with other sources of emissions to meet all system requirements, whether market driven or policy imposed at minimum energy system cost [10].

OPERA does not optimize over a time horizon. Rather, it looks into specific years of importance, such as 2030 and 2050. In OPERA, the price of future technologies is not modelled endogenously with using learning curves. Technology options present in the National Energy Outlook (NEO) are used to represent the business-as-usual scenario in OPERA. For these technologies, information regarding input/output characteristics are extracted from the NEO. They remain as option for other scenarios as well. Technologies which are rather new, for example technologies related to power-to-liquids, are not part of NEO and characteristics on these technologies come from sectoral experts. Techno-economic data of many of such new technologies is extracted from factsheets from the website www.energy.nl [96]. In addition, for specific technologies like wind energy, where costs will change a lot over the time horizon, cost reduction is included in different scenarios within OPERA. For other technologies or energy carriers where the future is highly uncertain, OPERA provides the possibility to perform a sensitivity analysis. Examples are sensitivity analyses on biomass price, amount of CCS in the future system, social issues associated with availability of nuclear energy and wind availability both onshore and offshore.

In OPERA, a set of sectors is identified and a set of technology options is assigned to each sector to satisfy the sectoral electricity and heat demand. From NEO, it receives the information on total emissions, energy service demand per sector, conversion characteristics of technologies used, volume and capacities of technologies and prices of primary energy carriers. Furthermore for electricity, H2, NG and heat, the user can allow all explicit connections within a sector, i.e. individual supply options are connected to all individual demand option for a particular energy carrier. Alternatively, supply and demand options are connected to each other via a central connection point, instead of direct links between all possible individual options within a sector. This is useful for several energy carriers, namely heat, electricity, and NG. However, for H2, the connections are explicit. In reality also, H2 flow is more sequential as compared to other energy carriers.

OPERA structure detailed description

Fig. A.1 represents a generic flowchart indicating interactions between and within different sectors, i.e. sectoral coupling over different transmission grids. The flow of energy is from primary energy carriers to different sectors having technology options to convert to either an intermediate
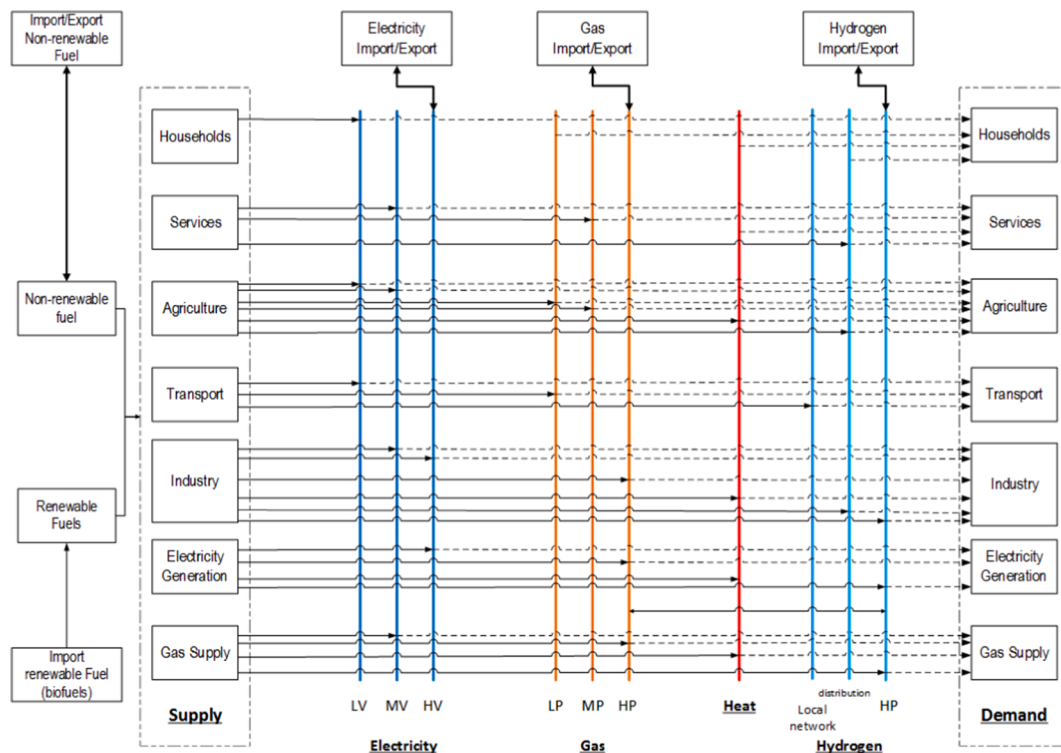

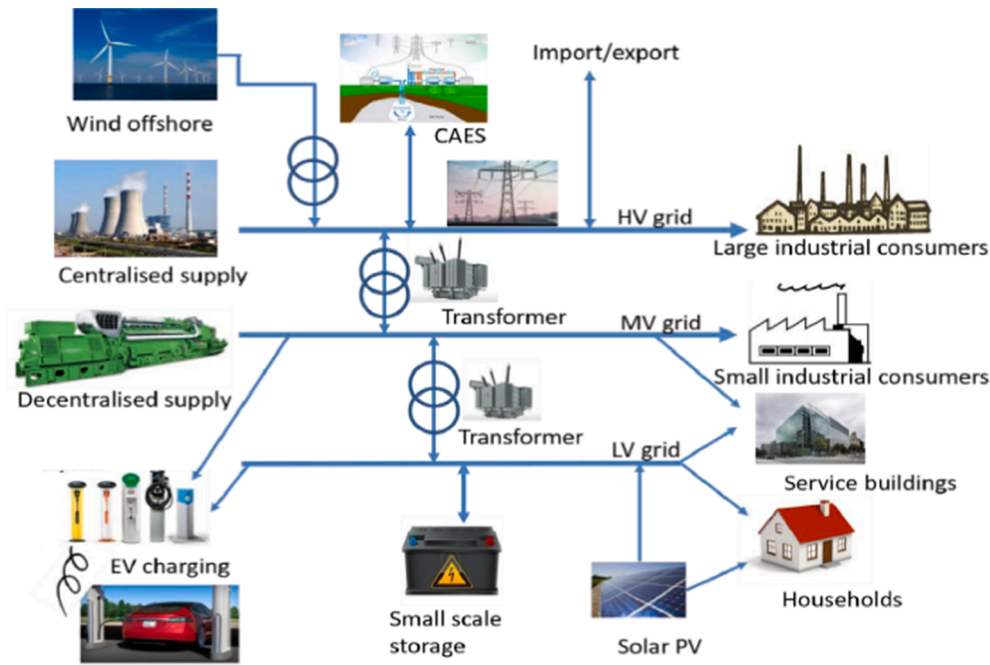**Fig. A.1.** Schematics of OPERA.

Fig. A.2. Electricity sector schematics in OPERA [32].

energy carrier or a final energy carrier within the sector, before being carried to the transmission grid. The other end of the transmission grid is the demand sector, utilizing energy coming from the grid, either as some intermediary energy carrier or as final energy use. The general assumption for making Fig. A.1 is sectoral interactions occur via the grid infrastructure, i.e. supply and demand are connected via a node. In this case, the sector supplying energy is present on the supply side and the sector receiving energy is represented on the demand side. Intermediary processes or feedstocks representation within/between different sectors are not represented for clarity purposes. The figure shows all the sectors on both the supply and demand side. The supply side sectors use primary energy sources that are further subdivided into non-renewable and renewable sources. Non-renewable fuels in this context are mainly coal, NG, gasoline, and uranium and renewable sources are mainly wind, solar, biomass, and geothermal. The gas grid represents all the gases, such as NG, bio-methane or synthetic natural gas (SNG). OPERA has a separate H_2 grid because in the Dutch context, the future contribution from H_2 is likely to expand [97]. In addition, OPERA provides the possibility of admixing H_2 and NG. The H_2 network is well represented in OPERA with three levels: a) a high pressure distribution network (HP (H_2)); b) a low pressure distribution network (DN); and c) a local network corresponding to H_2 filling stations (FS). OPERA considers different GHGs, air pollutants, and several system and user defined constraints. Heat is represented by one generic energy carrier.

In general, some reference technology options from the NEO are available for all sectors in OPERA. In addition, combining additional technological options is possible that can result in lowering GHG emissions for different sectors in different scenarios. Thus, OPERA provides an opportunity for new technologies to compete with reference technologies for the analysis of different future scenarios. Since OPERA has a technology portfolio to choose from, many technologies may not be selected, as those are not cost effective. However, the technologies just above the margin are also important and a little technology push or suitable policy might make them cost effective. Energy saving and emission reduction options can be achieved by improvements in the energy labels of different building types within the built environment (BE). Additionally, electricity-related savings can be achieved by the use of efficient equipment in BE. Similarly, for several industrial activities, savings are achieved by replacing the reference process by a more efficient process. These processes can also achieve emission savings. In (almost) all the sectors, energy savings can be applied based on the energy savings potential of the sector as a whole.

Table A.1 provide important sectoral attributes and their technology options in OPERA. Detailed sector-wise description of the OPERA model follows:

a.1) Households

Currently, in OPERA the housing sector is subdivided into three dwelling types: apartments, terraced houses, and other dwellings. These dwellings types are independent activities with million housing or 'Mh' as their unit to represent heat demand. Every dwelling type is again constituted of five different energy labels: GFE, DC, B, A, and A+. Households provide the possibility to supply electricity to the LV grid for electricity (such as, through solar PVs) – refer Fig. A.1. On the demand side, OPERA allows electricity, gas, heat, and H_2 requirements to be fulfilled from the LV, low pressure (LP) grid of gas, heat, and DN grid of H_2, respectively. Furthermore, there are electricity saving options related to efficient equipment. The unit of remaining final energy demand is PJ.

a.2) Services

Similar to the housing sector, the services sector is constituted of five service building types: offices, education, industrial halls, hospitals, and rest service buildings. Each building type has square kilometer of gross floor area or 'km^2' as their unit independent activity to represent heat demand.

Again, similar to the households sector, every service building type is constituted of five different energy labels: GFE, DC, B, A, and A+.

Sector-specific technology options include boilers (solar, geothermal, NG, hybrid with NG and air), micro-CHP (H_2, NG), and HP (ground source). In addition, service sector includes electricity saving options, such as halogen to compact fluorescent lamp and presence detection. In addition, mobile machinery (electric, hybrid) is also part of the sector. On the supply side, gas, electricity, heat, and H_2 are connected to the HP (gas), MV, heat, and DN transmission grids respectively. Furthermore, gas, electricity, heat and H_2 are constrained to not flow outside the sector. The unit of remaining final energy demand is PJ.

a.3) Agriculture

In OPERA, this sector includes activities and technology options related to crop production and livestock. Some examples of such technology options in agriculture are manure digestion, geothermal, CHPs, HPs and boilers. This sector is sub-divided into two major parts: a) horticulture and related technology options, which is a major crop cultivation activity in the Netherlands; and b) other crop cultivation and livestock including energy savings and emission reduction options. Some examples of emission reduction options considered in OPERA are precision fertilization, lifetime extension of dairy products and lowering protein content of grass.

Technology options, such as CHPs related to horticulture are connected to the MV grid so as to provide a possibility of supplying excess electricity to the electricity grid. The presence of large CHPs in horticulture within the agriculture sector results in the supply of electricity and H_2 through MV and DN grid, respectively. However, other parts of agriculture, which do not need large quantities of heat or electricity are connected to the LV and LP network of electricity and gas grid, respectively. In OPERA, mobile machinery are associated with energy saving options. The unit of final energy demand for both agriculture and mobile machinery is PJ.

a.4) Mobility

In OPERA, road transportation is provided by different varieties of cars, e-cars, plug-in vehicles, light-duty vehicles, such as vans and heavy-duty vehicles, such as trucks (with NG and H_2). Local transport modes, such as metro, bus, and tram are aggregated with national transport modes, such as rail and inland navigation, i.e. movement by each of these transport mode is not explicitly represented because of their low energy consumption. For example, energy consumption associated with rail movement is quite low, i.e. around 1% in 2017 of the total sectoral energy demand [98]. Other aggregated options are movement by motorcycles and inland navigation. Thus, OPERA includes all the transport technology options present in NEO. In OPERA, some energy savings and emission reduction options are included, such as drag reduction and rolling resistance reduction in trucks. The unit of demand is 'billion_vehicle_km' or Bvkm for passenger movement, namely cars and vans, and freight movement, namely trucks. For the remaining part of the transport sector, the unit is PJ[1].

Table A.1
Description of all the sectors and their important technology options in OPERA.

Sectors	Description	Technology options
Households	- Dwellings are subdivided into apartments, terraced houses, and other dwellings - Each dwelling type is further subdivided into five energy labels: GFE, DC, B, A, and A+ - Unit of activity is million houses (Mh) to account for heat demand in dwellings - Unit of remaining final energy demand is peta joule (PJ)	- micro-combined heat and power (CHP), solar thermal, boiler, geothermal, and heat pumps (HPs) - Solar PV and micro-CHP - Electricity saving options,[a] such as wash-dryers, and dishwashers
Services	- Service buildings are subdivided into offices, education, industrial halls, hospitals, and rest service buildings - Each service building type is further subdivided into five energy labels: GFE, DC, B, A, and A+ - Unit of activity is gross floor area measured in km^2 to account for heat demand in service buildings - Unit of remaining final energy demand is peta joule (PJ)	- micro-CHP, solar thermal, boiler, geothermal, and HPs - Solar PV and micro-CHP - Electricity saving options
Agriculture	- Separate representation for horticulture, and other agriculture - Includes livestock - Unit of measurement is PJ for both subsectors	- CHPs, boilers, manure digestion technologies, and mobile machinery - Energy saving and emission reduction options
Mobility	- Explicit representation of each of road passenger cars, road freight trucks, road passenger vans and the rest of the vehicle fleet - Cars, vans, and trucks are represented with billion-vehicle-km as the standard unit and the rest of the mobility modes are aggregated with PJ as the driving force - Includes infrastructures related to H_2 (filling station), and EVs (charging station, vehicle itself)	- cars, such as electric, H_2, hybrid, and biofuel - Vans and freight, such as H_2 - Trucks, such as NG and H_2 - Standard fuel driven remaining vehicle fleet - Energy saving options
Industry	- Separate subsector representation for base metal (steel and aluminum), fertilizers (ammonia), chemicals (chloro-alkali, salt, and high value chemicals), food and beverage industries (sugar, potato products, dairy products), rest ETS industries, and rest non-ETS industries - steel, aluminum, fertilizer, salt, chlorine, dairy products, potato products, and sugar production is expressed as million ton (Mt) of final product and rest of the sub-sectoral activities including remaining final energy demand of different subsectors are represented by PJ	- Boilers, HPs, CHPs, - Other technology specific options - Energy saving and emission reduction options
Electricity	- For high voltage (HV), capacity and network-related constraints are included, including losses - Includes lump-sum infrastructure costs related to medium voltage (MV) and low voltage (LV) grid - Unit of measurement is PJ	- battery storage - large-scale wind (onshore and offshore), and solar (onshore) - Centralized plants with CCS option and nuclear
Gas	- For high pressure (HP) network of NG and H_2, capacity and network-related constraints are included, including losses - Includes lump-sum infrastructure costs related to medium pressure (MP) and low pressure (LP) pipelines for NG, and distribution and local network for H_2 - Unit of measurement is PJ	- H_2 (coal and biomass gasification, methanation, and electrolysis) - Green gas (manure digestion, and biomass gasification)

[a] In OPERA model, savings of energy is treated in a way that is similar to energy production

---

[1] Only cars, vans, and trucks movements are individually balanced, i.e. demand in 'billion_vehicle_km' for each of these movement type is explicitly met by different supply options. These movement modes are individually represented because they contribute to a large energy consumption and emission within the sector. However, for the remaining movement within the transport sector, the demand is aggregated and different supply options can meet the demand.

a.5) Industry

The industry sector within OPERA is split into the following subsectors: a) base metal (includes iron/steel and primary aluminum); b) chemicals (chloro-alkali, salt, and high value chemicals); c) refineries; d) fertilizers (such as ammonia); e) food and beverage industries (dairy products, potato products, and sugar); f) other Emission Trading System (ETS) includes waste incineration and the remaining part of the industry that fall under the ETS category; and g) non ETS includes remaining part of the industry that does not fall under the ETS system.

In the current OPERA structure, base metal is connected to HP (gas), HV, heat and HP (H_2) grid both for supply and demand side. Refineries, fertilizers, and other ETS industries follow the same connection pattern. However, food and beverage industries and non-ETS industries are connected to MV instead of HV and rest of the connections are the same as other sub-categories. Currently, the unit of final energy demand for steel, aluminum, fertilizer, salt, chlorine, high value chemicals, dairy products, potato products, and sugar production is expressed as million ton (Mt) of final product. The remaining industrial subsectors include PJ as the unit of final energy demand.

a.6) Power generation

The electricity generation sector includes existing power plants, in particular coal, gas, biomass and nuclear power plants. Technology options also include biomass and coal gasification, wind onshore and offshore, solar PVs, geothermal and storage options (such as batteries, compressed air energy storage , and Superconducting magnetic energy storage (CAES)). OPERA has a representation of different grid networks along with transformers (refer Fig. A.2)[2]. Network and transmission-related losses are considered for the high voltage grid, but not for medium and low voltage grid. This sector additionally includes CCS options along with some of the above-mentioned technologies. Sectoral unit energy demand is expressed in PJ.

a.7) Gas supply

Similar to the power generation sector, this sector includes the option of LP (gas), MP (gas) and HP (gas) for low, medium and high pressure network, respectively, and transformers for changing pressure levels as a part of network infrastructure[3]. This sector also includes H_2 related technology options, such as methanation, and electrolysis. The H_2 infrastructure includes HP (H_2), distribution grids, and local network.

Appendix B. Detailed description of analyzed regions and OPERA modeling changes

B.1) Detailed description of analyzed region

Our analyzed region is the northern part of the Netherlands (NNL). The region has a total area of 8,300 km^2, accommodating 1.8 million inhabitants (10% of the Dutch population), with a population density of just over 200 person/km^2, which is modest by Dutch standards. Other Important atypical features of the region include (see also Fig. 2):

- Industry: The region is rich in food and beverage industries, including dairy products, potato products, and sugar, compared to the rest of the Netherlands (RNL) [37]. In addition, the NNL has a few chemical industries such as chloro-alkali and salt [37]. Among basic metal industries, the region is the only producer of primary aluminum [37]. However, it lacks other major industries such as petrochemicals, high value chemicals, and other basic metal industries [39–42].
- Energy: The region is characterized by a high average wind speed [39,40] and a modest population density, which provide favorable conditions for establishing wind farms (Fig. 2 [c]). In addition, the region has significant potential for geothermal energy production [42] (Fig. 2 [d]) and large-scale solar PV systems [43]. It is also connected to a large offshore section of the North Sea which is also characterized by high wind speeds [99].

B.2) Detailed OPERA modeling changes
The Built environment modeling

OPERA had Peta Joule (PJ) as the measure of unit activity, i.e. sectoral driving force, for households and services. As the number of houses is a more appropriate measure of dwellings, we changed the unit activity to "millions housing" (Mh). Therefore, the model now needs to meet a certain number of Mh demand (input parameter) to achieve convergence. Given that service buildings occupy a much larger area than residential buildings, floor area is an appropriate measure of sectoral activity. Therefore, we introduced km^2 of gross floor area (GFA) as the unit of activity for service buildings.

We introduced new building types and energy labels in OPERA. In line with these changes, we introduced the following new modeling equations in OPERA. The symbols used in the equations (B.1)–(B.3) are defined in Table B.1.

$$\sum_l DW_{n,dt,l} = \mathbf{DW}_{n,dt} \quad \forall n, \ dt, \tag{B.1}$$

Table B.1
Definitions of variables, parameters, and indices used in the equations (B.1)–(B.3).

Index		Variable	
n	regions/nodes	DW	the number of dwellings or GFA of service buildings at a particular energy label, l
dt	building types	D	energy demand
l	energy labels	Parameter	
t	time slice	$\mathbf{DW}$	the total number of dwellings expressed in 'Mh' or GFA of service buildings expressed in 'km^2'
c	energy carrier	$\mathbf{NE}$	normalized heat demand per household building or per km^2 of service building
i	change in energy label	$\mathbf{M}$	a matrix with rows representing current energy label and columns representing energy use associated with improved energy label
		$\mathbf{DW}_r^{reference}$	DW_r in the reference case

---

[2] For HV only, the model considers capacity and transmission related constraints, including losses. The connections between regions is through nodes.

[3] Similar to the electricity sector, the gas sector can consider transmission and capacity constraints related to HP grid network. Currently, this grid does not implement constraints as the capacity of the gas network is already over-dimensioned in the Netherlands.

$$D_{t,n,dt,l,c} = \mathbf{NE}_{t,n,dt,l,c} * DW_{n,dt,l} \quad \forall t, \ n, \ dt, \ l, \ c, \ \text{and} \tag{B.2}$$

$$\sum_{l,i} DW_{n,dt,l} * \mathbf{M}_{l,i} \leq \sum_{i} \mathbf{DW}_{n,dt}^{reference} * M_{l,i} \quad \forall n, \ dt, \tag{B.3}$$

Industries

We introduced new industrial subsectors with their new activities expressed in million tons (Mt) of final main product, as these units of activities are more appropriate measures of the final products stock or demand than the final energy demand. For example, the activity unit for chloro-alkali is Mt of gaseous chlorine.

For industries, we added the following equations in the OPERA model related to new activities or industrial subsectors addition:

$$\sum_{pa} FP_{n,pa,a} = \mathbf{FP}_{n,a} \quad \forall n, \ a, \ \text{and} \tag{B.4}$$

$$D_{t,n,c,a} = \sum_{pa} \mathbf{EP}_{t,n,c,a,pa} * FP_{n,pa,a} \quad \forall t, \ n, \ c, \ a, \tag{B.5}$$

where *pa* and *a* (indices) respectively denote a process within an activity and the activity itself. *FP* (variable) is the final product produced by a process and **FP** (parameter) is the projected final product demand. *D* (variable) is the energy demand associated of an activity. **EP** (parameter) denotes the energy demand of the process.

After we have allocated energy demands to different industrial activities, mainly related to new industrial subsector creation, we allocated both heat and electricity demands (in PJ) to the remaining activities for every industrial subsector (refer Fig. 6). For this purpose, we used the Dutch Emissions authority (NEa in Dutch) database [100]. This database provides information on current carbon dioxide (CO_2) emissions information of industries in the Netherlands. First, we segregated industrial activities in the NEa database based on the industrial subsectors and activities in OPERA. We then categorized the remaining industries that were not part of any explicit OPERA activities in the database into one of the industrial subsectors and grouped them by regions in OPERA. Lastly, we aggregated the CO_2 emissions of industries within a region and a subsector and allocated regional energy demands to the remaining subsector activities based on their share of regional CO_2 emissions (see also Fig. 6). Data on national energy demands of these activities were derived from our scenario (see Table 5).

Other activities

For agriculture, the regional allocation of sectoral energy demands and related mobile machinery (both of which has PJ as the unit of activity) was based on land use for horticulture. For mobility, we calculated the regional share of activities for passenger cars, light duty vehicles, and heavy duty vehicles by the same unit activity. All these activities have their standard unit described in billion vehicle kilometer (Bvkm).

Appendix C. Database related to household and service buildings or the BE

For service buildings, our building type categorization are offices, education, industrial halls, hospitals, and others. For households buildings, our building type categorization are apartments, terraced buildings, and other dwellings. The common energy label categorization for all BE building

Table C.1
Service buildings shell improvement costs compared to GFE label (€/m² GFA) [36].

Energy label	Service buildings shell improvement costs compared to GFE label (€/m² GFA)				
	Offices	Education	Industrial halls	Hospitals	Others
DC	25	30	20	30	30
B	115	135	80	135	135
A	140	165	105	165	165
A+	170	195	125	190	195

Table C.2
Service buildings normalized heat demand for each energy label (GJ/m² GFA) [36].

Energy label	Service buildings normalized heat demand (GJ/m² GFA)				
	Offices	Education	Industrial halls	Hospitals	Others
GFE	0.783	0.386	0.322	0.825	0.571
DC	0.373	0.201	0.161	0.446	0.303
B	0.293	0.16	0.128	0.383	0.255
A	0.218	0.12	0.096	0.293	0.19
A+	0.177	0.098	0.078	0.244	0.155

Table C.3

GFA for service buildings at the national level for the reference case (km^2) ([36], own assumptions).

Energy label	GFA for service buildings at the national level for the reference case (km^2)				
	Offices	Education	Industrial halls	Hospitals	Others
GFE	0	13.14	45	7.46	79.44
DC	38.93	8.28	28.63	3.47	27.65
B	22.79	22.7	109.60	15.44	113.07
A	6.85	0.09	0.08	0.08	0.47
A+	11.48	0.09	0.08	0.08	0.47

Table C.4

Number of household buildings at the national level for the reference case (Mh) and the normalized heat demand per household building type for different energy labels (PJ/Mh).

Energy label	Number of million household buildings at the national level for the reference case (Mh) ([36], own assumptions)			Normalized heat demand per million household buildings for different energy labels (PJ/Mh) [36]		
	Apartments	Terraced houses	Other dwellings	Apartments	Terraced houses	Other dwellings
GFE	0	0	0	30.1	45.6	70.4
DC	0.337	0.193	0.4	28.7	38.4	60.6
B	0.9	0.7	0.418	25.7	34.3	53.4
A	1	1	2.07	19	25.4	39.5
A+	0.312	0.264	0.403	15.4	20.6	32

Table C.5

Household buildings shell improvement cost compared to GFE label (€/h) [36].

Energy label	Household buildings shell improvement costs compared to GFE label (€/h)		
	Apartment	Terraced houses	Other dwellings
DC	2099	2795	1587
B	7307	8652	15,308
A	9716	12,085	21,623
A+	12,126	15,517	27,939

Table C.6

Current distribution of different household buildings in different regions (Mh) [67].

Region/Node	Current distribution of different household buildings in different regions (Mh)		
	Apartment	Terraced house	Others
Groningen municipality	0.04	0.02	0.01
Groningen rest	0.03	0.03	0.12
Friesland	0.04	0.05	0.19
Drenthe	0.03	0.04	0.14
Rest of the Netherlands	2.13	1.79	2.48

Table C.7

Current energy label distribution for 'office' buildings in different regions (km^2) [62,77].

Region/Node	Current energy label distribution for 'office' buildings in different regions (km^2)				
	GFE	DC	B	A	A+
Groningen municipality	0.56	0.32	0.11	0.07	0.22
Groningen rest	0.17	0.10	0.03	0.02	0.07
Friesland	0.82	0.44	0.09	0.11	0.27
Drenthe	0.49	0.22	0.06	0.07	0.16
Rest of the Netherlands	23.50	12.31	3.28	6.58	10.77

Table C.8
Current distribution of different service buildings in different regions (km^2) [62,68,69].

Region/Node	Current distribution of different service buildings in different regions (km^2)				
	Offices	Education	Industrial halls	Hospitals	Others
Groningen municipality	1.28	0.21	0.79	0.13	1.83
Groningen rest	0.38	1.39	3.39	0.9	3.88
Friesland	1.73	1.33	6.7	0.77	6.72
Drenthe	1	0.71	5.3	0.61	4.58
Rest of the Netherlands	56.44	30	123.18	17.74	15.1

types are GFE, DC, B, A, and A+. The normalized heat demand and shell improvement costs for different BE building types are assumed to be the same in different regions and at the national level. These data at the national level are obtained from the ENSYSI database [36]. Tables C.1–C.3 presents data on service buildings; and Tables C.4 and C.5 present data on the household buildings. Tables C.1 and C.5 provide information on shell improvement cost compared to GFE label in €/(m^2 GFA) and €/h, respectively. Tables C.2 and C.4 present normalized heat demand for each energy label in GJ/(m^2 GFA) and PJ/Mh, respectively. Tables C.3 and C.4 present reference case buildings distribution for different energy labels in km^2 and Mh, respectively. For the service buildings reference case, we assume that no office buildings will have 'GFE' label and all new services buildings constructed after 2018 will have 'B' label. Similarly, in household buildings reference case, there will be no 'GFE' label buildings in 2050 and all buildings constructed after 2012 have A+ label as the latest buildings data is available for 2012.

Tables C.6–C.8 present input parameters for BE related to buildings and energy label distribution on a regional level. Table C.6 presents current distribution of different household buildings in different regions with million housing or Mh as the standard unit. Table C.7 presents current energy label distribution in 'office' buildings in different regions in the Netherlands. We do not have regional energy label data for the remaining service buildings. Therefore, we considered the same proportion of energy label in different regions as the national level for the remaining service buildings. The data source is ECN part of TNO reports [62,77]. Table C.8 presents current distribution of different service buildings in different regions/nodes in the standard unit km^2. The data sources are ECN part of TNO [62,63] and CBS [101] databases. Since we do not have any data on the regional distribution of energy labels of any of the household buildings, we use the same regional share of the households buildings as the national share in Table C.5, data on which is obtained from the ENSYSI report [36].

Appendix D. Description of approach to determine region-specific RES potentials

We categorize solar PV into small scale (in different sectors) and large scale. For regional allocation of small-scale solar PV in BE, we consider the rooftop space potential. Since we do not have information on rooftop space information of all our exclusive regions, we assumed that rooftop space is similar to the current land-use dedicated to BE. As we assume similar conditions for all regions, we simply calculated the regional share. For agriculture, small-scale solar PV is linked to horticulture due to its intensive energy requirement, i.e. regional space potential share for agriculture solar PV is based on land dedicated to horticulture. To allocate the potential for solar PV alongside roads [102], we consider the regional share of provincial roads. Similarly, for small-scale industrial PV, we considered the land dedicated to industries. Current land-use data on BE, horticulture, major roads, and industries are obtained from CBS [78]. Large-scale (i.e. >1 MW) PV, is part of the energy sector and is subdivided into ground-based and inland water. For ground-based photovoltaics (GB-PV) regional allocation, we considered the provincial allocation from the ENSPRESO project [43]. The project scenario considers 17% of agricultural area and 100% of non-agricultural area for GB-PV. For inland water, provincial data is obtained from CBS [78].

Wind is subdivided into onshore and offshore. For onshore regions, the future capacity proportion is the same as short-term provincial targets [79]. The offshore capacity is determined by the space allocated according to Scenario IV of a PBL-based study [80]. This scenario is aggressive with respect to the future offshore space potential. Explicit wind profiles are created for each onshore region by considering a hub height of 125 m and wind-speeds at 150 m from the national meteorological institute KNMI [39]. Offshore wind profiles are extracted from KNMI as well at 150 m. For offshore wind, the power velocity curve of a 1 GW wind farm at a hub height of 155 m as used in [103] has been considered.

Geothermal potential is another important supply-related spatial parameter [104,105]. We used the GIS-based 'overview technical potential' raster map of TNO [41,81]. For calculating nodal values, we overlaid our five region NL vector polygon map over the raster map. For each node, we calculated the geothermal technical potential using the 'Zonal Statistics' tool in QGIS [106].

We considered seven types of biomass: wet manure; co-substrate for manure digestion; biogenic waste for incineration; crop-based biomass, such as sugar and starch, for bioethanol production; vegetable, fruits, and garden (VFG) waste or green waste from households; sewage sludge; and primary and secondary residues from forests, including households wood waste, or woody biomass.

Livestock population is a good indicator of wet manure production [107] and is predominantly produced by cattle, pigs, and chickens in the Netherlands [82]. For obtaining nodal manure production, we added the product of each of the above-mentioned livestock population [75] with its manure production [82]. We used the same regional share for potential allocation of co-manure for digestion.

Collecting and burning municipal solid waste (MSW) is an important industrial activity in the Netherlands with significant regional differences [83]. Nodal allocation is based on annual MSW burnt in existing incinerators, taking data from the Ministry of Infrastructure and Waterways or Rijkswaterstaat [83].

The amount of VFG or organic green waste produced in households is strongly dependent upon household size. Nodal allocation, therefore, is based on population distribution. Sewage sludge production is widespread in the Netherlands [108], implying we could here also use population distribution

Table D.1
Sensitivity cases for the year 2050 and their difference with the reference scenario.

Sensitivity case name and regional distribution						Differences compared to the reference scenario in the regionalized OPERA model and the reason of the case selection
High onshore wind (*C1*), national total = 32 GW						Our analysis shows onshore wind capacity allocation of 16 GW is fully utilized fully in the reference scenario. So, we doubled the onshore wind potential of each region in the NL for a national total of 32 GW as future wind aggressive regional policies might enable installation of such a high capacity on land. This would require an onshore space of 1800 km^2 in the NNL (assuming a power density of 5 MW/km^2 [110]).
Regional distribution	D	F	GM	GR	RNL	
Onshore wind (GW)	1.6	2.9	0	4.5	23	
(all other supply-side distributions remains the same as in the reference scenario)						
Very low onshore wind (*C2*), national total = 6 GW						Here, we take into account the fact that further installation of onshore wind turbines are not allowed due to social resistance, except meeting the near-term national target of 6 GW at predefined locations [79]. This represents an highly conservative situation with regards to wind farm installation in every region.
Regional distribution	D	F	GM	GR	RNL	
Onshore wind (GW)	0.29	0.53	0	0.86	4.32	
(all other supply-side distributions remains the same as in the reference scenario)						
Low ground-based PV (*C3*), national total = 30 GW						In our model runs with the reference scenario nearly 60 GW of large-scale ground PV is utilized at the national level, even though the potential was 74 GW. So, there is no use to consider higher capacity for GB-PV. Therefore, this represents a sensitivity case where we reduced the solar GB-PV capacity to half of the actual realized capacity potential, i.e. 30 GW. Thus, this is a conservative case with regards to large-scale ground PV.
Regional distribution	D	F	GM	GR	RNL	
Ground PV (GW)	3	2.1	0	3	21.9	
(all other supply-side distributions remains the same as in the reference scenario)						
Less geothermal (*C4*), national total = 70 PJ						Similar to GB-PV, only 140 PJ of geothermal is utilized at the national level, even though the scenario potential is 200 PJ. Therefore, in this case, we reduced the geothermal potential to half of the actual realized potential, i.e. 70 PJ. This represents a conservative situation for geothermal heat potential for every region.
Regional distribution	D	F	GM	GR	RNL	
Geothermal (PJ)	3.5	16.1	0.7	6.3	43.4	
(all other supply-side distributions remains the same as in the reference scenario)						
Large woody biomass (*C5*), national total = 50 PJ						As the allocated future potential of 26.7 PJ of woody biomass is fully utilized in the reference scenario. In this case, we try to understand the impact of almost doubling the woody biomass potential in every region to obtain a national total of 50 PJ. This is an aggressive case with respect to woody biomass potential in every region.
Regional distribution	D	F	GM	GR	RNL	
Woody biomass (PJ)	1.7	1.6	0	1.37	45.32	
(all other supply-side distributions remains the same as in the reference scenario)						
Less woody biomass (*C6*), national total = 10 PJ						Here, we consider that households and other sectors component of woody biomass (nearly 17 PJ) from Elbsersen *et al.* [84] is almost negligible compared to the reference scenario. Therefore, the woody biomass potential in this case is 10 PJ. This represents a conservative case of biomass potential in every region.
Regional distribution	D	F	GM	GR	RNL	
Woody biomass (PJ)	0.34	0.32	0	0.27	9.06	
(all other supply-side distributions remains the same as in the reference scenario)						
Strong renewables potential NNL only (*C7*)						Here, onshore wind and woody biomass, ground PVs capacity/potential for each of the nodes in the NNL is doubled. The capacity/potential for all the above-mentioned sources remains the same for the RNL node. This case is technically feasible since our model shows a complete utilization of every resource potential. This case represents an aggressive case for the NNL. Thus, this case represents a combination of C1 and C5 cases for the NNL.
Regional distribution	D	F	GM	GR	RNL	
Onshore wind (GW)	1.6	2.9	0	4.5	11.5	
Woody biomass (PJ)	1.7	1.6	0	1.37	24.2	
(all other supply-side distributions remains the same as in the reference scenario)						
Less renewables deployment NNL only (*C8*)						As we know that our reference scenario represents an aggressive situation with respect to renewables, which might not happen in reality in the NNL regions due to a lack of strong regional policies. Therefore, in this case, we simultaneously consider reducing the capacity/potential of onshore wind, ground PVs, geothermal, and woody biomass for all the NNL nodes to half, without affecting the RNL node. This represents a highly conservative case for the supply side in the NNL. Thus, this case represents a combination of C2, C3, C4, and C6 cases for the NNL.
Regional distribution	D	F	GM	GR	RNL	
Onshore wind (GW)	0.29	0.53	0	0.86	11.5	
Ground PV (GW)	3	2.1	0	3	54	
Geothermal (PJ)	3.5	16.1	0.7	6.3	124	
Woody biomass (PJ)	0.34	0.32	0	0.27	24.2	

for nodal allocation.

There are significant regional differences in the potentials/constraints in sugar and starch availability for bioethanol production and woody biomass for combustion purposes [84,109]. Elbersen *et al.* [84] estimated future biomass potentials by considering existing land-use policy measures, i.e. business-as-usual, for different provinces in the Netherlands. We used their database [84] to perform our regional allocation of bioethanol and woody biomass potentials.

Table D.1 presents sensitivity cases on renewable potentials, their regional distributions, differences compared to the reference scenario, and the reason for the case selection.

Appendix E. Detailed scenario description

We used a scenario based on 2050 targets set for different categories in the 'National management' scenario from the Berenschot and Kalavasta study [90]. We used the complete set of results for [90] from the 2050 run of energy transition model (ETM) [111], to derive underlying assumption relevant for our analysis. The 'National management' scenario focuses on centralized RES supply for energy self-sufficiency, large demand for H_2 from RES, and a low energy exchange with neighboring countries [90]. OPERA does not need all the data considered in [90] as OPERA can extract demand figures related data from NEOMS used in the NEO, in particular related to physical quantities such as million ton of product, billion vehicle kilometers, and square kilometers of service buildings. Remaining sectoral demand that is expressed in PJ is derived from the national management scenario. Table E.1 presents main energy demand parameters related to major activities or subsectors for the whole of the Netherlands in the national management scenario, i.e. NM2050. Unit column represents the standard unit of activity.

In the original NM2050 scenario of Berenschot and Kalavasta several capacities have been taken as fixed, while in OPERA it is a potential, so a lower realization is also possible. For example, the NM2050 scenario of Berenschot and Kalavasta fixates the wind offshore capacity at 72 GW, while in OPERA the realization is determined by the optimization. We explicitly mention the following few deviations as compared to [90] in Table E.2. For example, we assumed CCS is available in future scenarios in contrast to [90]. In addition, we allowed an onshore HV transmission grid expansion of

Table E.1
OPERA energy demand parameters for the Netherlands in NM2050 scenario.

Main demand parameters	Unit	NM2050
Demand for electricity - Chemicals	PJ	23.53
Demand for heat - Chemicals	PJ	70.10
Physical demand - Chemicals	MT HVC	4.04
Demand for electricity - Iron and steel	PJ	9.20
Demand for heat - Iron and steel	PJ	33.23
Physical demand - Iron and steel	Mt steel	7.20
Demand for electricity - Ammonia	PJ	0.00
Demand for heat - Ammonia	PJ	7.90
Physical demand - Ammonia	Mt NH_3	1.28
Demand for electricity - Refineries	PJ	3.50
Demand for heat - Refineries	PJ	0.00
Physical demand - Salt	Mt_Salt	7.048
Physical demand - chlorine	Mt_Chlorine	0.958
Physical demand – liquid Aluminum	Mt_liquid_Aluminum	0.138
Demand for electricity - FBI	PJ	24.79
Demand for heat - FBI	PJ	44.27
Physical demand - dairy	Mt_dairy_products	1.204
Physical demand - Sugar	Mt_Sugar	1.195
Physical demand - potato	Mt_potato_product	1.682
Demand for electricity - Rest industry ETS	PJ	26.16
Demand for heat - Rest industry ETS	PJ	35.93
Demand for electricity - Rest industry non-ETS	PJ	41.89
Demand for heat - Rest industry non-ETS	PJ	56.98
Demand for electricity - households	PJ	89.80
Physical demand - apartments	Mh	2.55
Physical demand – terraced houses	Mh	2.158
Physical demand – other dwellings	Mh	3.292
Demand for electricity - service sector	PJ	105.78
Physical demand - offices	km^2	80.048
Physical demand – education	km^2	44.308
Physical demand – Industrial halls	km^2	183.398
Physical demand – hospitals	km^2	26.543
Physical demand – rest services	km^2	221.097
Demand for mobility – Passenger cars	BVKm	122.41
Demand for mobility – Light Duty Vehicles (LDVs)	BVKm	20.68
Demand for mobility – High Duty Vehicles (HDVs)	BVKm	8.58
Energy fuel - Rest domestic transport	PJ	60.24
Energy electricity - Rest domestic transport	PJ	0.00
Energy consumption for international aviation	PJ	170
Energy consumption for international shipping	PJ	543
Demand for electricity - Agriculture	PJ	86.37
Demand for heat - Agriculture	PJ	78.86
Mobile machinery - Agriculture	PJ	16.80
Mobile machinery - Industry	PJ	25.36
Mobile machinery - Service sector	PJ	7.50

Table E.2

Scenario parameter and restrictions for 2050 as used by OPERA in this paper compared to the values of the NM2050 scenario developed by Berenschot and Kalavasta [90].

Category	Unit	2050 OPERA scenario	Fixed 2050 values in NM2050 [90]
Capacity PV	GW	168	106
CO_2 storage capacity in CCS	Mt/yr	25	5.9[a]
Biomass availability	PJ/yr	115	248
Maximum import of NG	TeraWatt hour (TWh)/yr	0	0
Trade profile electricity	TWh/yr	Output from COMPETES	Unclear
H_2 trade	TWh/yr	Not allowed	Not allowed
SMR without CCS	–	Allowed	Allowed
Maximum admixing % in the methane grid	–	15% [113]	Unclear
Expansion HV grid as compared to the currently capacity	–	2.5×	2.0×

[a] Berenschot and Kalavasta (2020) [90] assumes an overall CCS capacity (offshore) of 1700 Mt. In their NM2050 the actual use of CCS amounts to 5.9 Mt in 2050 (implying that, on average, the overall CCS capacity is available for 289 year).

2.5× the current capacity in 2050 as compared to 2× considered in [90]. Since, the electricity grid is internationally connected, we used trade flows from the COMPETES model [85,112] based on the LSES study [91]. Additionally in [90], H_2 admixing in the NG network is unclear for 2050. However, we assumed 15% admixing in the current analysis based on study by New Energy Coalition [113].

Appendix F. District heating network analysis

We follow the equations from [49,114] to identify among others, parameters needed to create a DH network, such as, average pipe diameter, and linear heat density. The equations follow:

$$c_d = \frac{a(c_1 + c_2 * d_a)}{p * \alpha * q * w} \ (€/GJ) \tag{F.1}$$

$$p = \frac{P}{A_L} \ (number/m^2) \tag{F.2}$$

$$\alpha = \frac{A_B}{P} \ (m^2/capita) \tag{F.3}$$

$$e = p * \alpha \ (-) \tag{F.4}$$

$$q = \frac{Q_s}{A_B} \ (GJ/m^2 a) \tag{F.5}$$

$$w = \frac{A_L}{L} = 61.8 * e^{-0.15} \ (m) \tag{F.6}$$

$$or, \ for \ 0 < e < 0.4; w = 137.5e + 5, \ e > 0.4; \ w = 60 \ (m) \tag{F.7}$$

$$d_a = 0.0486 * ln\left(\frac{Q_s}{L}\right) + 0.0007 \ (m) \tag{F.8}$$

where 'C_d' is the distribution capital cost, and 'a' is the annuity. For this, we assume interest rate of 3% and a lifetime of 30 years for DH network, similar to [49]. 'C_1' and 'C_2' represents the construction cost constant (€/m) and construction cost coefficient (€/m²) respectively. 'P', 'A_L', and 'A_B' represents total population (number), total land area (km²), and total building space area (hectare) respectively. 'p' and 'α' represents population density and total building space per capita, respectively. 'e' represents plot ratio that informs about the building density within a city area and is used to obtain 'w', the effective width of the network[4]. 'w' can then be used to calculate 'L'. 'Q_s/L', and 'd_a' represents linear heat density, and average pipe diameter respectively. Parameters 'e', 'q', 'C_1', 'C_2', and 'a' are obtained from [49]. At a standard value of e = 0.5, we obtained C_d = 2. This is in line with heat roadmap Europe that suggests an annualized marginal cost of DH network for Groningen to be between 2 and 5 €/GJ for most part of Groningen municipality. In addition, our calculation cannot take into account heat transmission and connection cost or total distribution cost. [49] identifies that distribution capital cost is more than half of total distribution cost. Thus, we take the standard value of 3.5€/GJ as total heat distribution cost for Groningen municipality.

Appendix G. Industry database for OPERA

This section presents the database related to activities added for different subsectors in the OPERA model. The activities added are highly relevant for the north of the Netherlands (NNL). The activities added in the OPERA database are primary aluminum, gaseous chlorine, dairy product, potato product, salt, and sugar production.

---

[4] 'e' in the eq. (E6) represents plot ratio and not natural logarithm base.

Table G.1

Database related to primary aluminium production [115].

Process Name	Unit Activity	Investment cost [M€/yr/unit activity]	Variable cost [M€/yr/unit activity]	Electricity consumption [GJ/unit activity]	Emission [per unit activity] CO$_2$[a] [Mt CO$_2$]	F-gases[b] [Mt CO$_2$_eq]
REF Hall-Héroult process	Mt liquid Al	0	0	54,75	1,58	0,55[c]
Implementing BATs	Mt liquid Al	4500	0	49	1,58	0,55[d]
Incremental EE improvements	Mt liquid Al	125	0	54	1,58	0,55[d]
Dynamic AC magnetic field	Mt liquid Al	80	0	48	1,58	0,55
Wetted cathodes	Mt liquid Al	520	0	43,8	1,58	0,14
Inert anodes	Mt liquid Al	90	0	65,56	0[e]	0
Carbothermic reduction of Alumina	Mt liquid Al	3000	0	37	0	0
Hall_Héroult + CCS[f]	Mt CO$_2$	210	28[g]	0,46 + 5,63[h]	−1[i]	−

[a] We have excluded 0.044 (mining) and 1.37 (alumina refining) = 1.414 MT CO$_2$ emissions. In addition, we do not consider emission associated with anode production, i.e., 0.28 Mt CO$_2$ emissions.

[b] F-gasses here represents CF$_4$ and C$_2$F$_6$ and not actual Fluoride gas emitted from the process

[c] We do not consider SO$_2$ emissions. In addition, we do not consider indirect emission associated with prebaked C anodes, AlF$_3$, and Al$_2$O$_3$ production process as these are mainly imported to the Netherlands.

[d] We assume there is no change in PFC emission as compared to the Hall Heroult's process.

[e] Some literature studies show that there is not 100% reduction of CO$_2$ emission due to presence of inert anodes. However, [115] considers 100% reduction of CO$_2$ emission (in combination with wetted cathode process)

[f] In OPERA, we consider this as an add-on or retrofit option rather than completely new option

[g] operation cost excludes extra energy costs associated with CCS

[h] this is the heat requirement for CCS on top of existing heat requirement, which is assumed to be zero for every other option

[i] '−' sign indicates that CO$_2$ is absorbed as opposed to other cases where CO$_2$ is released.

Table G.2

Database related to gaseous chlorine production [37].

Process Name	Unit Activity	Investment cost [M€/yr/unit activity]	Variable cost [M€/yr/unit activity]	Energy consumption [PJ/unit activity] ('-' sign indicates production) Electricity	Heat	Hydrogen	(woody) biomass	Geothermal
REF Membrane Electrolysis	Mton gaseous Chlorine	0	0	8.23	1.89	−3.78	0	0
Zero gap membrane electrolyzer	Mton gaseous Chlorine	3.64	0.55	7.606	1.89	−3.78	0	0
Electric boiler	PJ	5.78	4.45	1.01	−1	0	0	0
Biomass boiler	PJ	11.15	1.49	0	−1	0	1.25	0
Ultra-deep geothermal boiler	PJ	53.74	3.1	0.067	−1	0	0	0.93

Table G.3

Database related to dairy product production [37,116,117].

Process Name	Unit Activity	Investment cost [M€/yr/unit activity]	Variable cost [M€/yr/unit activity]	Energy consumption [PJ/unit activity] Electricity	Heat	Hydrogen	Biogas (FBI)	Geothermal
REF production	Mt_dairy product	0	0	0.95	7.39	0	0	0
Zeolite spray drying	Mt_dairy product	26.90	0.81	0.95	5.73	0	0	0
Reverse osmosis evaporation	Mt_dairy product	26.95	8.40	0.85	6.89	0	0	0
MVR evaporation	Mt_dairy product	18.22	0.55	1.15	6.59	0	0	0
Heat pumps evaporation	Mt_dairy product	104.63	2.54	1.26	6.17	0	0	0
Electric boilers	Mt_dairy product	43.62	3.34	8.57	0	0	0	0
Hydrogen boilers	Mt_dairy product	35.92	4.62	0.95	0	8.21	0	0
Biogas boiler	Mt_dairy product	26.43	0.77	0.95	0	0	7.39	0
Ultra-deep geothermal energy station	Mt_dairy product	733.13	29.33	1.27	0	0	0	7.07

Table G.4

Database related to potato product production [37,118].

Process Name	Unit Activity	Investment cost [M€/yr/unit activity]	Variable cost [M€/yr/unit activity]	Energy consumption [PJ/unit activity] ('-' sign indicates production)							
				Electricity	Heat	Biogas (FBI)	Biomethane	(woody) biomass	waste heat (FBI)	Geothermal	Hydrogen
REF process	Mt potato product	0	0	0.25	5	0	0	0	0	0	0
Eco steam potato peeler and processer	Mt potato product	0.24	0	0.25	4.87	0	0	0	0	0	0
Biogas production (UASB digestion) + CHP	Mt potato product	21	0.214	0	4.80	0	0	0	0	0	0
Biogas production	Mt potato product	15.72	0.002	0.26	5	−0.34	0	0	0	0	0
Biogas upgrading - water scrubbing	Mt potato product	3.773	0.0946	0.26	5	0.34	−0.2	0	0	0	0
Condensing biogas steam boiler	Mt potato product	0.67	0.02	0.25	4.68	0.34	0	0	0	0	0
Solid biomass steam boiler	Mt potato product	89.93	6.94	0.25	0	0	0	5.56	0	0	0
MVR (blanching)	Mt potato product	4.48	0.15	0.29	4.70	0	0	0	0.26	0	0
Heat pumps (blanching)	Mt potato product	28.13	0.63	0.33	4.70	0	0	0	0.23	0	0
Electric boilers	Mt potato product	29.51	0.19	5.51	0	0	0	0	0	0	0
Ultra-deep geothermal energy station	Mt potato product	434.03	18.58	0.47	0	0	0	0	0	4.78	0
Hydrogen boilers	Mt potato product	24.31	3.13	0.25	0	0	0	0	0	0	5.56

Table G.5

Database related to salt production [37].

Process Name	Unit Activity	Investment cost [M€/yr/unit activity]	Variable cost [M€/yr/unit activity]	Energy consumption [PJ/unit activity] ('-' sign indicates production)		
				Electricity	Heat	Hydrogen
REF process	Mt_salt	0	0	0.26	1.6	0
MVR brine vaporization	Mt_salt	30.2	1.5	0.7	0.94	0
Hydrogen boiler	PJ	6.24	0.44	0	−1	1.03
Electric boiler	PJ	5.78	4.45	1.01	−1	0

Table G.6

Database related to sugar production [37].

Process Name	Unit Activity	Investment cost [M€/yr/unit activity]	Variable cost [M€/yr/unit activity]	Energy consumption [PJ/unit activity] ('-' sign indicates production)				
				Electricity	Heat	Hydrogen	waste heat (FBI)	Biomass (FBI)
REF process	Mt_sugar	6.19	0.36	0.55	2.8	0	0	0
MVR using waste heat vapor	PJ	79.76	6.56	0.1	−1	0	0.9	0
Hydrogen boiler	PJ	5.74	0.41	0	−1	1.03	0	0
Biogas boiler	PJ	24.31	0.69	0.02	−1	0	0	1.11
Electric boiler	PJ	222.43	4.45	1.01	−1	0	0	0

Table G.7

Current distribution of final products in different regions for important industrial activities in the north of the Netherlands [37].

Regions	Current distribution of final products in different regions for important activities in the north of the Netherlands					
	Basic Metal	Food and beverage industry (FBI)			Chemicals	
	Primary Aluminum (Mt liquid aluminum)	Dairy Products (Mt dairy products)	Potato Products (Mt potato products)	Sugar (Mt sugar)	Chlorine (Mt gaseous chlorine)	Salt (Mt salt)
Drenthe	0	0.28	0	0	0	0
Friesland	0	0.64	0.13	0	0	0.88
Groningen municipality	0	0	0	0.47	0	0
Groningen rest	0.08	0.14	0.03	0	0.12	2.77
Rest of the Netherlands	0	0.7	1.98	0.47	0.73	3

Table G.1 presents primary aluminum production-related database. The unit of this activity is 'Mton liquid aluminum'. Investment cost is annualized with respect to one unit of activity, i.e. M€/yr/unit activity. Variable cost also has the same unit. As primary aluminum production is the electrolysis part of the whole aluminum production process, we consider electricity consumption as the only energy demand for this production process. The electricity demand is expressed as 'GJ per unit activity'. The electrolysis process releases both CO_2 and F gases. The unit of both of these emissions component is 'Mt_CO2 eq.'. The CCS process is considered as a retrofit option for the standard Hall-Héroult's process. The unit of this process is 'Mt-CO_2'.

Table G.2 presents gaseous aluminum production-related database. The unit of the standard production process is 'Mton gaseous chlorine'. The standard gaseous chlorine production is electrolysis-related process called 'membrane electrolysis'. There is only one alternative production process 'zero gap membrane electrolyzer'. Other processes are generic heat production processes with 'PJ' as the unit of activity. For these processes, energy demanding carriers are electricity, heat, woody biomass, and geothermal, and the energy producing carrier is H_2. There is no direct emissions from any of these processes.

Table G.3 presents database related to production of dairy products. The unit of activity is 'Mt dairy product' for all the processes. Energy carriers related to energy demand are electricity, heat, H_2, biogas related to food and beverage industries or biogas (FBI), and geothermal. All the FBI-related energy carriers are limited within the FBI subsector. Ultra-deep geothermal energy station process has the highest investment and variable cost with values corresponding to €733 million/yr/unit activity and €29 million/yr/unit activity, respectively.

Table G.4 presents potato products production-related database. The unit of activity is 'Mt potato product'. Energy carriers involved with the processes are electricity, heat, biogas (FBI), biomethane, (woody) biomass, waste heat (FBI), geothermal, and H_2. Investment cost and variable cost are expressed in 'M€/yr/unit activity'.

Table G.5 presents database related to salt production. The reference process has 'Mt salt' as the unit of activity. There one alternate process called mechanical vapor recompression with the same unit of activity. Other processes are standard process with 'PJ' as the unit activity. Energy carriers involved with the processes are electricity, heat, and H_2.

Table G.6 presents database related to sugar production. The reference process has 'Mt sugar' as the unit of activity. There are no alternate process for sugar production; however, other processes can substitute energy carriers involved with the reference process. These processes have 'PJ' as the unit activity. Energy carriers involved with the activity are electricity, heat, H_2, waste heat (FBI), and biomass (FBI). Table G.7 presents current distribution of final main products in different regions for important industrial activities in the north of the Netherlands, based on the MIDDEN reports [37]. The unit activity is 'Mt final product'. Groningen rest has high production volumes in the north compared to other regions.

Appendix H. Infrastructure-related information

Table H.1 provides a comparison between existing lump-sum prices (in k€/MW) and new prices as a function of distance (i.e. k€/(MW*km)) along with references for these new prices. Table H.2 presents distances between nodes/regions and lower and upper capacity limits for the electricity HV-network infrastructure between regions.

While representing regions with nodes and creating network infrastructures between those nodes, we formulated a much simplistic network to

Table H.1
Comparison between existing lump-sum prices and new prices related to annualized investment costs.

Network type	Existing lump-sum prices (k€/MW)	New prices (k€/(MW*km))	References new prices
Electricity HV network	364	6.6	Expert consultation
NG HP pipeline	57.8	0.34	Indicative, based on ECN part of TNO report [119]
H_2 pipeline	86.7	0.43	Based on HP NG, but 80% of the pipe capacity considered as per Infrastructure Outlook 2050 report [120]

Table H.2
Distances between regions and capacity constraints for electricity energy infrastructure analysis.

Region 1	Region 2	Distances (km)	Network Capacity (MW)	
			Minimum [86]	Maximum (own Assumption)
Groningen rest	Friesland	72	1830	2830
Groningen rest	Drenthe	58	2635	6635
Groningen rest	Groningen municipality	24	880	1380
Rest of the Netherlands	Friesland	150	1900	3900
Rest of the Netherlands	Drenthe	154	2635	6635

Fig. H.1. Network infrastructures representation of the Netherlands (only for illustrative purposes) [121,122]. (L) represents high voltage electricity network from TenneT and (R) represents gas network from Gasunie.

allow energy carrier flow between regions. The present actual electricity and gas networks presented in Fig. H.1 (L) and Fig. H.1 (R), respectively, are more complicated and difficult to present in our modeling structure.

Appendix I. Detailed analysis of the results

Fig. I.1 presents a comparison of the primary energy mix between the single- and multi-node models. For obtaining regional allocation in the single-node model, we provided the regional population share. All the nodes in the multi-node model have lower primary energy demand, except Groningen rest (GR). GR has a significantly high onshore wind energy supply (44 PJ) resulting in higher overall primary energy supply in the multi-node model. Similarly, Friesland and Drenthe have higher wind energy supply (29 and 15 PJ, respectively) in the multi-node model compared to the single-node model (11 and 8 PJ, respectively). Similarly, solar energy supply in the multi-node model (13 PJ) in Drenthe is higher than the single-node model (8 PJ). On the other hand, oil consumption in Friesland and Drenthe is higher in the single-node model (23 and 18 PJ, respectively) compared to the multi-node model (~0 and 1 PJ, respectively). In the multi-node model, GM has energy demand mainly from the BE sector. Therefore, for GM, primary energy supply is significantly lower in the multi-node model compared to the population-based average in the single-node model.

Fig. I.2 presents total system cost comparison between the single- and multi-node models. The regional allocation is based on population share in the single-node model. The total system cost is split into supply, demand, infrastructure, and storage-related costs. Infrastructure and storage costs are

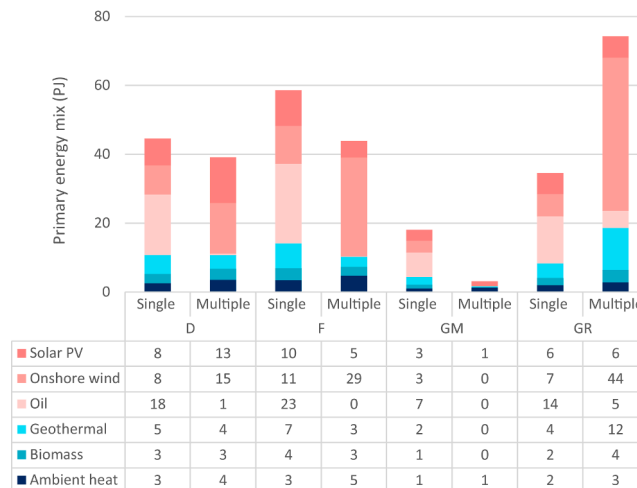|	Single	Multiple	Single	Multiple	Single	Multiple	Single	Multiple
	D		F		GM		GR	
Solar PV	8	13	10	5	3	1	6	6
Onshore wind	8	15	11	29	3	0	7	44
Oil	18	1	23	0	7	0	14	5
Geothermal	5	4	7	3	2	0	4	12
Biomass	3	3	4	3	1	0	2	4
Ambient heat	3	4	3	5	1	1	2	3

Fig. I.1. Primary energy mix comparison between the single- and multi-node models (all data in PJ). The single-node model regional distribution is based on the population share.
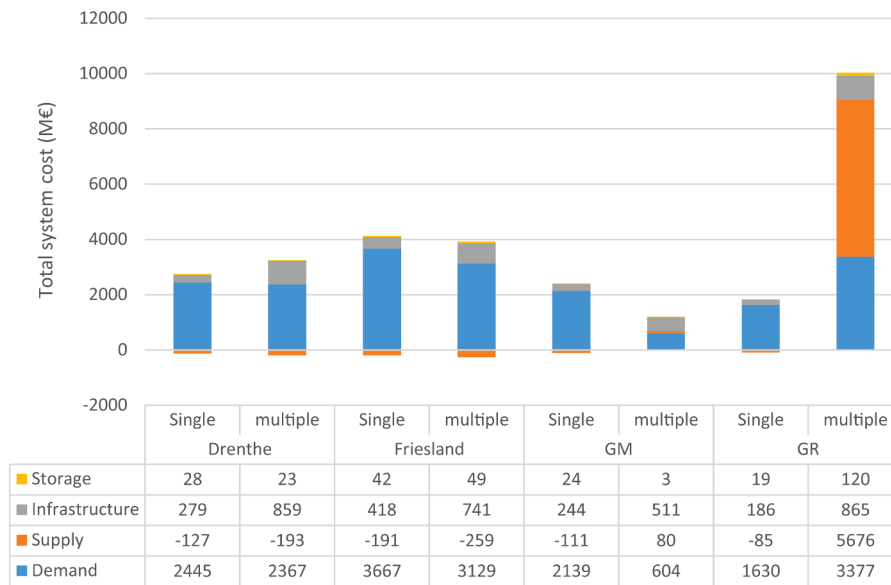
		Single	multiple	Single	multiple	Single	multiple	Single	multiple
		Drenthe		Friesland		GM		GR	
■ Storage		28	23	42	49	24	3	19	120
■ Infrastructure		279	859	418	741	244	511	186	865
■ Supply		-127	-193	-191	-259	-111	80	-85	5676
■ Demand		2445	2367	3667	3129	2139	604	1630	3377

Fig. I.2. Region-wise comparison of total system cost for the single- and multi-node models (all data in M€). The regional allocation in the single-node model is population based. Negative sign indicates reduction in the cost due to supply-related options.

always positive. Demand-related options generally have positive costs. These costs can be slightly negative if an option is related to energy savings and then the negative energy cost is higher than the positive remaining costs. Overall, negative costs demand options have significantly low values compared to positive options. Therefore, demand costs do not show negative values for any of the regions. Supply-side options can have high negative or positive costs. This cost is negative if the negative energy cost is higher than the remaining positive costs for the same option, for example offshore wind farms. In case the supply side has a total negative cost, it reflects a situation in which the sum of options with a negative total cost is higher than the sum of options with a positive cost, for example both models in Friesland.

There are differences between the single- and multi-node models, particularly for GR. In GR, all cost components are significantly higher in the multi-node model compared to population-based average. For example, demand, infrastructure, and storage costs in the multi-node model are 3377, 865, and 120 M€, respectively, whereas the corresponding values in the single-node model are 1630, 186, and 18 M€, respectively.

Disaggregation of total system cost

Fig. I.3 presents a breakdown of the total cost per option into the energy cost, the variable O&M cost, the fixed O&M cost, and CAPEX. All of the cost components are consistently positive, with the exception of the energy cost. The energy cost is calculated as the net consumption or production of an energy carrier multiplied by the energy price in the OPERA database. Therefore, if energy is produced by means of a technology option, with most of such options being on the supply side, then the energy cost will be negative, as in the case of the offshore wind-related technology option. To illustrate further, investment in wind-related infrastructure results in positive system cost. However, wind farms produce electricity which can be utilized by other system components decreasing the need to buy electricity. The positive infrastructure costs can be exceeded by the negative energy carrier cost. Therefore, wind farms reduce the total system cost depending upon the electricity price (input parameter). Since addition and subtraction calculations are internally associated with these energy-related options, cost associated with these types of options are called energy cost in OPERA.

Energy costs associated with almost all of the technology options were negligible for all the NNL nodes apart from GR in the multi-node model. The energy costs for many technology options on the demand and supply sides were high in GR. The total energy cost was low because the positive values associated with the sum of the demand-side options (€20.9 billion in total) were almost entirely compensated by negative values associated with the supply-side options (€20.2 billion), particularly those related to the energy sector (Fig. I.3 [a]). Therefore, the overall energy cost for GR was also negligible.

The variable O&M cost was in the range of millions of Euros (Fig. I.3 [b]). Here too, GR's energy sector contributed significantly to this cost at a sum of €73 million, of which €67 million were related to offshore wind. Similarly, GR's energy sector, mainly producing electricity, contributed significantly to CAPEX and fixed O&M costs (€5 billion and €2 billion, respectively), as shown in Fig. I.3 [c] and [d]. Drenthe, Friesland, and GR also incurred costs of €1 billion, each, for CAPEX in the B€, which was mainly associated with changes in the energy labels of different building types.

Sectoral energy mixes

Fig. I.4 shows net energy carrier consumption in different nodes in the NNL of the multi-node model for both the BE and industries. Within the NNL, net electricity consumption was the highest within the BE for every region, followed by H_2. Electricity accounted for 54% (9 PJ), 51% (10 PJ), 61% (3 PJ), and 45% (5 PJ) of the net total energy consumption of Drenthe, Friesland, GM, and GR, respectively, in the BE (Fig. 18 [a]). Within the industrial sector, the net electricity consumption was also the highest, followed by geothermal energy consumption. To illustrate, electricity accounted for 54% (4 PJ), 65% (7 PJ), and 57% (21 PJ) of the net total energy consumption in the industrial sectors of Drenthe, Friesland, and GR, respectively.
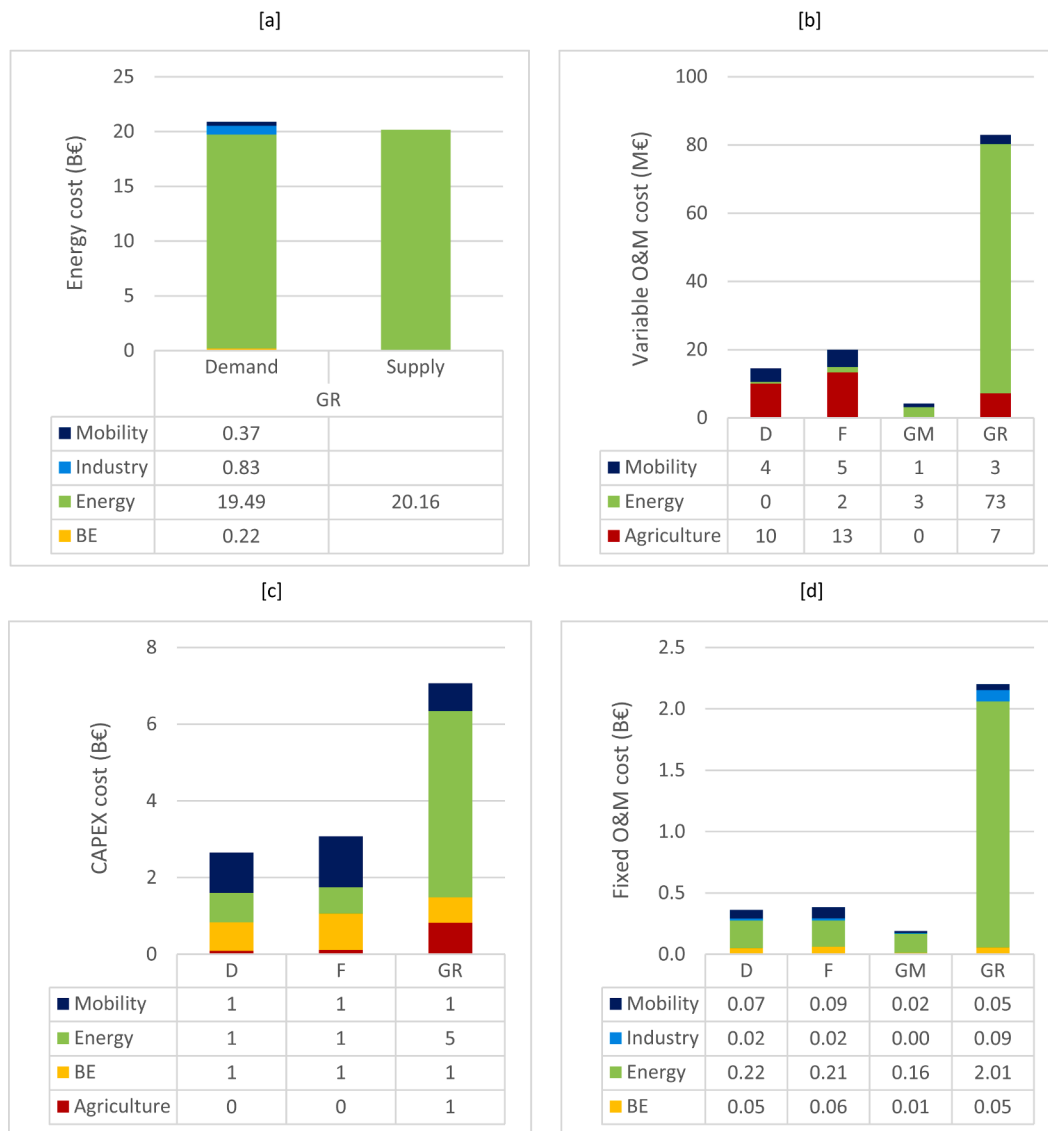
Fig. I.3. Sector-wise disaggregation of different components of total system cost in the multi-node model for different nodes in the NNL. [a], [b], [c], and [d] show energy costs of GR (in B€), variable O&M costs (in M€), CAPEX costs (in B€), and fixed O&M costs (in B€), respectively. [c] does not have GM-related x-axis because GM does not have any CAPEX cost.
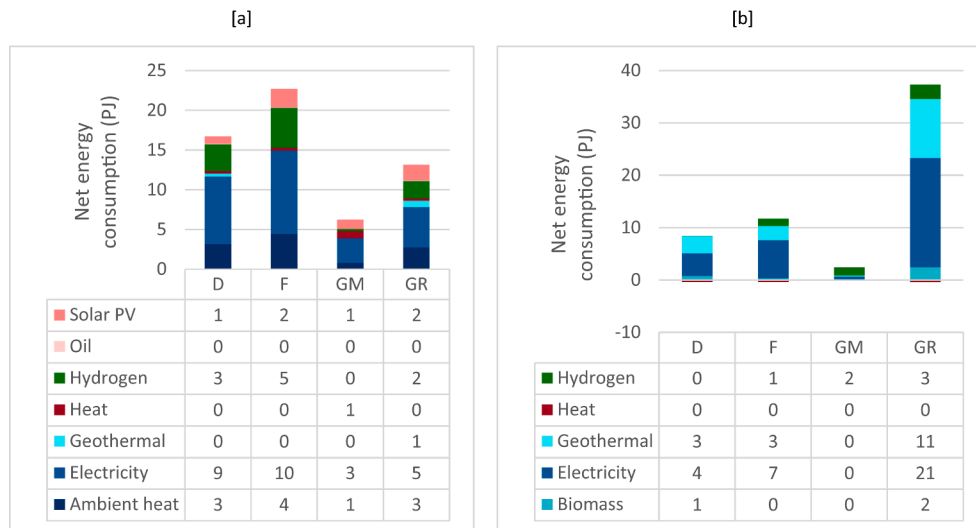
[a]

[b]

	D	F	GM	GR
Solar PV	1	2	1	2
Oil	0	0	0	0
Hydrogen	3	5	0	2
Heat	0	0	1	0
Geothermal	0	0	0	1
Electricity	9	10	3	5
Ambient heat	3	4	1	3

	D	F	GM	GR
Hydrogen	0	1	2	3
Heat	0	0	0	0
Geothermal	3	3	0	11
Electricity	4	7	0	21
Biomass	1	0	0	2

Fig. I.4. Net energy consumption of different energy carriers in the NNL in the multi-node model (all data in PJ). [a] and [b] present the BE and industries, respectively.

References

[1] de Boer J, Zuidema C. Towards an integrated energy landscape. In: AESOP-ACSP Jt. Congr.; 2013. p. 1–16.
[2] Smil V. Energy in nature and society: general energetics of complex systems. MIT Press; 2008.
[3] Bridge G, Bouzarovski S, Bradshaw M, Eyre N. Geographies of energy transition: Space, place and the low-carbon economy. Energy Policy 2013;53:331–40. https://doi.org/10.1016/j.enpol.2012.10.066.
[4] Ministry of Economic Affairs. Energy Agenda. Den Haag; 2017.
[5] Dutch ministry of Economic Affairs and Climate Policy. Integrated National Energy and Climate Plan 2021-2030: The Netherlands; 2019.
[6] PBL. National Energy Outlook 2017 - PBL Netherlands Environmental Assessment Agency; 2017. https://www.pbl.nl/en/publications/national-energy-outlook-2017 [accessed December 3, 2018].
[7] Commission E. 2030 Energy Strategy - European Commission n.d. https://ec.europa.eu/energy/en/topics/energy-strategy-and-energy-union/2030-energy-strategy [accessed October 9, 2018].
[8] Eurostat. Key figures on Europe; 2019. doi: 0628.
[9] Coalitieakkoord Groenlinks, PvdA, ChristenUnie, VVD, CDA, D66. Verbinden versterken vernieuwen 2019-2023 (in Dutch); 2019.
[10] de Joode J, Dalla Longa F, Smekens K, Daniels B. Integrating energy systems at the regional level: A model based assessment of the Dutch energy system; 2016.
[11] Seljom P, Tomasgard A. Short-term uncertainty in long-term energy models - A case study of wind power in Denmark. Energy Econ 2015;49:157–67.
[12] Daly HE, Scott K, Strachan N, Barrett J. Indirect CO2 Emission Implications of Energy System Pathways: Linking IO and TIMES Models for the UK. Environ Sci Technol 2015;49(17):10701–9. https://doi.org/10.1021/acs.est.5b01020.
[13] Van der Zwaan B, Keppo I, Johnsson F. How to decarbonize the transport sector? Energy Policy 2013;61:562–73. https://doi.org/10.1016/j.enpol.2013.05.118.
[14] Keramidas K, Kitous A, Després J, Schmitz A. POLES-JRC model documentation; 2017. doi:10.2760/225347.
[15] Ramachandra TV. RIEP: Regional integrated energy plan. Renew Sustain Energy Rev 2009;13(2):285–317. https://doi.org/10.1016/j.rser.2007.10.004.
[16] NEPLAN AG 8700 Küsnacht - Zürich Switzerland. NEPLAN n.d. https://www.neplan.ch/ [accessed March 28, 2019].
[17] Vitecsoftware. NETSIM n.d. https://www.vitecsoftware.com/en/product-areas/energy/products/netsim-grid-simulation/ [accessed March 28, 2019].
[18] Keirstead J, Samsatli NJ, Shah N. Syncity: an integrated tool kit for urban energy systems modelling. Energy Effic. cities Assess. tools benchmarking Pract. World Bank, 2010, p. 21–42.
[19] Girardin L, Marechal F, Dubuis M, Calame-Darbellay N, Favrat D. EnerGis: A geographical information based system for the evaluation of integrated energy conversion systems in urban areas. Energy 2010;35(2):830–40. https://doi.org/10.1016/j.energy.2009.08.018.
[20] Tiba C, Candeias ALB, Fraidenraich N, Barbosa EMdeS, de Carvalho Neto PB, de Melo Filho JB. A GIS-based decision support tool for renewable energy management and planning in semi-arid rural environments of northeast of Brazil. Renew. Energy 2010;35(12):2921–32. https://doi.org/10.1016/j.renene.2010.05.009.
[21] Howells M, Rogner H, Strachan N, Heaps C, Huntington H, Kypreos S, et al. OSeMOSYS: The Open Source Energy Modeling System An introduction to its ethos, structure and development. Energy Policy 2011;39(10):5850–70. https://doi.org/10.1016/j.enpol.2011.06.033.
[22] Short W, Blair N, Sullivan P, Mai T. ReEDS Model Documentation : Base Case Data and Model Description. Renew Energy 2009.
[23] Energy Information Administration. The National Energy Modeling System : An Overview 2018; 2019.
[24] Heaton C, Bunn DW. Modelling Low-Carbon Energy System Designs with the ETI ESME Model. Energy Technol Inst 2014:1–27.
[25] Günther S, Krien U, Hilpert S, Kaldemeyer C, Plessmann G, Wingenbach C. The Open Energy Modelling Framework (oemof) - A new approach to facilitate open science in energy system modelling. Energy Strateg Rev 2018;22:16–25. https://doi.org/10.1016/j.esr.2018.07.001.
[26] E3Mlab/ICCS. PRIMES Model 2017:50. doi:10.1038/sj.hdy.6800728.
[27] Riva F, Gardumi F, Tognollo A, Colombo E. Soft-linking energy demand and optimisation models for local long-term electricity planning: An application to rural India. Energy 2019;166:32–46. https://doi.org/10.1016/j.energy.2018.10.067.
[28] Li B, Thomas J, De Queiroz AR, Decarolis JF. Open Source Energy System Modeling Using Break-Even Costs to Inform State-Level Policy: A North Carolina Case Study. Environ Sci Technol 2020;54:665–76. https://doi.org/10.1021/acs.est.9b04184.
[29] Bennett JA, Trevisan CN, DeCarolis JF, Ortiz-García C, Pérez-Lugo M, Etienne BT, et al. Extending energy system modelling to include extreme weather risks and application to hurricane events in Puerto Rico. Nat Energy 2021;6(3):240–9.
[30] Tsiropoulos I, Hoefnagels R, van den Broek M, Patel MK, Faaij APC. The role of bioenergy and biochemicals in CO2 mitigation through the energy system – a scenario analysis for the Netherlands. GCB Bioenergy 2017;9(9):1489–509. https://doi.org/10.1111/gcbb.2017.9.issue-910.1111/gcbb.12447.
[31] van den Broek M, Faaij A, Turkenburg W. Planning for an electricity sector with carbon capture and storage. Case of the Netherlands. Int J Greenh Gas Control 2008;2(1):105–29. https://doi.org/10.1016/S1750-5836(07)00113-2.
[32] Van Stralen J, Longa FD, Daniëls B, Smekens K, Van Der ZB. OPERA: A New High-Resolution Energy System Model for Sector Integration Research. Environ Model Assess 2020. https://doi.org/10.1007/s10666-020-09741-7.
[33] Fattahi A, Sánchez Diéguez M, Sijm J, Morales España G, Faaij A. Measuring accuracy and computational capacity trade-offs in an hourly integrated energy system model. Adv Appl Energy 2021;1:100009. https://doi.org/10.1016/j.adapen.2021.100009.
[34] Sánchez Diéguez M, Fattahi A, Sijm J, Morales España G, Faaij A. Modelling of decarbonisation transition in national integrated energy system with hourly operational resolution. Adv Appl Energy 2021;3:100043. https://doi.org/10.1016/j.adapen.2021.100043.
[35] Schure KM, De Haan FH, Boot PA, Boendermaker C, Geelhoed JJ. Investeringen Energietransitie En Financierbaarheid Uitdagingen met betrekking tot investeringen 2020-2040; 2017.
[36] PBL. ENSYSI - a simulation model for the Dutch energy system; 2015.
[37] PBL Netherlands Environmental Assessment Agency. MIDDEN: Manufacturing Industry Decarbonisation Data Exchange Network publications | PBL Planbureau voor de Leefomgeving n.d. https://www.pbl.nl/en/middenweb/publications [accessed June 24, 2020].
[38] PBL. National Energy Outlook 2016 | PBL Netherlands Environmental Assessment Agency n.d. https://www.pbl.nl/publicaties/nationale-energieverkenning-2016 [accessed December 9, 2019].
[39] KNMI - Koninklijk Nederlands Meteorologisch Instituut. Klimaatatlas n.d. http://www.klimaatatlas.nl/klimaatatlas.php [accessed June 3, 2019].
[40] The World Bank. The Netherlands - Wind Speed and Wind Power Potential Maps | Data Catalog n.d. https://datacatalog.worldbank.org/dataset/netherlands-wind-speed-and-wind-power-potential-maps [accessed May 31, 2020].

[41] TNO. Map Viewer | Thermogis n.d. https://www.thermogis.nl/en/map-viewer [accessed September 2, 2019].

[42] Kramers L, van Wees J-D, Pluymaekers MPD, Kronimus A, Boxem T. Direct heat resource assessment and subsurface information systems for geothermal aquifers; The Dutch perspective. Geol En Mijnbouw/Netherlands J Geosci 2012;91(4): 637–49. https://doi.org/10.1017/S0016774600000421.

[43] Wouter N. JRC Data Catalogue - European Commission 2019. https://data.jrc.ec.europa.eu/collection/id-00138 [accessed December 26, 2019].

[44] RUG G. Basic Data Portal n.d. https://geodienst.xyz/data/ [accessed April 5, 2020].

[45] Topo RD n.d. https://www.arcgis.com/home/item.html?id=7aea6fa913a94176a1074edb40690318 [accessed April 5, 2020].

[46] Luchtfoto 2018 - 25 cm n.d. http://esrinl-content.maps.arcgis.com/home/webmap/viewer.html?useExisting=1&layers=c9fe154fef63455a8450f6e13a19e3c5 [accessed April 5, 2020].

[47] Lund H, Thellufsen JZ. EnergyPLAN: Advanced Energy Systems Analysis Computer Model. www.EnergyPLAN.eu; 2018.

[48] Wiese F, Bramstoft R, Koduvere H, Pizarro Alonso A, Balyk O, Kirkerud JG, et al. Balmorel open source energy system model. Energy Strateg Rev 2018;20:26–34. https://doi.org/10.1016/j.esr.2018.01.003.

[49] Persson U, Werner S. Heat distribution and the future competitiveness of district heating. Appl Energy 2011;88(3):568–76. https://doi.org/10.1016/j.apenergy.2010.09.020.

[50] Möller B, Wiechers E, Persson U, Grundahl L, Lund RS, Mathiesen BV. Heat Roadmap Europe: Towards EU-Wide, local heat supply strategies. Energy 2019; 177:554–64. https://doi.org/10.1016/j.energy.2019.04.098.

[51] Europa-Universität Flensburg Halmstad University, Aalborg University. Peta4 – Heat Roadmap Europe n.d. https://heatroadmap.eu/peta4/ [accessed September 2, 2019].

[52] CBS. StatLine - Energy consumption private dwellings; type of dwelling and regions 2018. https://opendata.cbs.nl/statline/#/CBS/en/dataset/81528ENG/table?ts=1550249238313 [accessed February 15, 2019].

[53] RVO. Heat Atlas n.d. https://rvo.b3p.nl/viewer/app/Warmteatlas/v2 [accessed May 31, 2020].

[54] CBS. NUTS-2 Regions (Provinces) n.d. https://www.regioatlas.nl/indelingen/indelingen_indeling/t/nuts_2_regio_s_provincies [accessed May 30, 2019].

[55] Hers JS, Özdemir Ö, Kolokathis C, Nieuwenhout FDJ. Net Benefits of a New Dutch Congestion Management. System. 2009.

[56] Peters J, Volkers C. Korte modelbeschrijving NEV-RS (in Dutch) 2019. https://www.pbl.nl/sites/default/files/downloads/pbl-2019-korte-modelomschrijving-nev-rs_3870.pdf [accessed November 26, 2020].

[57] Sijm J, Gockel P, van Hout M, Ozdemir O, Van Stralen J, Smekens K, et al. Demand and supply of flexibility in the power system of the Netherlands, 2015-2050; 017.

[58] Daniëls B, Seebregts A, Joode J, Smekens K, Van Stralen J, Dalla Longa F, et al. Exploring the role for power-to-gas in the future Dutch energy system. Dnv Gl 2014:121.

[59] Bedir M, Hasselaar E, Itard L. Determinants of electricity consumption in Dutch dwellings. Energy Build 2013;58:194–207. https://doi.org/10.1016/j.enbuild.2012.10.016.

[60] Guerra Santin O, Itard L, Visscher H. The effect of occupancy and building characteristics on energy use for space and water heating in Dutch residential stock. Energy Build 2009;41(11):1223–32. https://doi.org/10.1016/j.enbuild.2009.07.002.

[61] Brounen D, Kok N, Quigley JM. Residential energy use and conservation: Economics and demographics. Eur Econ Rev 2012;56(5):931–45. https://doi.org/10.1016/j.euroecorev.2012.02.007.

[62] Sipma J, Kremer A, Vroom J. Energielabels en het daadwerkelijk energieverbruik van kantoren; 2017.

[63] Sipma J, Niessink R. Energielabels en het daadwerkelijk energieverbruik van scholen en tehuizen in de zorg; 2018.

[64] Energy USD of. Model documentation report: Residential sector demand module of the national energy modeling system. www.eia.gov; 2018. doi:10.2172/563838.

[65] Energy USD of. Model Documentation Report : Commercial Sector Demand Module of the National Energy Modeling System. vol. 066. www.eia.gov; 2018.

[66] Martinsen D, Krey V, Markewitz P, Vögele S. A New Dynamical Bottom-Up Energy Model for Germany: Model Structure and Model Results. In: 6th IAEE Eur Conf; 2004. p. 17.

[67] CBS. StatLine - Homes; main resident / household, 1998-2012 n.d. https://opendata.cbs.nl/statline/#/CBS/nl/dataset/7409wbo/table?dl=217F9 [accessed December 4, 2019].

[68] Sipma J, Rietkerk MDA. Ontwikkeling energiekentallen utiliteitsgebouwen; 2016.

[69] R.L.Bak. KANTOREN IN CIJFERS 2017. NVM Business; 2017.

[70] U.S. EIA. Model Documentation Report: Industrial Demand Module of the National Energy Modeling System. Washington DC; 2018.

[71] E3mlab. PRIMES model; 2018.

[72] Lehmann H. SimREN: Energy Rich Japan; 2003.

[73] Planbureau voor de Leefomgeving, Rijksinstituut voor Volksgezondheid en Milieu, CBS, Rijksdienst voor Ondernemend Nederland, TNO. Klimaat en Energieverkenning 2019 (Dutch); 2019.

[74] van den Wijngaart R, Folkert R, Elzenga H. Heating the built environment more sustainably by 2050; 2012.

[75] CBS. StatLine - Agriculture; crops, livestock and land use by general farm type, region 2019:1. https://opendata.cbs.nl/statline/#/CBS/en/dataset/80783eng/table?ts=1560159415718 [accessed December 4, 2019].

[76] Rijkswaterstaat. Klimaatmonitor n.d. https://klimaatmonitor.databank.nl/dashboard/ [accessed April 1, 2019].

[77] Arnoldussen J, Zwet R van, Koning M, Menkveld M. Verplicht energielabel voor kantoren; 2016.

[78] CBS. StatLine - Land use; all categories, municipalities n.d. https://opendata.cbs.nl/statline/#/CBS/en/dataset/70262eng/table?dl=3DD4 [accessed July 26, 2020].

[79] Ministerie van Infrastructuur en Milieu, Ministerie van Economische Zaken. Structuurvisie Windenergie op land; 2014.

[80] Matthijsen J, Dammers E, Elzenga H. De toekomst van de Noordzee. De Noordzee in 2030 en 2050: een scenariostudie; 2018.

[81] Vrijlandt MAW, Struijk ELM, Brunner LG, Veldkamp JG, Witmans N, Maljers D, et al. ThermoGIS update: a renewed view on geothermal potential in the Netherlands. In: Eur. Geotherm. Congr. 2019, Den Haag; 2019. p. 11–4.

[82] Wageningen UR. Manure - A valuable resource; 2014. doi:10.7748/ns2003.12.18.12.88.c3512.

[83] Rijkswaterstaat Ministerie van Infrastructuur en Waterstaat. Afvalverwerking in Nederland, gegevens 2017; 2018.

[84] Elbersen B, Staritsky I, Hengeveld G, Jeurissen L, Lesschen J-P. Outlook of spatial biomass value chains in EU 28; 2014.

[85] Özdemir Ö, Hers JS, Fisher EB, Brunekreeft G, Hobbs BF. A nodal pricing analysis of the future german electricity market. In: 2009 6th Int. Conf. Eur. Energy Mark. EEM 2009, 2009. https://doi.org/10.1109/EEM.2009.5207112.

[86] TenneT_Nederland. TenneT Assets (hoogspanning) 2020. https://www.arcgis.com/home/item.html?id=646a6dee22bf485587bc4daf98da1306 [accessed March 14, 2020].

[87] Zvingilaite E, Balyk O. Heat savings in buildings in a 100% renewable heat and power system in Denmark with different shares of district heating. Energy Build 2014;82:173–86. https://doi.org/10.1016/j.enbuild.2014.06.046.

[88] Nielsen S, Möller B. GIS based analysis of future district heating potential in Denmark. Energy 2013;57:458–68.

[89] Danish Energy Agency. Technology Data Generation of Electricity and District heating; 2020.

[90] Berenschot, Kalavasta. Klimaatneutrale scenario's 2050 – Scenariostudie ten behoeve van de integrale infrastructuurverkenning 2030-2050. (in Dutch); 2020.

[91] Sijm J, Janssen G, Morales-España G, Van Stralen J, Hernandes-Serna R, Smekens K. The role of large-scale energy storage in the energy system of the Netherlands, 2030-2050. Amsterdam; 2020. doi:TNO 2020 P11106.

[92] Avebe, Gemeente Emmen, Nedmag, Provincie Fryslan, Gemeente Groningen, New Energy Coalition, et al. The Northern Netherlands Hydrogen Investment Plan 2020: Expanding the Northern Netherlands Hydrogen Valley; 2020.

[93] van der Niet S, Rooijers F, van der Veen R, Voulis N, Wirtz A, Lubben M. Systeemstudie energie-infrastructuur Groningen & Drenthe (in Dutch). Delft; 2019.

[94] Provincie Groningen. Regional Energie Strategie (in Dutch). n.d.

[95] Sijm J, Gockel P, Hout M van, Özdemir Ö, Stralen J van, Smekens K, et al. The supply for flexibility of the power system in the Netherlands, 2015-2050; 2017.

[96] TNO. Fact sheets 2020. https://energy.nl/geavanceerd-zoeken/?fwp_content_type=factsheets [accessed December 17, 2020].

[97] Gigler J, Weeda M. Outlines of a Hydrogen Roadmap; 2018.

[98] Netherlands Institute for Transport Policy Analysis. Key Transport Figures 2018. 2018.

[99] World Bank Group, ESMAP, Technical University of Denmark, VORTEX. Global Wind Atlas 2021. https://globalwindatlas.info/ (accessed January 19, 2021).

[100] National Emissions Authority (NEa). Emissiecijfers 2013 - 2019 2020;53. https://www.emissieautoriteit.nl/documenten/publicatie/2020/04/16/emissiecijfers-2013-2019 [accessed September 9, 2020].

[101] Schoots K (ECN), Hamming P (PBL). Nationale Energieverkenning 2015 2015: 1–276. doi:ECN-O–16-035.

[102] Spijkerboer RC, Zuidema C, Busscher T, Arts J. Institutional harmonization for spatial integration of renewable energy: Developing an analytical approach. J Clean Prod 2019;209:1593–603. https://doi.org/10.1016/j.jclepro.2018.11.008.

[103] Ruijgrok EC., van Druten E., Bulder B. Cost Evaluation of North Sea Offshore Wind Post 2030; 2019.

[104] Pluymaekers MPD, Kramers L, van Wees J-D, Kronimus A, Nelskamp S, Boxem T, et al. Reservoir characterisation of aquifers for direct heat production: Methodology and screening of the potential reservoirs for the Netherlands. Geol En Mijnbouw/Netherlands J Geosci 2012;91(4):621–36. https://doi.org/10.1017/S001677460000041X.

[105] Limberger J, Calcagno P, Manzella A, Trumpy E, Boxem T, Pluymaekers MPD, et al. Assessing the prospective resource base for enhanced geothermal systems in Europe. Geotherm Energy Sci 2014;2(1):55–71. https://doi.org/10.5194/gtes-2-55-201410.5194/gtes-2-55-2014-supplement.

[106] Open source community. QGIS n.d. https://qgis.org/en/site/ [accessed October 5, 2020].

[107] Batzias FA, Sidiras DK, Spyrou EK. Evaluating livestock manures for biogas production: A GIS based method. Renew Energy 2005;30(8):1161–76. https://doi.org/10.1016/j.renene.2004.10.001.

[108] CBS. Biomass - Renewable energy in the Netherlands 2019. https://longreads.cbs.nl/hernieuwbare-energie-in-nederland-2019/biomassa/ [accessed November 25, 2020].

[109] Luo L, van der Voet E, Huppes G. Biorefining of lignocellulosic feedstock - Technical, economic and environmental considerations. Bioresour Technol 2010; 101(13):5023–32. https://doi.org/10.1016/j.biortech.2009.12.109.

[110] Ruiz P, Nijs W, Tarvydas D, Sgobbi A, Zucker A, Pilli R, et al. ENSPRESO - an open, EU-28 wide, transparent and coherent database of wind, solar and biomass energy potentials. Energy Strateg Rev 2019;26:100379. https://doi.org/10.1016/j.esr.2019.100379.

[111] Quintel. Energy Transition Model n.d. https://energytransitionmodel.com/?locale=en [accessed December 10, 2019].

[112] Özdemir Ö, Munoz FD, Ho JL, Hobbs BF. Economic Analysis of Transmission with Demand Response and Quadratic Losses by Successive LP. IEEE Trans Power Syst 2016;31:1096–107. https://doi.org/10.1109/TPWRS.2015.2427799.

[113] New Energy Coalition. Study: Offshore reuse potential for existing gas infrastructure in a hydrogen supply chain - New Energy Coalition n.d. https://newenergycoalition.org/study-offshore-reuse-potential-for-existing-gas-infrastructure-in-a-hydrogen-supply-chain/ [accessed December 9, 2019].

[114] Persson U, Wiechers E, Möller B, Werner S. Heat Roadmap Europe: Heat distribution costs. Energy 2019;176:604–22. https://doi.org/10.1016/j.energy.2019.03.189.

[115] Kortes H, Dril T van. Decarbonization option for the Dutch Aluminum Industry; 2019.

[116] Moejes SN, Visser Q, Bitter JH, van Boxtel AJB. Closed-loop spray drying solutions for energy efficient powder production. Innov Food Sci Emerg Technol 2018;47: 24–37. https://doi.org/10.1016/j.ifset.2018.01.005.

[117] Suárez A, Fernández P, Ramón Iglesias J, Iglesias E, Riera FA. Cost assessment of membrane processes: A practical example in the dairy wastewater reclamation by reverse osmosis. J Memb Sci 2015;493:389–402. https://doi.org/10.1016/j.memsci.2015.04.065.

[118] Carlini M, Mosconi EM, Castellucci S, Villarini M, Colantoni A. An economical evaluation of anaerobic digestion plants fed with organic agro-industrial waste. Energies 2017;10:1–15. https://doi.org/10.3390/en10081165.

[119] Lise W, De Joode J, Boots MG. Druk in de gasleiding (in Dutch); 2005.

[120] Gasunie, TenneT. Infrastructure Outlook 2050; 2019.

[121] TenneT. TenneT - Our high voltage grid n.d. https://www.tennet.eu/nl/ons-hoogspanningsnet/ [accessed July 14, 2020].

[122] Gasunie. About Gasunie » N.V. Nederlandse Gasunie 2018. https://www.gasunie.nl/en/about-gasunie [accessed October 24, 2018].